

Coded Wireless

Video Broadcast/Multicast

by

James She

A thesis

presented to the University of Waterloo

in fulfillment of the

thesis requirement for the degree of

Doctor of Philosophy

in

Electrical and Computer Engineering

Waterloo, Ontario, Canada, 2009

© James She 2009

I hereby declare that I am the sole author of this thesis. This is a true copy of the thesis, including any required final revisions, as accepted by my examiners.

I understand that my thesis may be made electronically available to the public.

Abstract

Advancements in video coding, compact media display, and communication devices, particularly in emerging broadband wireless access networks, have created many foreseeable and exciting applications of video broadcast/multicast over the wireless medium. For efficient and robust wireless video broadcast/multicast under fading, this thesis presents and examines a novel cross-layer framework that exploits the interplay between applying protections on a successively refinable video source and transmitting through a layered broadcast/multicast channel. The framework is realistically achieved and evaluated by using multiple description coding (MDC) on a scalable video source and using superposition coding (SPC) for layered broadcast/multicast transmissions. An analytical model using the total received/recovered video bitstreams from each coded wireless broadcast/multicast signal is developed, which serves as a metric of video quality for the system analysis and optimization. An efficient methodology has demonstrated that optimal power allocations and modulation selections can be practically determined to improve the broadcast/multicast video quality. From the information-theoretical perspective, a general closed-form formula is derived for the end-to-end distortion analysis of the proposed framework, which is applicable to any (n, k) protection code applied on a successive refinable source with a Gaussian distribution over layered Gaussian broadcast channels. The results reveal the scenarios for the proposed framework to lead to a lower distortion than a legacy system without any protection. By analyzing the characteristics of the closed-form formula, an efficient $O(n \log n)$ algorithm is developed to determine optimal k values in the (n, k) protection codes that minimize the distortion under the framework. Finally, a cross-layer design of logical SPC modulation is introduced to achieve layered broadcast/multicast for scalable video. It serves as an alternative for practically implementing the proposed framework of coded wireless video broadcast/multicast, if the

hardware-based SPC component is not available in a wireless system. In summary, the thesis presents comprehensive analyses, simulations, and experiments to understand, investigate, and justify the effectiveness of the proposed cross-layer framework of coded wireless video broadcast/multicast. More importantly, this thesis contributes to the advancement in the related fields of communication engineering and information theory by introducing a new design dimension in terms of protection. This is unique when compared to previously-reported layered approaches that are often manipulating conventional parameters alone such as power and modulation scheme. The impact of this dimension was unapparent in the past, but is now proven as an effective means to enable high-quality, efficient, and robust wireless video broadcast/multicast for promising media applications.

Acknowledgements

Over the years while commencing my studies at the University of Waterloo, many of my lifelong lessons were learned through exceptional individuals who have made distinctive influences on me, in both subtle and unsubtle ways.

First, I express my deepest gratitude to my supervisor, Professor Pin-Han Ho, for supporting me over the years with endless generosity, for giving me so much freedom and open-minded guidance to explore and discover exciting research ideas, and for cultivating me to become an independent researcher and life-long learner with his inspiring encouragement. I also present a special appreciation to my Ph.D. exam committee member, Professor En-hui Yang, for helping me to build a solid background and cultivate creative thinking for new areas of research, for sharing generous and stimulating discussions with me, and for being my role-model of a passionate teacher and persistent researcher with wide-range of wisdoms. My appreciation extends to Professor Liang-Liang Xie, who has been resourceful to me with his valuable advices to my research, and charismatic to me with his teaching style as one of my best learning experiences in his class at Waterloo. I would like to thank Professor Johnny Wong as my external committee and Professor Danny H.K. Tsang as my life-long mentor, who opened my eyes and minds through the journey of my Ph.D. study. I would also like to deeply thank Professor Xiaohong Jiang to serve as my external committee with his generous time and support.

I lovingly extend my gratitude to Dr. Flora Li for her adoring support and care during final stages of this work. I would like to thank Xiang Yu and James Ho, who have been my wonderful friends and research collaborators. There were many impactful and enjoyable moments in the discussions with them that inspire me endlessly for my research ideas. I would also like to thank many friends and colleagues at Waterloo, with whom I have had the pleasure to work with over the

years. These include Fen Hou, Jing-qing Mei, Gary Yeung and all the helpful individuals such as Wendy Boles, Annette Dietrich, and Karen Schooley in the Electrical and Computer Engineering Department.

My warmest thanks extend to Scott Inwood and Khosrow Modarressi for bringing useful outsiders' perspective to the thesis, and encouraged me to make it more accessible to non computer scientists. Finally, I would like to thank Dr. Orlan Lee, David Li, Tom Pham, Professor Justin Wan Eva and Sid Wong, Anahid and Wanis Der-Boghossian for their support and care throughout my Ph.D. study.

I acknowledge the financial support from Natural Sciences and Engineering Research Council (NSERC) of Canada, Ontario Centres of Excellence (OCE), and University of Waterloo. Lastly, I want to thank everyone who have educated, inspired, and enlightened me along the way, to make my academic journey at University of Waterloo a truly remarkable and colorful experience.

“Do not go where the path may lead, go instead where there is no path and leave a trail.”

~Ralph Waldo Emerson

Dedication

To

my Parents, Nai-yu She and Sit-leung Kam,

who have been unconditionally supportive since the start of my life journey.

and

Dr. Flora M. Li,

who brought me special meanings that redefine the understanding of my life journey.

Table of Contents

List of Tables	xii
List of Figures.....	vii
Chapter 1 Introduction.....	1
1.1 Wireless Broadband Access Networks and Video Applications	2
1.2 Wireless Video Broadcast/Multicast and Challenges	3
1.2.1 Multi-user Channel Diversity	3
1.2.2 Error Control.....	4
1.3 Thesis Motivation and Objectives	4
1.4 Thesis Contributions	5
1.5 Thesis Organization	7
Chapter 2 Background and Literature Review.....	9
2.1 Scalable Video Source – Background	9
2.2 Superposition Coding - Background	11
2.3 Error Controls	14
2.3.1 Erasure coding	14
2.3.2 Layered MDC - Background	15
2.4 Cross-layer Designs	17

2.5	Related Information-theoretical Bounds.....	18
-----	---	----

Chapter 3 A Cross-Layer Framework of Coded Wireless Video Broadcast/Multicast

	20
3.1	Superposition Coded Broadcast/Multicast.....	20
3.1.1	A preliminary cross-layer design.....	20
3.1.2	Simulation and Results	21
3.1.3	Lessons Learnt.....	24
3.2	A Proposed Cross-layer Framework of Wireless Coded Video Broadcast/Multicast	25
3.2.1	System Model	26
3.2.2	Modification of Layered Multiple Description Coding.....	27
3.2.3	Integration For Wireless Coded Video Broadcast/Multicast.....	29
3.3	Performance Evaluation.....	38
3.3.1	Selection of N and K_l	39
3.3.2	A Case Study for Optimization.....	40
3.4	Simulation Results	43
3.5	Summary	47

Chapter 4 Information-theoretical Analysis Under Gaussian Broadcast Channels...49

4.1	System Model and Notations.....	50
4.1.1	Protected Successive Refinement and Layered Broadcast	50
4.1.2	Channel Demodulation and Source Reconstruction	52
4.2	Distortion Analysis	53
4.3	A Novel Search Algorithm	61
4.3.1	The Global Minimum	62
4.3.2	Proposed Search Algorithm.....	69

4.4	Numerical Analysis	72
4.5	Summary.....	76
Chapter 5 Logical Superposition Modulation		78
5.1	Proposed Logical Superposition Coded Modulation	79
5.1.1	One-shot Modulation at Transmitter	79
5.1.2	A Cross-layer Mapping at Transmitter	81
5.1.3	Leveraging Existing Receiver Demodulators	83
5.1.4	Software Support at Receiver	85
5.2	Analysis Of Symbol Errors – A Case study	86
5.2.1	Feasibility of using a Standard 8-QAM Demodulator	86
5.2.2	Analysis of Symbol Error Rate (SER).....	89
5.3	Generalized Formulations for Logical SPC.....	92
5.3.1	Bounds on β	92
5.3.2	General Formulation of SER	93
5.4	Numerical Results.....	96
5.4.1	Overall System Performance with Multi-User Channel Diversity	96
5.4.2	Achieving Comparable Optimal System Performance	98
5.5	Testbed Results.....	102
5.6	Summary.....	104
Chapter 6 Contributions and Conclusions		106
6.1	Major Research Contributions.....	106
6.2	Future Works	109
6.2.1	EPON-WiMAX Network - A hybrid wired/wireless access network	109
6.2.2	Cooperative Coded Video Multicast	111

6.3	Final Remarks.....	115
	References	116

List of Tables

Table 3-1.	Simulation parameters and the average SNR of each SS.	23
Table 4-1.	Only 7 possible trends of the distortion function with respect to k_1	68
Table 5-1.	Equivalency in the number of constellation symbols between logical and conventional SPC modulations.	81
Table 5-2.	Upper and lower bounds for β under various	93

List of Figures

Figure 1-1. Examples of digital signages for advertisement.	2
Figure 2-1. Scalable bitstreams with L quality layers.	10
Figure 2-2. Distortion and bitstream boundaries in a GoF.	11
Figure 2-3. Power disparities in a wireless network.	12
Figure 2-4. Superposition coded (SPC) modulation: (a)-(c) encoding; (d)-(e) decoding.	13
Figure 2-5. Generation of conventional Layered MDC packets.	17
Figure 3-1. The multicast signal based on 2-level SCM with 16-QAM and BPSK.	23
Figure 3-2. Video quality at SS1 and SS10 using the legacy scheme (denoted normal) and proposed scheme.	24
Figure 3-3. An overview of five major processes in the proposed cross-layer framework.	27
Figure 3-4. Generation of MDC packets based on modified layered MDC with the decreasing ordering of K values from the lower layer to the higher one.	29
Figure 3-5. PUs of layer i formed by a RS code (N, K_i)	30
Figure 3-6. PUs of layer 1 and 2 stored in B1 and B2 buffers forming cross-layer superposition coded multicast signals.	31
Figure 3-7. BS transmits all PUs of all quality layers of video bitstreams with superposition coded multicast.	32
Figure 3-8. Enhancement video data loss at time $t = 2$ and $t = 4$	34
Figure 3-9. Enhancement video data loss at time $t = 3$ and $t = 4$	34
Figure 3-10. Both base and enhancement data loss at time $t = 3$	34
Figure 3-11. Illustrations of (a) SNRs, (b) layer error rates, (c) modulation schemes, and (d) total received/recovered bitstreams with respect to different power allocation.	43
Figure 3-12. PSNR of Foreman between the proposed framework and the SCM.	46
Figure 3-13. PSNR of Paris between the proposed framework and the SPCM.	46
Figure 3-14. Better video qualities and less PU loss for both the best and worst channel receivers under the proposed framework.	47

Figure 4-1.	A generic cross-layer architecture of protected successive refinement over layered broadcast channels.....	51
Figure 4-2.	Two-stage optimization for the cross-layer framework.....	60
Figure 4-3.	A function of f_1+f_3	65
Figure 4-4.	$-(f_1+f_3)'$	65
Figure 4-5.	A function of f_2+f_4	65
Figure 4-6.	$(f_2+f_4)'$	65
Figure 4-7.	Four possible cases.....	66
Figure 4-8.	The system with a higher average compound symbol error, $p_{M,1}$. (optimized protections are $k_1^* = 5$ and $k_2^* = 2$).....	74
Figure 4-9.	The system with a lower average compound symbol error, $p_{M,1}$. (optimized protections are $k_1^* = 14$ and $k_2^* = 2$).....	74
Figure 4-10.	The system with a higher average compound symbol error, $p_{M,2}$. (optimized protection in layer 2 - $k_2^* = 3$).....	75
Figure 4-11.	The system with a lower average compound symbol error, $p_{M,2}$. (optimized protection in layer 2 - $k_2^* = 1$).....	75
Figure 4-12.	The expected distortions of two systems with respect to various $p_{M,1}$ and $p_{M,2}$	76
Figure 5-1.	Mapping a 3-bit symbol block to one of the 8 constellation symbols. “ \otimes ” stands for superposition operation.	82
Figure 5-2.	Operation and interactions between layers of the required software support.....	84
Figure 5-3.	The bounds and impacts of β towards the location of constellation points limited by the decision boundary of a standard 8-QAM detector.....	87
Figure 5-4.	Sample first quadrant of QPSK/16QAM constellation denoting reference to each decision region using i and j	94
Figure 5-5.	Overall system throughput of L-SPC and C-SPC for combinations: (a) BPSK/QPSK, (b) QPSK/16QAM, (c) 16QAM/64QAM, over varying β values under the Normal distributions with various means for the multi-user channel histogram.....	99
Figure 5-6.	Overall system throughputs of the proposed and standard approaches over different values under the normal distribution with various standard deviations for the SPC combination (a) QPSK/BPSK, (b) QPSK/16QAM and (c) 16QAM/64QAM.....	100
Figure 5-7.	Comparable optimal system performance between the proposed and conventional approaches under various multi-user channel histograms modeled using Normal distributions of different means and variances.....	101
Figure 5-8.	Received PSNR from the transmission of a scalable HDTV video trace using 2 layered L-SPC and mono-rate BPSK.....	103
Figure 6-1.	Integrated access network architecture based on EPON and WiMAX.....	110
Figure 6-2.	Multiple ONU-BSs and 4 SSs in the polar coordinates.....	113

Figure 6-3. Achievable SINRs and best supportable modulation pair for both quality layers by
SSs in different interference areas. 114

Chapter 1

Introduction

Imagine the advertising signages at prime areas in city downtowns, billboards at eye-catching locations along highways (as illustrated in Figure 1-1), and posters in high-traffic exhibitions, events, and restaurants, all wirelessly networked and fueled with digital media. Up-to-date, high-quality, animated, and even interactive information are customizable in real-time according to location and ambient environment of the signages, timing, and targeted audience. Such information is delivered simultaneously to a large number of destinations on-the-fly through wireless, pervading to both indoor/outdoor locations, to both fixed digital signage/display, and even portable/mobile media devices. These are no longer just the visions seen in science-fiction movies, but possibly realizable in the near-future as a result of advancements in video coding, electronic display and portable/mobile media devices, and particularly, Broadband Wireless Access (BWA) networks based on emerging wireless technologies of IEEE 802.16 (WiMAX) [1] and 4G Long Term Evolution [2].



Figure 1-1. Examples of digital signages for advertisement. [3]

1.1 Wireless Broadband Access Networks and Video Applications

A broadband access network (BAN) refers to the portion of a high-speed data communication network that connects to a subscriber's device, residence, place of business, or mobile location. Based on the type of “last-mile” transmission medium, BANs can be divided into two categories: one is the wired network, such as Digital Subscriber Line (DSL) network, coaxial cable network, and optical fiber network; the other is the wireless network, such as IEEE 802.11-based Wireless Local Area Network (WLANs) or WiFi, IEEE 802.16-based Wireless Metropolitan-Area Network (WMANs), WiMAX, 3G or 4G Long Term Evolution (LTE) cellular networks. The wired and wireless networks currently co-exist in the broadband access market. For higher profitability and competitive services, telecoms and network services providers are actively migrating their infrastructures to a single Internet Protocol (IP) platform to offer triple/quadruple-play services (voice, video, data or/and mobility). Therefore, all-IP BWA networks are being aggressively developed in recent years for new Internet access service through wireless and mobility, along with

many exciting bandwidth-intensive media applications such as mobile/wireless Internet Protocol Television (IPTV), wireless digital signages, mobile online games, and video conferencing.

1.2 Wireless Video Broadcast/Multicast and Challenges

Potential wireless media applications, such as digital signages and wireless/mobile IPTV, require simultaneous duplicated deliveries of the same bandwidth-intensive video data to all/multiple interested locations/devices. Conventional cellular networks simply wirelessly transmit these common video streams on a 1-by-1 basis to all interested destinations. Under the limited radio spectrum and system transmission capacity, this approach is entirely neither scalable nor manageable when the number of destinations grows. An alternative is to transmit the video data through a single common broadcast/multicast radio signal that is simultaneously received and shared by all interested receivers within the same radio coverage. Although a higher radio spectrum efficiency and system scalability can be achieved by the use of this wireless video broadcast/multicast approach, delivering a high-quality video efficiently and robustly are subjected to the following two generic challenges.

1.2.1 Multi-user Channel Diversity

A challenge in wireless video broadcast/multicast is the transmission rate of a shared broadcast/multicast radio signal. It is unfortunately limited to the lowest data rate that is supported by the receiver with the poorest channel condition. Hence, this broadcast/multicast signal can be demodulated by the channel conditions of largest possible number of interested receivers at the same time. However, because the fluctuations in wireless channels and the diversity of channel conditions among receivers are inevitable at any reception moment in a wireless network, wireless

video broadcast/multicast eventually prohibits the delivery of higher-quality video to qualified receivers with better channel condition that support a faster data rate. This is a generic bottleneck to wireless broadcast/multicast radio systems, and is known as the multi-user channel diversity problem.

1.2.2 Error Control

Due to the time-varying nature of wireless channels and possibly user mobility, transmission loss yields a significant portion of the end-to-end distortion at the recipient for the transmitted information. For receiving broadcast/multicast radio signals continuously, different receivers can experience extremely diverse temporary deafness in their wireless channels. Although repetitive transmission or re-transmission may alleviate certain transmission loss problems, it is neither efficient nor scalable in the broadcast/multicast scenario. Since the loss of data varies from one receiver to another, retransmitting for a particular data lost only benefits the recovery for some receivers and could cause acknowledgement explosion if every data lost is retransmitted.

1.3 Thesis Motivation and Objectives

With exciting and promising media broadcasting/multicasting applications in BWA networks, significant industrial development and business opportunities with great potentials in advancing the use of wireless for our digital lifestyles are presented. Therefore, researching scalable, efficient, and robust wireless video transmission frameworks over BWA networks that addresses the challenges of multi-user channel diversity and error control is an important and timely topic. These evolving trends present the major motivations of this thesis on coded wireless video broadcast/multicast with the following research objectives:

- To develop practical, scalable, and robust wireless video broadcast/multicast transmission frameworks through joint considerations of advanced source, channel and protection coding and viable engineered wireless system designs;
- To understand the fundamental information-theoretical limits of the proposed frameworks for optimal system configuration and resource allocation to minimize information distortion.

1.4 Thesis Contributions

The research contributions are summarized as follows.

- To cope with the multi-user channel diversity, a cross-layer framework, called Superposition Coded Multicast (SCM), is proposed by exploring the intrinsic layered natures of advanced scalable video coding (e.g., H.264/MPEG-4 AVC) and the use of superposition coding at the channel. Extensive simulations and experiments with the real trace files of high-definition television (HDTV) are conducted to compare a system using the proposed framework and a legacy multicast scheme that always transmits with the best supported modulation rate. The results revealed the benefits of jointly considering a successive refinement coding at the source and layered broadcast coding at the channel for wireless video broadcast/multicast. Such coded wireless video broadcast/multicast signal practically utilized the diverse channel conditions of all individual receivers at each reception moment. Each receiver can therefore acquire a better video quality regardless of its average channel condition.

- Another novel cross-layer framework of the interplay between applying protections on successively refinable video source and layered modulation at the channel is proposed. An analytical model using the total receivable/recoverable video bitstreams from each coded wireless broadcast/multicast signal is developed, which serves as a video quality measurement for system analysis and optimization. An efficient optimization technique is developed to practically determine the optimal power allocations and modulation selections that improve the broadcast/multicast video quality at the receivers. Most importantly, this framework can be realistically implemented by using scalable video source, a modified multiple description coding (MDC) as the protection, and SPC at the channel for layered broadcast/multicast. Comprehensive simulations are conducted on various standard video sequences, which confirm the effectiveness of this framework of coded wireless video broadcast/multicast for effectively tackling with the problems of multi-user channel diversity and error control.
- From the information-theoretical point of view, a closed-form formula is derived for the distortion analysis of the proposed framework using any (n, k) protection code in a successive refinable source with Gaussian distribution over a layered Gaussian broadcast channel. The closed-form formula can determine if and when such coded wireless video broadcast/multicast can yield a lower distortion than a system with any protection. An efficient iterative search algorithm is developed that can always identify the global optimal at the worst-time complexity of $O(n \log n)$, where n is the number of channel symbols required to send a source symbol after protection. Numerical analyses for performance evaluation are conducted to show the effectiveness of the proposed search algorithm. The results confirmed that the optimized k values searched by the $O(n \log n)$ algorithm can yield the lowest distortion.

- A novel cross-layer design framework of logical SPC modulation is proposed as an alternative to realize SPC modulation if the hardware support for SPC is not available. It takes advantage of the successively refinable feature of scalable video bitstreams and a logical mapping onto the constellation of SPC modulated signals. Generalized closed-form formulations were derived to evaluate and analyze the proposed logical SPC approach in terms of symbol error rate (SER). Numerical experiments were conducted, and the results showed that the proposed logical SPC modulation/demodulation can achieve much better performance than that by using only mono-rate modulation in the multicast of scalable video bitstreams. In contrast with the scheme of conventional hardware-based SPC with SIC, the proposed logical SPC modulation can completely avoid additional hardware at the sender and receivers without any compromise in the overall performance by manipulating the value of β . *Abed* is developed based on GNU Radio to demonstrate the implementability and its advantages of the proposed framework.

It is envisioned that the outcomes from this research on coded wireless video broadcast/multicast will contribute to the development and advancement of video delivery for a new generation of all-IP BWA networks, media communication devices, and other pertinent applications.

1.5 Thesis Organization

The organization of the remainder of the thesis is as follows. Chapter 2 provides the background knowledge and a survey of state-of-the-art technologies, where the issues of multi-user channel diversity and error control are reviewed. Chapter 3 starts with a practical preliminary cross-layer framework, known as Superposition Coded Multicast (SCM), that only adopts the superposition

coding at the channel to tackle the multi-user channel diversity problem. The chapter then presents a comprehensive cross-layer framework, called Coded Video Broadcast/Multicast, that fully overcomes the multi-user channel diversity and error-control problems through the interplay of scalable video coding at the source, modified multiple description coding for erasure protection, and superposition coding at the channel. From the information-theoretical point of view, Chapter 4 investigates the end-to-end distortion of the proposed framework based on any (n, k) protection code on a successive refinable source with Gaussian distribution over Gaussian broadcast channels. Chapter 5 presents a cross-layer design of logical SPC as an alternative to hardware-based SPC for realizing layered broadcast/multicast transmission of scalable video. Finally, conclusions and future research work are described in Chapter 6.

Chapter 2

Background and Literature Review

This chapter first provides the background in relation to the scalable video source, superposition coding, and multiple description coding that are required throughout this thesis. Literature review presents related works with focus on the areas in cross-layer designs for multi-user channel diversity and error control, as well as the related information-theoretical analysis.

2.1 Scalable Video Source – Background

Advanced video coding techniques enable the same video content to be encoded once while supporting heterogeneous conditions of transport and end-user devices. It allows the same content to be simultaneously decoded by multiple fixed and mobile receivers with different performances of devices and/or communication channels. H.264/MPEG-4 was recently standardized by the International Telecommunications Union-Telecommunication (ITU-T), and designed to packetize video data with real-time transport protocol (RTP) [4]. It shows a substantial improvement over MPEG-2 performance, especially for both HDTV and scheduled video-on-demand (VoD) content. Other scalable video codecs are proposed to further improve the spatial-temporal scalability of

video communications. The encoded bitstreams (i.e., the encoded bit string) for low-end performing devices and communication channels are embedded as subsets of bitstreams for high-end ones. This facilitates the video broadcasting/multicasting due to the ability of partial decoding at a variety of resolutions and quality levels (or conceptual quality layers) based on individual receiver capabilities. The proposed frameworks in this thesis generically exploit this property of any advanced video coding, which generates scalable bitstreams with multiple quality layers. An advanced video coder based on Joint Scalable Video Model (JSVM) from Heinrich-Hertz-Institute is employed in this thesis, which is a scalable extension of H.264/MPEG-4, part 10 -AVC. With JSVM, a group of frames (GoF) are encoded into a scalable bitstreams with L quality layers as shown in Figure 2-1, which supports both the temporal and spatial scalabilities at the same time. The bitstreams is strategically split into bitstream segments according to the boundaries of each quality layer. The boundaries of a layer l in the bitstreams of a GoF is denoted by bits b_{l-1} and b_l , such that $0 = b_0 \leq b_1 \leq \dots \leq b_L$, and the corresponding distortion of video quality by $D(b_l)$, where $D(b_0) \geq D(b_l) \geq D(b_L)$ as illustrated in Figure 2-2.

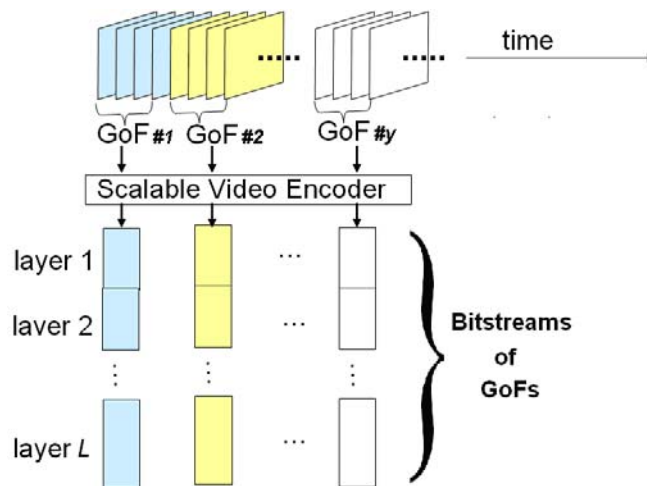


Figure 2-1. Scalable bitstreams with L quality layers.

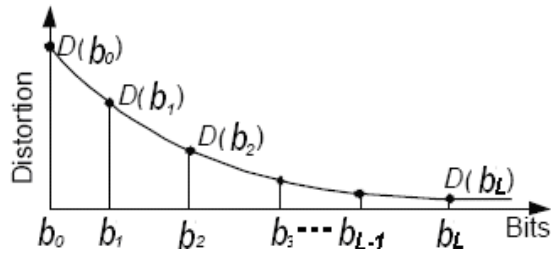


Figure 2-2. Distortion and bitstream boundaries in a GoF.

2.2 Superposition Coding - Background

For a long time, superposition coding (SPC) was introduced at the channel to increase the overall capacity of a wireless communication system by exploiting the spatial or temporal power disparities perceived by multiple receivers for common broadcast signals [28]. The intrinsic goal of SPC is to facilitate the transmission of two independent receiver's information in a single wireless transmission block by the superimposition of the two signal's symbol blocks. An example of SPC is illustrated in Figure 2-3, cited from [24]. The receivers, M_1 , M_2 , and M_3 are indexed in an increasing order according to their distance from the base station (BS). As shown in the figure, when the BS transmits signals to M_3 at the targeted signal-to-noise ratio (SNR) level, the SNR experienced by both M_1 and M_2 is much greater than their targeted SNR levels (by the amount of $A + B$ and C , respectively). Similarly, when the BS transmits signal to M_2 , M_1 receives additional A dB of power above its targeted SNR level. This implies that M_1 has sufficient SNR to decode the messages intended for both M_2 and M_3 , and M_2 has sufficient SNR to decode the messages intended for M_3 . The power disparities at receivers M_1 , M_2 , and M_3 suggest that the information for M_1 can be included in the transmission to M_2 or M_3 through the adoption of superposition coding. Similarly, the information for M_2 can be included while transmitting information to M_3 . The dotted line in

Figure 2-3 indicates that the BS transmits information to M_2 while transmitting to M_3 at the targeted SNR level by employing superposition coding.

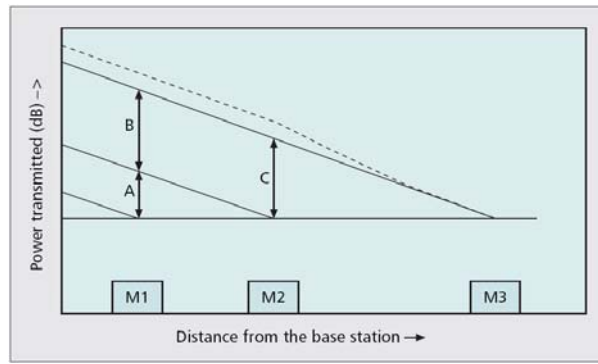


Figure 2-3. Power disparities in a wireless network cited from [24].

From the view of a constellation diagram during the encoding and decoding process, the superposition of two signals is analogous to the vector addition of the signal constellation symbols. As shown in Figure 2-4, x_1 and x_2 are information for receiver M_1 modulated using QPSK and information for receiver M_2 modulated using BPSK, respectively. Modulation using QPSK has the capability to achieve a higher transmission rate over BPSK at the expense of robustness when subject to a noisy channel. The superimposed signal, x , is a vector sum of the two modulated signals governed by $x = x_1 + x_2$. In Figure 2-4(c), vector x consists of symbol '0' from Figure 2-4(b) and symbol '01' from Figure 2-4(a). Signal x is the SPC symbol, launched as a single wireless transmission block, and received by two receivers with diverse channel conditions concurrently within the same coverage.

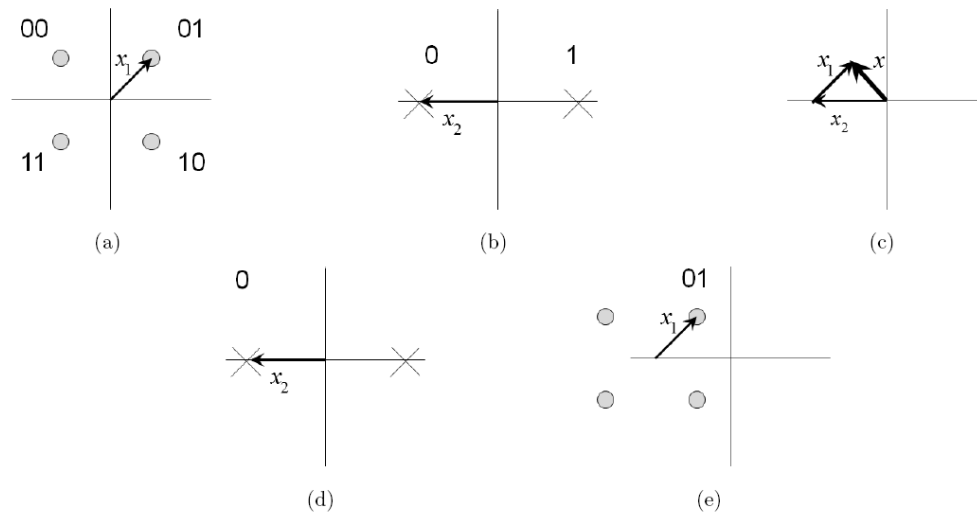


Figure 2-4. Superposition coded (SPC) modulation: (a)-(c) encoding; (d)-(e) decoding.

The received signal is expressed as $y_j = x + z_j$, where z_j is the noise perceived by receiver M_j . The conventional technique to decode the received SPC signals is known as Signal-Interference Cancellation (SIC), which is used at receiver M_j to identify the signal components meant for the noise and other receivers. Hence, receiver M_j can obtain its own information by subtracting the undesired signal components belonging to other receivers from the received signal y_j . For example, for receiver M_1 to decode its data from y_1 , it must first use the demodulator (i.e., BPSK) corresponding to the information used for receiver M_2 , x_2 , and then use SIC to subtract x_2 from the received signal y_1 . The result of the subtraction using SIC is x_1 , which is usually distorted by the noise experienced at receiver M_2 , z_1 .

2.3 Error Controls

2.3.1 Erasure coding

Note that retransmission of lost information/packets is only an effective countermeasure in the case of point-to-point transmission instead of broadcast/multicast. To tackle the transmission loss problem, especially under a broadcast/multicast scenario, a partial solution is to apply the erasure coding at the transport layer such as *Digital Fountain Code* [12] or *multiple description coding* (MDC) at the application layer [14].

The basic idea of *Digital Fountain* is to encode k original data packets into n packets, where $n = k + h$, and $h > 0$ is the number of redundant packets, so that the original packets can be recovered from any k received encoded packets in a computationally efficient manner. A cross-layer scheme was proposed in [15] that combines the *Digital Fountain* code with a MAC layer multicast policy based on a statistical value *Threshold-T*. One redundant packet can be used by different receivers to recover different lost packets. However, only some but not all receivers can receive this packet successfully in each transmission, and hence, it only helps a limited number out of T receivers in the scheme. Similarly, the idea of MDC is to encode a set of video bitstreams data into N packets, which are then transmitted from a source to receiver(s) over channel(s) with spatial or temporal diversity. In general, the more MDC packets a receiver obtains, the better video quality it can enjoy. This idea was further engineered in [19] to achieve the robustness on unreliable channels and adaptation to heterogeneous receivers, where base layer descriptions for lower video quality can be transmitted to low bandwidth clients, while both base and enhancement layer descriptions for full quality can be transmitted to high bandwidth clients.

In general, however, MDC was designed for wireline infrastructures in the past without reference to modulation/demodulation schemes used at the PHY layer. MDC packets generally are

assumed to be completely lost or received as a whole. There is not any notion in utilizing partially received MDC packets. In addition, a very limited number of papers have been identified using MDC in a cross-layer broadcast/multicast over single-hop wireless networks.

2.3.2 Layered MDC - Background

Many schemes of MDC are developed over the years for the uses in packet based media transmission systems as a means to overcome both packet loss and infrastructure failures. A MDC scheme designed in the proposed framework is modified from a layered MDC proposed by Chou et al. [19]. Packets of multiple descriptions in that MDC scheme are generated based on the Priority Encoding Transmission (PET) technique, which was first introduced by Albanese et al. [20]. PET is a packetization scheme that combines scalable layered video coding with unequal erasure protection. As illustrated in Figure 2-5, since each GoF is independently encoded into scalable bitstreams with multiple quality layers of different importance, the bitstream of each layer l is then partitioned into source blocks of K_l equal length bytes. Each source block of K_l bytes is encoded and expanded into a series of protected units (PUs) of length N bytes using an (N, K_l) Reed-Solomon (RS) code. Other network coding techniques, such as *LT* codes and *Digital Fountain* codes, are also applicable to encode the source block into PUs as alternative protection codes.

Without loss of generality, suppose there are exactly L layers, i.e., $l = 1, 2, \dots, L$, which are indexed in order of non-increasing importance such that layer l is protected with an (N, K_l) RS code. In general, the value of K_l for partitioning layer l video bitstream is determined by a number of factors, including the significance of that layer for the final video reconstruction and the protection required by that layer in the transmission channel. A smaller K_l implies better protection for the bitstream data in layer l against loss/error and component failures. The PUs in each layer are then packetized in a way that the i -th byte in each row of PUs in that layer will be assigned to the i -

th MDC packet for transmission, where $i = 1, \dots, N$. In this sense, all these N MDC packets are equally important, where only the *number* of MDC packets received determines the reconstructed video quality of the GoF. Thus, the layered MDC is also a form of the generic MDC, where the i -th MDC packet constitutes the i -th description of a GoF, and contains bitstream data of multiple quality layers in the GoF. A sequence of the i -th MDC packets for GoFs constitutes the i -th description for the whole media stream.

Conventionally, a smaller K value is used to partition a lower video quality layer while a larger one is selected for partitioning a higher layer, because the final video reconstruction is more dependent on the lower layer than the higher one. For example, due to the higher importance of bitstream data in a lower quality layer, the layered MDC proposed by Chou et al. based on the original PET and its other variations allocate more or equal protection overheads to source blocks of a lower quality layer than those of higher quality layers (i.e., $N - K_1 \geq N - K_2 \geq \dots \geq N - K_L$). This is because an MDC packet with PUs containing bitstreams of multiple quality layers can be either completely lost or received as a whole, and as such, the data of higher quality layers becomes totally useless if a lower quality layer cannot be recovered from the number of MDC packets successfully received.

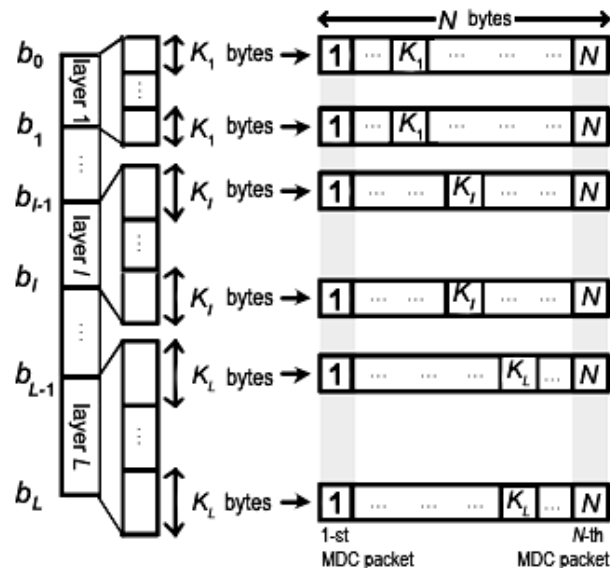


Figure 2-5. Generation of conventional Layered MDC packets.

2.4 Cross-layer Designs

Many studies on cross-layer designs have been reported to improve the unicast video quality and system performance, which commonly adjust/use strategic parameters across different system layers at the transmission system. The parameters include the application-layer delay bound of a video frame delay, the number/priority of Automatic Repeated reQuest (ARQ) retransmission attempts at the MAC layer, and the number of OFDM sub-carriers at the PHY layer. [5],[6],[7],[8],[9],[10]. Emerging attentions for IPTV services using cross-layer designs are also recently witnessed in Wireless Local Area Networks (WLANs). Due to the small scale of a WLAN, some approaches even adapt the video quality at the source with the real-time channel conditions [12]. However, all these approaches are only optimizing the transmission performance based on the condition of a single receiver, which is entirely not applicable for a large scale of broadcast/multicast scenario in a BWA network. For delivering the same video to multiple

receivers, none of these previous cross-layer designs are scalable to utilize the limited radio spectrum when the number of receivers increases. In this case, it is highly desirable to preserve the use of broadcast/multicast to avoid duplicated deliveries of the same video.

A few emerging cross-layer designs [33], [34], [35], [36] including our early work [37] are reported in very recent years for scalable video broadcast/multicast using multi-resolution modulated radio along with layered video bitstreams. The cross-layer framework in [[32]] incorporates adaptive power allocation and channel coding strategies by considering the interference-limited and bandwidth-limited characteristics of a broadcast/multicast CDMA system. The video encoder is effectively matched with an embedded multi-resolution modulation scheme to simultaneously deliver a basic quality-of-service (QoS) to less capable receivers while maximizing both the QoS for more capable receivers. However, they do not address the loss of video data (usually those in higher quality layers) due to the common short-term channel fluctuation in wireless systems, which prohibit the broadcast/multicast of high-quality video.

2.5 Related Information-theoretical Bounds

Previous information-theoretical studies on the performance bound on superposition coding have been well reported [28], [30],[31]. In recent years, the studies in [32], [33], [35] identified the end-to-end distortion bound from a cross-layer perspective and the impact due to power allocation in successive refinable layers of data. The evaluation of distortion in these works is based on the expected number of layers that can be decoded under a constant channel realization, where no loss is assumed in the layers to be decoded. However, the truth is that a layer of data in a successively refined source may not be decodable if there is any loss of channel codeword even if the corresponding long-term channel realization is sufficient. Such a loss of codeword could be easily

due to the short-term Rayleigh fading effect, which leads to the failure of achieving the required instantaneous channel realization from time to time. This situation is particularly an issue to mobile users.

Even though there is an abundance of literature on MDC (see [25], [26], [27]), an information-theoretic characterization of MDC (i.e., the achievable region of MDC) is still unknown, even for general memoryless sources let alone the characterization for general stationary or non-stationary sources and algorithms for designing optimal MDC. Hence, a fundamental problem here is to investigate whether or not the use of an erasure coding, such as MDC or other (n, k_l) protection codes on successive refinable data coupled with SPC broadcast signals can improve distortion performance. Due to the infancy of this approach, a general information-theoretical analysis on the end-to-end distortion and the performance bound has yet to be determined.

Chapter 3

A Cross-Layer Framework of Coded Wireless Video Broadcast/Multicast

In this chapter, a preliminary cross-layer design is first introduced that adopts the scalable video coding at the source and the superposition coding at the channel to tackle the multi-user channel diversity problem. Key design factors are concluded from this preliminary design. These conclusions contribute to the development of a novel cross-layer framework of coded wireless video broadcast/multicast after this section, which overcomes both the multi-user diversity and error-control problems effectively.

3.1 Superposition Coded Broadcast/Multicast

3.1.1 A preliminary cross-layer design

As discussed in the background about SPC in Section 2.2 of Chapter 2, receiver M_1 with a higher-SNR channel first decodes the information, x_2 , for receiver M_2 from a received SPC signal, and

then subtracts it from the received SPC signal to obtain its own information, x_1 . Intuitively, it will be beneficial to receiver M_1 if the information, x_2 , is actually useful. This interestingly happens to be the case when using SPC for broadcasting/multicasting a scalable video. Rather than the conventional notion in using SPC for transmitting two unrelated information, a SPC signal here contains two streams of correlated information with one refining the information of another.

A 2-level superposition coded multicast (SCM) is therefore developed by using superposition coding at the channel and a scalable video coding at the source. The employment of SPC achieves the effect of multi-resolution modulation that exploits the successive refinable feature in each video frame with two quality layers (i.e., *base* and *enhancement*). Bitstreams of *base* and *enhancement* quality layers from each video frame are modulated individually by different orders of modulation schemes, and then superimposed together as a single 2-level SPC multicast signal. By receiving such 2-level SCM signal, it is believed that most receivers can demodulate and decode at least the basic video quality with high probability. Meanwhile, the receivers with good channel conditions can obtain both quality layers of video bitstreams from the same SPC signal.

3.1.2 Simulations and Results

Simulations are conducted to evaluate the proposed 2-level SCM in a WiMAX-based BWA network. An IPTV content with 2 quality layers is multicasted to multiple subscriber stations (SSs) as a group of multicast receivers with diverse channel conditions. Video frames are generated from the video source with a constant frame rate (e.g., 30 frames per second) directly connected to a BS as shown in Figure 3-1. The size of each frame depends on the type of frame and content of video sources, which is obtained from the trace file of a real HDTV content [11]. The bitstreams of each

frame are categorized into base quality data and enhancement quality data by a certain percentage ratio, and packetized into RTP/IP packets and then to MAC-layer protocol data units (MPDU) for wireless transmission. The average SNR of each SS and other simulation parameters are given in Figure 3-2. The proposed 2-level SCM is compared with a legacy multicast scheme, which always transmits at the fastest monotonic modulation rate that all receivers support. Without loss of generality, only two modulation schemes (i.e., BPSK and 16QAM) are considered, though the proposed framework can be applied to the case with any number/combination of modulation schemes. With the legacy scheme (denoted as “normal” in the figures), either BPSK or 16QAM will be chosen for each multicast transmission, depending on whether all SSs can support that modulation scheme at that transmission moment indicated by their channel feedbacks. Rayleigh fading is simulated at the channel of each SS, and assumed to vary at one frame after the other. It is assumed that the channel state of each SS is unchanged over the duration of each WiMAX transmission frame. A SS channel with a SNR above 16 dB indicates that the SS is “good” enough to support 16QAM, otherwise only BPSK is employed. The frame-by-frame video quality, in terms of peak signal-to-noise ratio (PSNR), perceived at SS10 and SS1 are measured, which correspond to the SSs with the best and worst average SNR at their channel, respectively. In the simulation, the percentage of base quality data of a video frame is 40 percent and 80 percent for generating the results in Figure 3-2 (a) and Figure 3-2 (b), respectively.

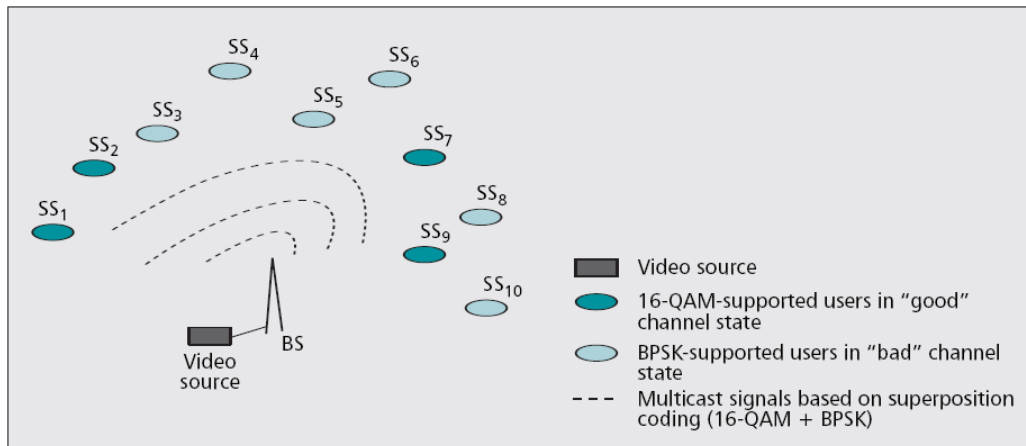


Figure 3-1. Each 2-level SCM signal decoded by both 16-QAM-supported and BPSK supported users simultaneously.

Table 3-1. Simulation parameters and the average SNR of each SS.

Number of SSs	Frame duration	Downlink sub-frame duration	Uplink sub-frame duration	FFT Size	Data subcarriers	OFDM symbol duration	Time slot duration			
10	2 ms	1ms	1 ms	256	192	11.46 ns	4 physical symbols			
Index of SS	SS1	SS2	SS3	SS4	SS5	SS6	SS7	SS8	SS9	SS10
Average SNR (dB)	10	12	14	16	18	20	22	24	26	28

The results show that the proposed 2-SCM always provides the better video qualities (higher PSNR values) for both SS1 and SS10 than those by the legacy scheme. Regardless of a receiver channel with a high or low SNR average, more video data of enhancement quality layer from the SCM signals are always obtainable during the ‘good’ channel condition. This explained the fluctuated increment of video qualities at both SS1 and SS10 from the results in Figure 3-2 (a) and Figure 3-2 (b). The difference of video qualities perceived by SS10 and SS1 is mainly due to the difference of average SNR in their channels. By comparing Figure 3-2 (a) and Figure 3-2 (b), it is

interesting to observe that the perceived video quality difference, in terms of PSNR, becomes larger when the percentage of base quality data in each frame reduces. That implies the video quality improvements brought by SCM or multi-resolution modulated broadcast/multicast signals have some sort of relations with the bitstreams boundaries between quality layers in the encoded video source. The details are indeed investigated and discussed in the next section.

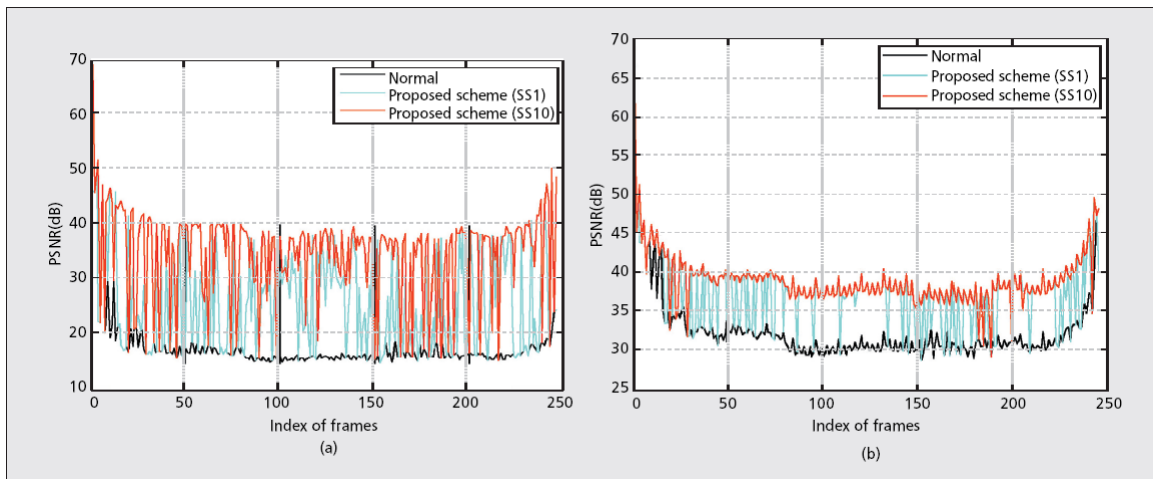


Figure 3-2. Video quality at SS1 and SS10 using legacy scheme (denoted normal) and the proposed scheme with the percentage of base quality data in each video frame as: (a) 40 percent; and (b) 80 percent.

3.1.3 Lessons Learnt

This preliminary cross-layer framework has demonstrated that it is critical to make use SPC or similar channel coding to generate multi-resolution modulated signals for video broadcast/multicast. Such multi-resolution modulated signal embedded with video data of multiple quality levels can enable a much scalable video broadcast/multicast performance at the transmission system, a better

channel utilization of at each receiver, and a higher quality experience for the receiver. These effectively address the multi-user diversity problem in a large-scale wireless video broadcast/multicast. Such a result is impossible when using a monotonic modulation in each broadcast/multicast transmission, even with the existence of a scalable video source. Hence, multi-resolution modulation at the channel and scalable video coding at the source are believed to be the two key factors in a cross-layer framework for scalable and efficient wireless video broadcast/multicast.

However, an undesirable limitation of this preliminary cross-layer design is the video quality fluctuation as shown in Figure 3-2. Since a receiver channel inevitably fluctuates regardless of with a high or low SNR on average, a receiver loses video data (usually in the enhancement layer), whenever the channel condition becomes poor and fail to demodulate the layer 2 in a SCM signal. This problem becomes more seriously pronounced when receivers experiences a frequent short-term fading, which brings the video quality fluctuations more obvious due to the error-propagations in the video decoding process. In addition, such data losses varies from one receiver to another in each broadcast/multicast transmission, a scalable solution for error control without trading off the video quality is the missing puzzle.

3.2 A Proposed Cross-layer Framework of Wireless Coded Video Broadcast/Multicast

In this section, a cross-layer framework of wireless coded video broadcast/multicast is introduced, where a modified MDC on a scalable video source and superposition coding at the channel are considered. Most importantly, the conventional layered MDC is modified and practically integrated with the preliminary framework in the previous section. When superposition coding is employed at

the channel, a MDC packet can be demodulated and received partially by different receivers with various data amount of multiple quality layers. Those partially received MDC packets are proved to be useful for recovering video data from transmission losses, which serve as a scalable error control mechanism across receivers with diverse channel conditions in a wireless video broadcast/multicast. It was originally impossible with the conventional MDC packets designed for a wired infrastructure, where a MDC packet containing video data of multiple quality layers was either completely lost, or successfully received as a whole. There is not any notion in utilizing those partially received MDC packets in the previous literatures with reference to SPC modulation/demodulation.

3.2.1 System Model

An overview of the system model for this proposed framework is illustrated in Figure 3-3 with five major processes: (1) A GoF from a video source is encoded by a scalable video encoder into scalable bitstreams, which generates multiple segments of bitstreams corresponding to multiple quality layers; (2) Before passing the bitstreams to the BS for broadcast/multicast transmissions, each segment is further encoded by a modified MDC for protection, which generates protected units (PUs) for each layer with an extended size; (3) PUs belonging to different quality layers are strategically queued into associated buffers and then modulated by corresponding modulation schemes before being superimposed altogether as a coded wireless video broadcast/multicast signal; (4) According to the channel condition of a receiver, the received signal is demodulated and decoded into a complete/partial MDC packet with various data amount of quality layers; (5) After receiving multiple complete/partial MDC packets, certain bitstreams in some layers of the GoF can be recovered from the losses/errors for the video decoder to reconstruct a better video quality.

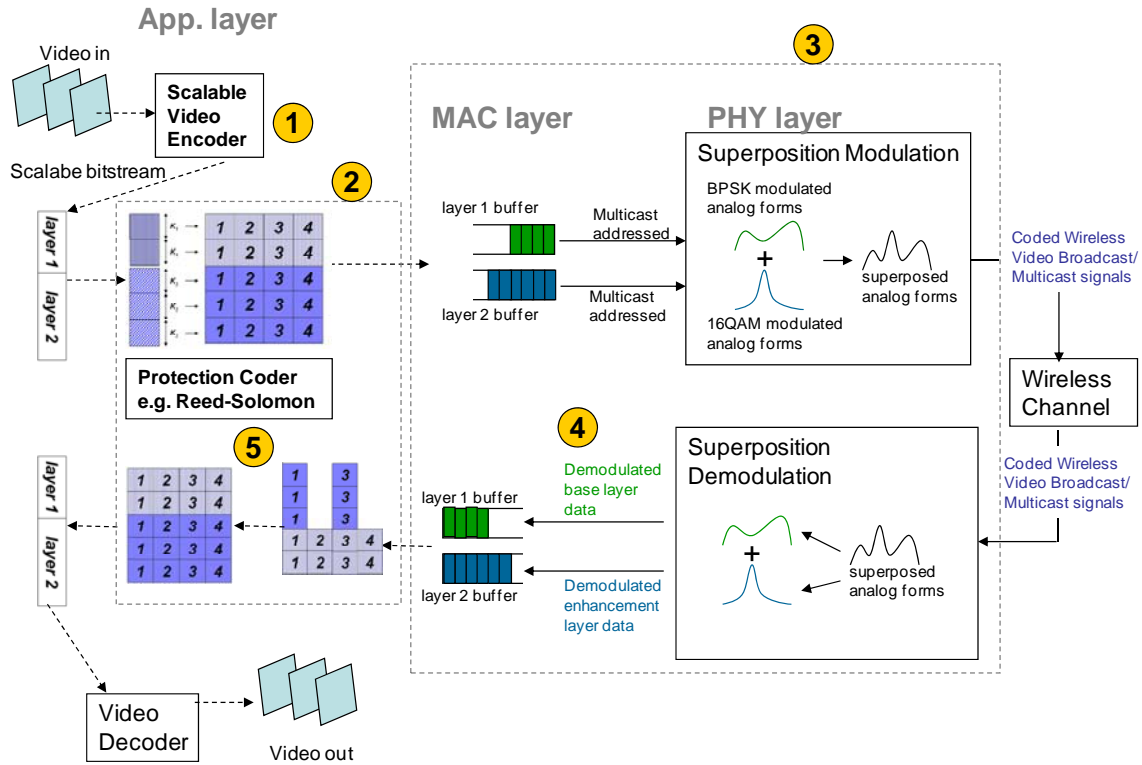


Figure 3-3. An overview of five major processes in the proposed cross-layer framework.

The following sections describe the proposed framework in detail. Since the framework involves the integration and interaction between the source and channel coding, the source coding based on a modified MDC will be presented first. It will be followed by the integration with the SPC channel coding through a series of examples. Finally, the advantages of the framework under multi-user channel diversity with fading are demonstrated.

3.2.2 Modification of Layered Multiple Description Coding

Modified from the conventional layered MDC described in Chapter 2, protection overheads allocated to a higher quality layer should be more than or equal to a lower one (i.e., $N - K_1 \leq N - K_2 \leq \dots \leq N - K_L$) as shown in Figure 3-4. Such decreasing orders of K values

from the lowest layer is motivated by the unique consideration of applying this modified layered MDC on scalable video source over superposition coding at the channel. Each MDC packet containing multiple quality layers will be transmitted through multi-resolution modulation under such special arrangement of protection overheads. The purpose is to make the recovery of a higher layer of video bitstreams relatively easier than the corresponding lower layers in a GoF, because it requires less numbers of partial MDC packets (i.e., lesser timeslots) to collect enough PUs for recovering that layer. When the PUs of a higher quality layer in an MDC packet is successfully demodulated by a receiver with the required SNR, those PUs of the corresponding lower layers of the same MDC packet must be already demodulated due to the intrinsic nature of using SIC demodulation technique. This reveals the fact that receivers in a broadcast/multicast scenario are generally easier to have the required SNRs for demodulating PUs of a lower quality layer than those of a higher quality layer in the same superposition coded MDC packet. By using a smaller K_l value (i.e., more protection) in a higher quality layer l , a set of layered MDC packets can recover the complete bitstreams of that higher quality layer l relatively easier with less MDC packets. This resolves the limitations of the preliminary cross-layer design and the recent previous works in [33], [34], [35], [36] in which receivers never receive/recover lost video data in higher quality layers, and their video quality fluctuates along with their time-varying channel conditions.

In summary, each source block with K_l bytes from the bitstream of quality layer l in a GoF is encoded into a row of PUs with N bytes long using a Reed Soloman (RS) code. A decreasing order of K values from the lowest layer is adopted in the proposed cross-layer framework. The N PUs of each quality layer are then packetized into a MDC packet like the conventional layered MDC. Note that PUs of different quality layers of a MDC packet are modulated by different modulation schemes to form a superposition coded broadcast/multicast signal as described as follows.

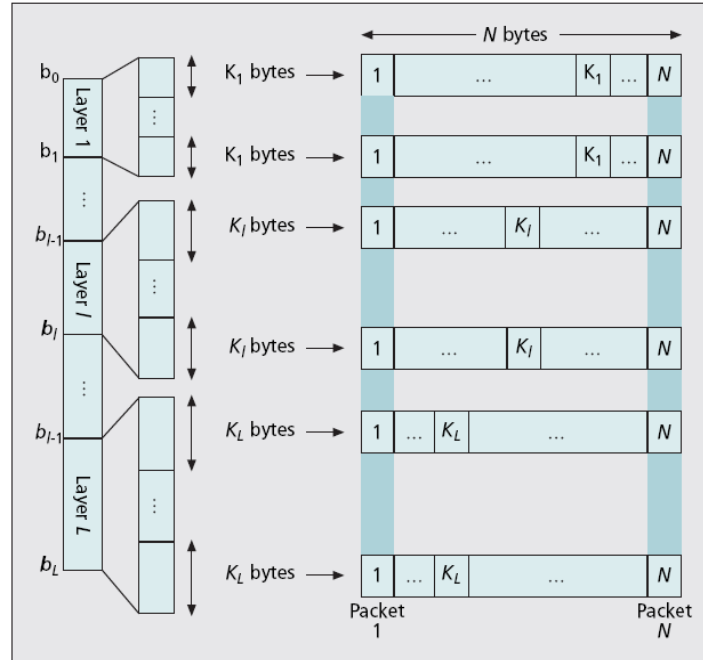


Figure 3-4. Generation of MDC packets based on modified layered MDC with the decreasing ordering of K values from the lower layer to the higher one.

3.2.3 Integration for Wireless Coded Video Broadcast/Multicast

The previous works using multi-resolution modulation alone have the limitation that a receiver never receives/recovers the data of higher quality layers lost during the timeslots under “bad” channel conditions. The proposed cross-layer framework here tackles this limitation by taking the joint advantage of novel protections through the modified layered MDC on a scalable video source and SCM at the channel.

Without the loss of generality, the proposed cross-layer framework is introduced as follows by way of a case study with 2 quality layers in the bitstreams of a GoF. PUs of bitstreams in layers 1 and 2 in Figure 3-5 are generated by the modified layered MDC using RS code with parameters

K_1 , K_2 , and N . PUs from layers 1 and 2 are then queued in buffers B1 and B2, respectively, at the BS with sequences based on the order of their associated MDC packets.

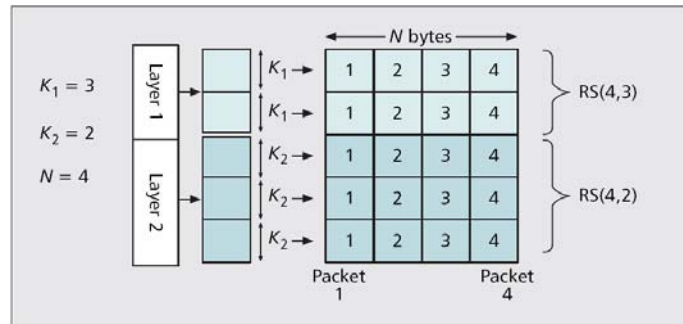


Figure 3-5. PUs of layer l formed by a RS code (N, K_l) .

Starting with the first available timeslot for broadcast/multicast transmission at time $t = 1$, PUs of layer 1 belonging to the 1st MDC packet in buffer B1 are modulated with a lower order of modulation scheme (e.g., BPSK). Within the same timeslot, PUs of layer 2 in buffer B2 belonging to the 1st MDC packet are modulated by a higher order of modulation scheme (e.g., 16QAM). For the same bit error rate (BER), a lower order modulation requires a lower SNR requirement than the higher order one to demodulate the corresponding data from the received signal. Both modulated signals from buffers B1 and B2 are superimposed together as shown in Figure 3-6 to form a coded broadcast/multicast signal for the 1st MDC packet. It is then transmitted by the end of the timeslot $t = 1$.

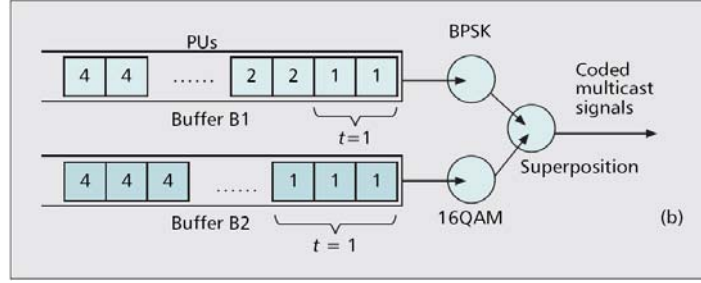


Figure 3-6. PUs of layer 1 and 2 stored in B1 and B2 buffers forming cross-layer superposition coded multicast signals.

Within each timeslot t , the transmission rate of a modulation scheme, $R_{M,l}$, applied on the buffer l must be fast enough to broadcast/multicast all the PUs of layer l in the corresponding MDC packet. Otherwise, either the duration of a timeslot, the K values, the size of bitstream segment of a quality layer, or the size of a PU (i.e., 1 byte each is assumed here) should be adjusted. This is a necessary condition for the BS to achieve the long-term stability, which is formulated into the following constraint for selecting a modulation scheme in each layer:

$$R_{M,l} \geq \frac{(b_l - b_{l-1})}{K_l} \times \frac{1}{t}, \quad (3.1)$$

where $R_{M,l}$ is the transmission rate (bit/second) of a modulation scheme from the set {BPSK, QPSK, 16QAM, 64QAM}, b_l is the bit position of the video bitstreams up to quality layer l , K_l is the value of the RS (N, K_l) code used in layer l , and t is the duration of a timeslot for each broadcast/multicast transmission assigned by a scheduling policy. The cross-layer framework repeats the same processes of protection and superposition modulations for the next set of PUs in all buffers for the 2nd MDC packet at the next available transmission timeslot (i.e., time $t = 2$) and so on. After PUs of all MDC packets in a GoF are superimposed and broadcasted/multicast, the

same processes continue with the next GoF as shown in Figure 3-7 until the end of the video stream.

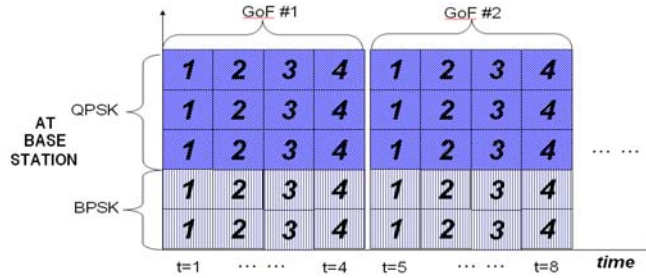


Figure 3-7. BS transmits all PUs of all quality layers of video bitstreams with superposition coded multicast.

Considering a BS transmits video bitstreams through this manner with an optimal scheduling policy for required transmission resources in a BWA network, different fixed/mobile subscriber stations (SSs) as the broadcast/multicast receivers may completely or partially demodulate the same coded wireless video signal according to the SNRs of their channel conditions. Each SS receives various amounts of PUs of some quality layers. For example, SS-1 in Figure 3-8(a) receives PUs of layer 2 from only the two timeslots at time $t = 1$ and $t = 3$, SS-2 receives PUs of layer 2 from the first two timeslots in Figure 3-9(a), whereas SS-3 in Figure 3-10(a) has lost the entire MDC packet at timeslot $t = 3$ due to deep fading.

Since the amount of data losses at each SS is tolerable by the protections in all quality layers, all SSs eventually recover their differently lost PUs in both layers. A complete set of bitstreams is obtained in each SS for the full video quality as shown in Figure 3-8 (b) and Figure 3-9 (b). Due to the use of RS(4, 2) code in layer 2, the recovery of lost PUs in each row of layer 2 among all SSs can succeed as long as the SS can successfully demodulate at least K_2 PUs (where $K_2 = 2$) from any

2 out of 4 timeslots. Even with the worst scenario at SS-3 in Figure 3-10 (a), where the entire MDC packet is lost at timeslot $t=3$, the complete set of video bitstreams in 2 quality layers is still recoverable like other SSs as shown in Figure 3-10 (b). In the following paragraphs, the performance of demodulating a layer l in a GoF by a receiver, SS- m , is evaluated in terms of the number of received/recovered bitstreams of layer l with respect to the average bit error rate (BER) in that layer. (Note: Collectively, Figure 3-8, Figure 3-9 and Figure 3-10 demonstrate that a complete set of video quality of a GoF is fully recovered at each SS with fading under the multi-user channel diversity.)

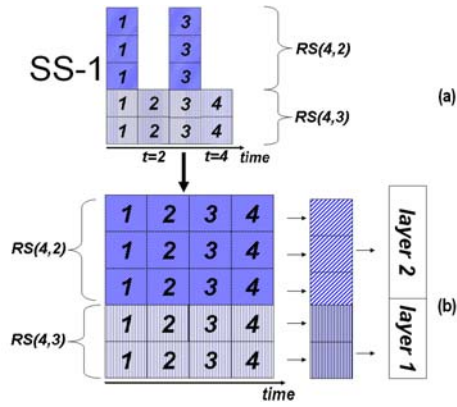


Figure 3-8. Enhancement video data loss at time $t = 2$ and $t = 4$.

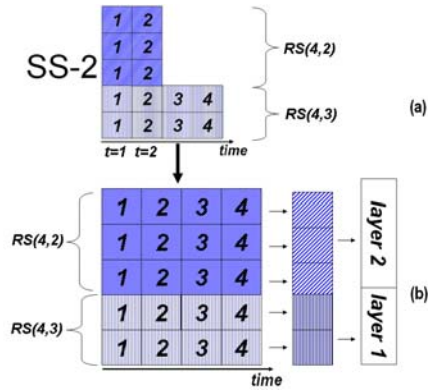


Figure 3-9. Enhancement video data loss at time $t = 3$ and $t = 4$.

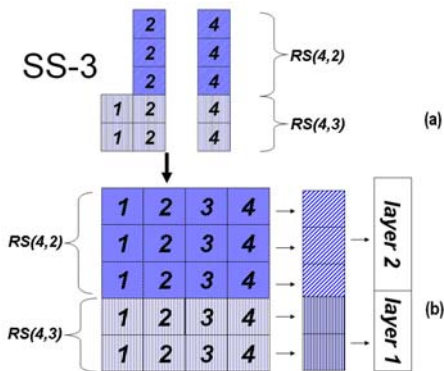


Figure 3-10. Both base and enhancement data loss at time $t=3$.

The SNR, $\gamma_{l,m}$, at SS- m is determined by the power p_l allocated by the BS to modulate the data of quality layer l , the distance, d_m , of SS- m from the BS, the path loss exponent α ($\alpha = 4$ for an urban area, or 3 for a rural area), and some other factors. Their relationship is shown as follows:

$$\gamma_{l,m} = \frac{c d_m^{-\alpha} p_l |h_m^2|}{N_0 W + \sum_{i=l+1}^L c d_m^{-\alpha} p_i |h_m^2|} \quad (3.2)$$

where c is a constant; $|h_m^2|$ is a random number with a Rayleigh fading distribution; W is the effective bandwidth seen by the SS; and N_0 is the average background noise power. In Eq. (3.2), the reason for having the second term in the denominator is due to the superimposing of modulated signals of other layers, where the demodulation of layer l treats all powers of higher layers as noise. To demodulate layer l , the SS demodulates the required signal by subtracting all the demodulated signals of layer 1 to $l-1$ from the received SCM signal.

Since the BS has selected the order of a modulation scheme, $R_{M,l}$ for layer l , a successful demodulation by SS- m using the same scheme, $R_{M,l,m}$, for the specific transmission rate can only happen, if its associated SNR, $\gamma_{l,m}$, of layer l at SS- m fulfills the required SNR lower bounds below:

$$R_{M,l,m}(\gamma_{l,m}) = \begin{cases} 64\text{QAM}, & \text{if } 18.5\text{dB} \leq \gamma_{l,m}, & \text{if } R_{M,l} = 64\text{QAM} \\ 16\text{QAM}, & \text{if } 11.5\text{dB} \leq \gamma_{l,m}, & \text{if } R_{M,l} = 16\text{QAM} \\ \text{QPSK}, & \text{if } 6\text{dB} \leq \gamma_{l,m}, & \text{if } R_{M,l} = \text{QPSK} \\ \text{BPSK}, & \text{if } 3\text{dB} \leq \gamma_{l,m}, & \text{if } R_{M,l} = \text{BPSK} \\ \text{fail}, & \text{otherwise} \end{cases} \quad (3.3)$$

These lower bounds are based on the WiMAX standards [1], whereas they can be extended with any new modulation scheme from future standards/systems. It is critical to fulfill the required SNR lower bound for a successful demodulation of layer l ; otherwise, the data fails to be decoded.

The expected BER, denoted as, $e_{l,m}$, for demodulating layer l using $R_{M,l,m}$ at SS- m is also affected by its SNR, $\gamma_{l,m}$, of the associated channel, which can be approximated by Eq. (3.4) according to the modulation scheme. These approximations of BERs are commonly assumed and provided in the literatures such as [21], [22]. They are employed here to derive the forthcoming formulations of the proposed framework, whereas they give the required accuracy and simplicity for practical computation in simulations and possible implementations. However, the following formulations and the proposed framework are still applicable when any of these BER approximations of a new or an existing modulation scheme is changed.

$$e_{l,m}(R_{M,l,m}, \gamma_{l,m}) = \begin{cases} Q(\sqrt{2\gamma_{l,m}}), & \text{if } R_{M,l,m} = \text{BPSK} \\ Q(\sqrt{\gamma_{l,m}}), & \text{if } R_{M,l,m} = \text{QPSK} \\ \frac{1}{4} \left[Q\left(\sqrt{\frac{\gamma_{l,m}}{5}}\right) + 3Q\left(\sqrt{\frac{\gamma_{l,m}}{5}}\right) + \frac{1}{2}Q\left(\sqrt{\frac{\gamma_{l,m}}{5}}\right) \right], & \text{if } R_{M,l,m} = 16\text{QAM} \\ \frac{1}{12} \left[Q\left(\sqrt{\frac{\gamma_{l,m}}{21}}\right) + Q\left(3\sqrt{\frac{\gamma_{l,m}}{21}}\right) + Q\left(5\sqrt{\frac{\gamma_{l,m}}{21}}\right) \right. \\ \left. + Q\left(7\sqrt{\frac{\gamma_{l,m}}{21}}\right) \right] \\ + \frac{1}{6}Q\left(\sqrt{\frac{\gamma_{l,m}}{21}}\right) + \frac{1}{6}Q\left(3\sqrt{\frac{\gamma_{l,m}}{21}}\right) + \frac{1}{12}Q\left(5\sqrt{\frac{\gamma_{l,m}}{21}}\right) \\ + \frac{1}{12}Q\left(7\sqrt{\frac{\gamma_{l,m}}{21}}\right) + \frac{1}{3}Q\left(\sqrt{\frac{\gamma_{l,m}}{21}}\right) + \frac{1}{4}Q\left(3\sqrt{\frac{\gamma_{l,m}}{21}}\right) \\ - \frac{1}{4}Q\left(5\sqrt{\frac{\gamma_{l,m}}{21}}\right) - \frac{1}{6}Q\left(7\sqrt{\frac{\gamma_{l,m}}{21}}\right) + \frac{1}{6}Q\left(9\sqrt{\frac{\gamma_{l,m}}{21}}\right) \\ \left. + \frac{1}{12}Q\left(11\sqrt{\frac{\gamma_{l,m}}{21}}\right) - \frac{1}{12}Q\left(13\sqrt{\frac{\gamma_{l,m}}{21}}\right) \right], & \text{if } R_{M,l,m} = 64\text{QAM} \end{cases}, \quad (3.4)$$

where $Q(\cdot)$ is a Q function.

Given $e_{l,m}$ and $(b_l - b_{l-1})$, an average loss probability, $\varepsilon_{l,m}$, that the whole column of PUs of layer l in a partial MDC packet becoming lost/erroneous at SS- m , can be derived as:

$$\varepsilon_{l,m} = 1 - (1 - e_{l,m})^{b_l - b_{l-1} / K_l} \quad (3.5)$$

Note that $(b_l - b_{l-1}) / K_l$ gives the number of rows of the PUs in layer l of in a partial MDC packet.

In the proposed framework, the erasure recovery of a quality layer at a receiver is strictly a function of the number of partial MDC packets (i.e., the number of columns of PUs) that are received for that layer in a GoF, rather than which of those packets (or columns of PUs) are received. Therefore, any row of N PUs long in layer l is recoverable at SS- m when at least K_l PUs of a row of layer l are successfully received. Let F_l denote a random variable that represents the number of packet erasures in a group of N partial MDC packets of layer l . Then, the probability of getting $N - K_l$ or fewer erasures in N partial MDC packets of layer l at SS m for a GoF can be approximated as:

$$P_{l,m} = \Pr\{F_l \leq N - K_l\} = \sum_j^{N - K_l} \binom{N}{j} (\varepsilon_{l,m})^j (1 - \varepsilon_{l,m})^{N - j} \quad (3.6)$$

By considering that the bitstreams of layer l is only useful if layer $l - 1$ is completely received/recovered, the average number of receivable/recoverable bitstreams of layer l in a GoF obtained by SS- m , denoted as $T_{l,m}$, can be calculated as the following:

$$T_{l,m} = (b_l - b_{l-1}) \prod_{i=1}^l P_{i,m} \quad (3.7)$$

Note that all involved loss events are assumed to be independent based on the fact that the bit errors distributed independently due to the interleaving of data transmissions between multiple services stream at the BS across continuous timeslots. Therefore, the total average number of

receivable/recoverable video bitstreams, T_m , (in bits) of a GoF with L layers by SS- m , can be expressed as:

$$T_m = \sum_{l=1}^L T_{l,m} \quad (3.8)$$

Since there is a direct relationship between the distortion and bitstream boundaries in a GoF as shown in Figure 2-2 in Chapter 2, the value of T_m can be regarded as a video quality measurement of a GoF at SS- m for the purpose of analysis and system optimization. When T_m of a GoF at SS- m is increased, a smaller distortion (i.e., a better video quality) of the GoF is perceived by SS- m . According to different application scenarios, a particular policy can be created to optimize T_m by selecting proper power allocations, modulation schemes or even the values of N and K in the RS codes for different layers, as well as other operational requirements.

3.3 Performance Evaluation

The problem formulation for maximizing Eq. (3.8) is obviously discrete and nonlinear, which is subject to a serious scalability problem when an optimal solution is desired. Hence, a heuristic optimization methodology is introduced in this section for solving the developed formulation. The basic idea of the proposed methodology entails two distinct aspects: (1) Instead of defining the parameters K and N in the optimization, they are defined through a policy-based operational condition. (2) The target of the optimization is to optimize the performance of the worst-channel receiver, which is also expected to improve the overall performance of the video broadcasting/multicasting.

3.3.1 Selection of N and K_l

The selection of K value for each layer strongly affects the perceived video quality and consumed redundancy. Given the size of bitstreams segment of layer l (i.e., $b_l - b_{l-1}$), the total number of PUs in layer l , denoted as J_l , that will be transmitted sequentially within each transmission timeslot t , can be expressed as, $J_l = (b_l - b_{l-1}) / 8K_l$, where each PU is assumed to be one byte. With Eq. (3.1), $t \geq 8J_l / R_{M,l}$ for $1 \leq l \leq L$ is obtained, where $R_{M,l}$ is the transmission rate (in bits/second) of the modulation scheme selected by the BS for layer l . For the best transmission efficiency, let $t = 8J_l / R_{M,l}$ for $1 \leq l \leq L$. It is also known that $R_{M,l} \leq R_{M,l+1}$ for $1 \leq l \leq L-1$ due to the use of SCM signals for allowing receivers with diverse channel conditions to decode various amount of information from the same broadcast/multicast signal. A lemma is therefore derived as follows to show that $K_1 \geq K_1 \geq \dots \geq K_L$ is a necessary condition in the proposed CLD framework.

Lemma 3.1: Given the relation of

$$\frac{(b_1 - b_0)}{R_{M,1}} \geq \frac{b_2 - b_1}{R_{M,2}} \geq \dots \geq \frac{b_L - b_{L-1}}{R_{M,L}},$$

$K_1 \geq K_1 \geq \dots \geq K_L$ is a necessary condition to enable the interplay of SPCM and modified MDC in the proposed cross-layer framework.

Proof:

Given

$$t = \frac{J_1}{R_{M,1}} = \frac{J_2}{R_{M,2}} = \dots = \frac{J_L}{R_{M,L}},$$

or, equivalently,

$$t = \frac{(b_1 - b_0)}{K_1 \times R_{M,1}} = \frac{(b_2 - b_1)}{K_2 \times R_{M,2}} = \dots = \frac{(b_L - b_{L-1})}{K_L \times R_{M,L}}.$$

$$\text{Since } \frac{(b_1 - b_0)}{R_{M,1}} \geq \frac{b_2 - b_1}{R_{M,2}} \geq \dots \geq \frac{b_L - b_{L-1}}{R_{M,L}},$$

$K_1 \geq K_2 \geq \dots \geq K_L$ must hold. ■

Note that the condition $\frac{(b_1 - b_0)}{R_{M,1}} \geq \frac{b_2 - b_1}{R_{M,2}} \geq \dots \geq \frac{b_L - b_{L-1}}{R_{M,L}}$ is common in a practical system scenario (such as WiMAX), since $R_{M,l+1}$ could be much larger than $R_{M,l}$, while $b_{l+1} - b_l$ can be reasonably configured at the video encoding process to be similarly or mildly larger than $b_l - b_{l-1}$ in a GoF. For example, in the case of using BPSK and 16QAM in a 2-layer SCM signal, $R_{M,2} = 8R_{M,1}$ is obtained. However, $b_{l+1} - b_l$ is not likely to be several times larger than $b_l - b_{l-1}$.

Given the pre-assigned K value of each quality layer, the corresponding uniform N value can be easily found in general due to the coding relationship of a RS code. Hence, the whole optimization problem is narrowed down to focus on the performance optimization for the worst-channel receiver. The performance here is evaluated in term of throughput and optimized over a time window long enough (e.g., a few seconds) for real-time computation. Denoting the worst-channel receiver as SS- j and its instantaneous throughput as T_j at a specific time window, optimizing T_j with respect to the fading factors will also improve the instantaneous throughput of the another receiver, SS- m , denoted as T_m and $m \neq j$. This arrangement is reasonable, since each SPCM signal is broadcasted/multicast and shared by a group of receivers simultaneously.

3.3.2 A Case Study for Optimization

For a practical case study, a video bitstream with two quality layers is assumed to be broadcasted/multicast through a WiMAX BS to a set of SSs with the average SNRs listed in Table 3-1. The channel condition of each SS is subject to a short-term Rayleigh fading, and is

evaluated according to the individual channel side-information (CSI) feedback over a time window denoted as ω . With the given N , K_1 and K_2 according to *Lemma 3.1*, T_m can be determined by a set of operating parameters, including the power and modulation scheme assigned to each quality layer, which in turn determines the resultant video quality experienced at SS- m .

Let SS- j^* be the receiver subject to the worst channel condition during the time window ω . Since the SPCM signal is shared and receivable by all SSs, an optimal set of power p_l and modulation rate $R_{m,l}$ is selected to improve the video quality of a GoF at SS- j^* . Hence, the objective is to maximize the number of total receivable/recoverable video bitstreams, T_{j^*} , of a GoF,

$$\text{i.e., max } T_{j^*} = \sum_{l=1}^L T_{l,j^*} \quad (3.9)$$

Adopting such an optimization objective is based on the assumption that any SS- m where $m \neq j^*$, will receive more video bitstreams than that by SS- j^* under a diverse and fading channel during the time window ω , thereby leading to a better video quality. The total receivable/recoverable bitstreams is emphasized, because the overall video distortion of a GoF monotonically decreases when the total received video bitstreams increases as discussed in Figure 2-2 of Chapter 2. In addition to the constraints defined in Eqs. (3.1) – (3.7) and *Lemma 3.1*, the optimization over all possible values of p_l and $R_{M,l}$ for both quality layers is subject to the following constraint:

$$\sum_{l=1}^L p_l \leq p_{total} \quad (3.10)$$

Obviously, $L = 2$ are in the constraints above, since there are only two quality layers of video data in our case study.

The objective function resulted from the analytical formulations above is non-linear and discrete. The optimal operating point $(p_l, R_{M,l})$ of each superposition coded broadcast/multicast transmission for a GoF cannot be solved by any commercially available integer program solver. However, the source coding parameters N and K can be eliminated from the optimization problem by using *Lemma 3.1*. The space of the total operating points of the proposed framework is reduced to a much smaller number of limited combinations. The optimization problem can therefore be efficiently handled by a less complicated but practical algorithm, such as an iterative search approach. The search space is formed by a limited combination of modulation schemes as well as a set of discrete ratio of power allocation pairs defined as (p_2 / p_{total}) and constrained by the total power. The associated SNRs, supportable pairs of modulation schemes, the resultant layer error rate (i.e., the probability that a quality layer is unrecoverable), as well as the total amount of received/recovered bitstreams, T_{j^*} , of an optimized broadcast/multicast transmission is evaluated under all possible ratios of power allocation pair (Note: Each ratio value is different from the previously evaluated one by 0.1. It is considered to be reasonably small enough to locate an optimal or near-optimal power allocation pair that gives the noticeable performance difference in practical operations). The searched results are illustrated in Figure 3-11(a) to (d), in which the optimal power allocation ratio is identified as (3.1:6.9) and the optimal pair of modulation schemes are QPSK and 16QAM for quality layer 1 and 2, respectively. Note that the contribution of this 2-fold heuristic optimization methodology allows the optimization problem to be efficiently solved and practically implemented in an actual WiMAX BS.

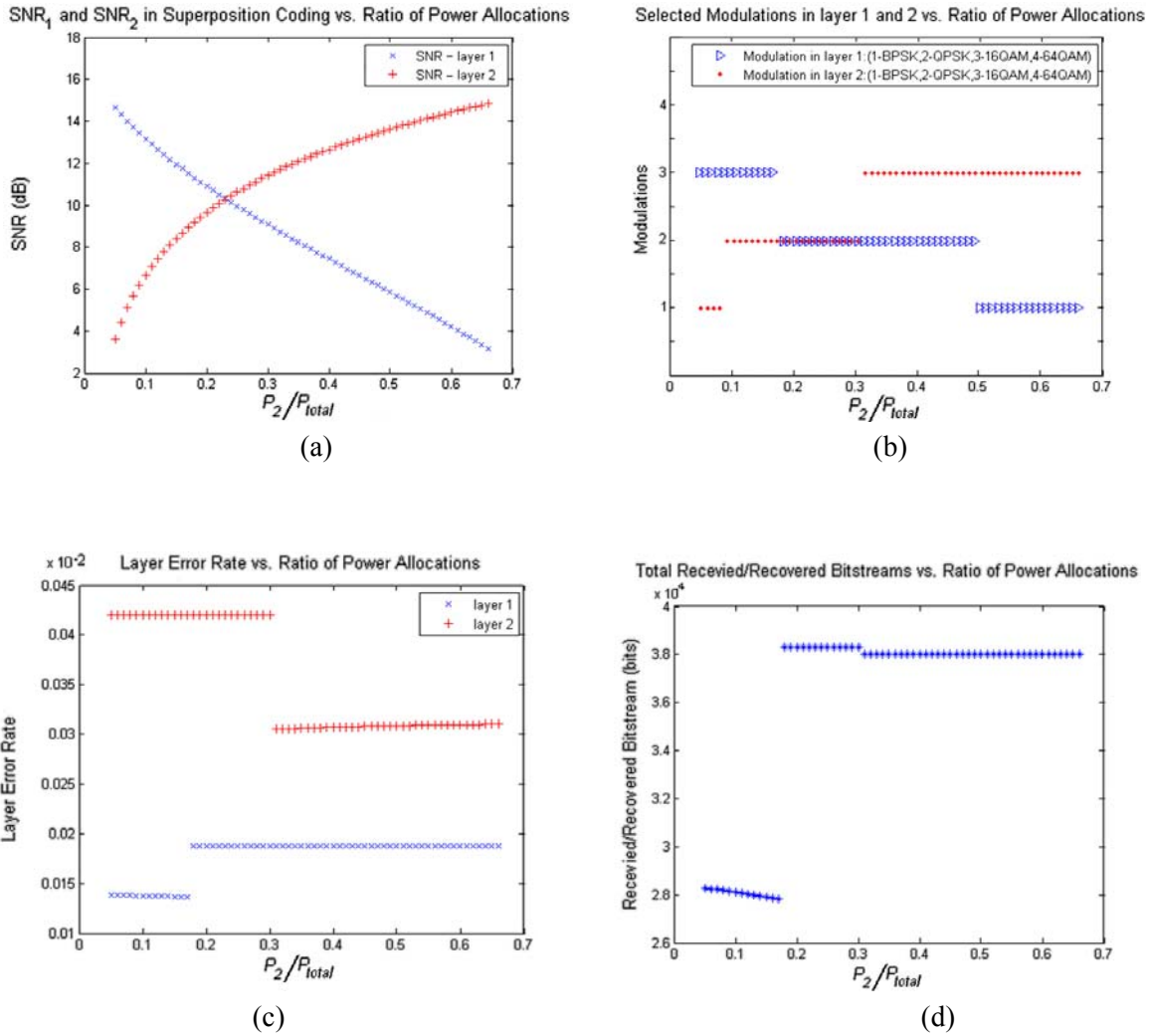


Figure 3-11. Illustrations of (a) SNRs, (b) layer error rates, (c) modulation schemes, and (d) total received/recovered bitstreams with respect to different power allocation.

3.4 Simulation Results

Comprehensive simulations with standard video sequences are conducted for evaluating the actual video quality perceived by a receiver. The transmissions using the proposed framework at a BS is simulated with optimized power allocations and modulation schemes obtained from the case study in Section 3.3.2. The goal is to compare the proposed framework with a broadcast/multicast

scheme simply using multi-resolution modulation alone such as in [32], [33], [34], [35], [36] under the multi-user channel diversity with a fading effect. The video sequences are encoded into bitstreams with 2 quality layers (i.e., $L = 2$), in which each GoF has 16 frames with the bitstreams boundaries of layer 1 and 2 at $b_1=1987712$ and $b_2 = 3266560$, respectively. Applying *Lemma 3.1* on these video settings, $N = 255$, $K_1=233$ and $K_2=192$ are obtained in the case study. Rayleigh distribution is adopted to simulate the channel fading from one WiMAX transmission frame after the other. The channel state of an SS is unchanged during the period of a transmission frame. The average SNRs of all SSs and other simulation parameters are the same as those in Table 3-1. Both systems under simulations were compared in terms of frame-by-frame video quality. The perceived video qualities in both systems are measured in peak signal-to-noise ratio (PSNR) at SS-10 and SS-1, which correspond to receivers with the best- and worst-channel condition on average, respectively. In the comparison, if the SNR of an SS is “good” enough, it demodulates data from both quality layers; otherwise, only data from quality layer 1 is demodulated when the channel is “bad”.

Through visual justifications, two sets of video sequences with very different natures of content are evaluated for demonstrating the effectiveness of the proposed framework. The first video sequence – “Foreman” is mainly the face of a person with limited movements in a simple and static video background, whereas the other one – “Paris” contains two persons with frequent movements along with other moving objects in a more complicated video background. When compared to a system simply using multi-resolution modulation such as SCM, the proposed framework generally gives a better video quality (i.e., higher PSNR values) in the video sequences of “Foreman” for both SS-1 and SS-10 as shown in Figure 3-12 due to the recovery of data lost in “bad” channels. The difference of the perceived video quality between SS-10 and SS-1 is mainly due to the difference of their average SNRs, which however, is significantly reduced under the proposed

framework. This is another benefit due to the recovery of data by way of the joint source-channel coding technique in the proposed framework. Similarly, distinguishable benefits were also concluded and observed in Figure 3-13 for the video sequence of “Pairs”, which has more movements and objects with a complicated background. In Figure 3-14 (a)-(d), the video quality perceived by SS-1 and SS-10 at the 105-th frame were sampled for a visual justification. Although it is very subjective to individuals by using the visual justification, the sampled snapshots are more or less still illustrating the concluded benefits above for the proposed framework. Such benefits are especially obvious when a receiver has a poor average channel condition like SS-10. Interestingly, SS-10 under the proposed framework seems to have a comparable visual quality to that of SS-1 which has a much stronger average channel but simply under multi-resolution modulation alone. Circles in Figure 3-14 (b) and (c) locate the similar scale of their distortions. (Note that there is no specific reason in picking the 105-th frame, whereas there are other frames supporting the same conclusions.)

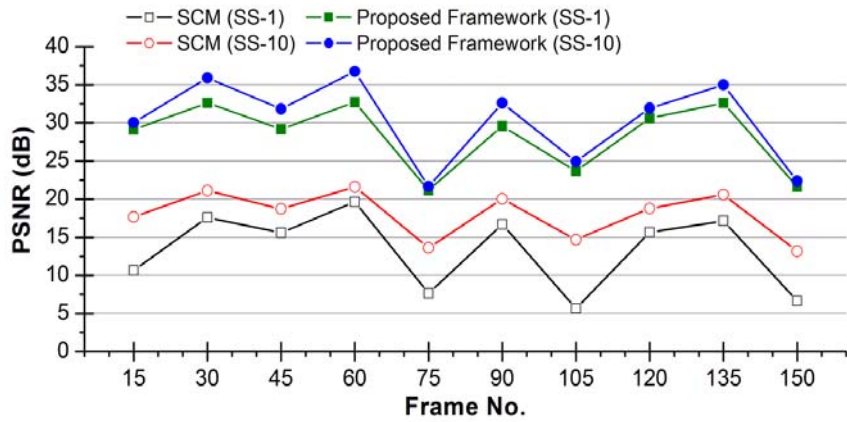


Figure 3-12. PSNR of Foreman between the proposed framework and the SCM.

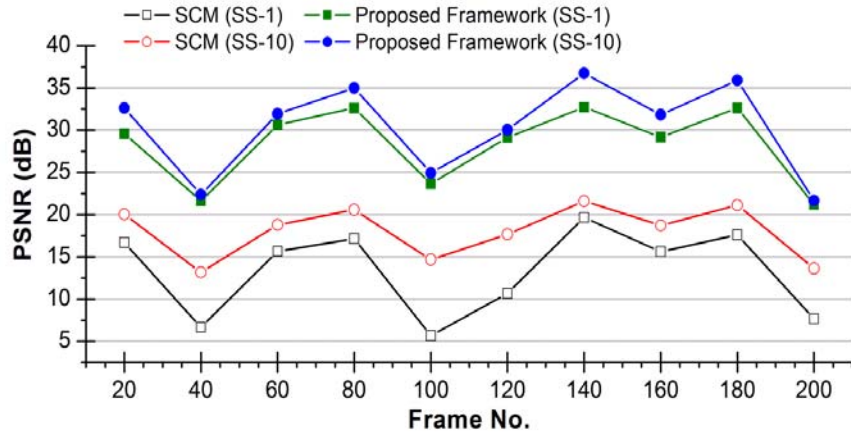


Figure 3-13. PSNR of Paris between the proposed framework and the SCM.



(a) SS-10 under the proposed framework



(b) SS-10 under multi-resolution modulation (such as SCM)



(c) SS-1 under the proposed framework



(d) SS-1 under SCM

Figure 3-14. Better video qualities at receivers brought by the proposed framework regardless of their average channel conditions.

3.5 Summary

In this chapter, a novel cross-layer framework of coded wireless video broadcast/multicast was introduced, where a joint design on source and channel coding techniques was investigated. Specifically, the proposed framework is characterized by a suite of manipulative mechanisms of

interplay between a novel modified MDC technique on scalable video source and a superposition coding technique at the channel. It is demonstrated that the proposed framework can effectively mitigate the impairments of video quality due to the short-fading effects and multi-user channel diversity. The framework was formulated as a nonlinear discrete optimization problem involving a number of key operational parameters, including the source coding parameters N and K , as well as power allocation and modulation scheme for each quality layer. A heuristic 2-fold methodology was developed for solving the optimization problem by determining the source and channel coding parameters in each quality layer separately. Comprehensive simulations were conducted based on real standard video sequences using the optimized parameters, which have demonstrated the effectiveness of the proposed framework to achieve a better video quality at the receivers. It is concluded that the proposed framework not only contributes to current WiMAX flavors, but also promises to serve as an important component for robust video broadcast/multicast in any other next-generation BWA networks.

Chapter 4

Information-theoretical Analysis under Gaussian Broadcast Channels

It is clear that the layered MDC based on RS codes on scalable video codes is a special type of MDC from an information theoretic perspective. Even though there is a relatively rich literature on MDC ([16][17][18]), an information-theoretic characterization of MDC (i.e., the achievable region of MDC) is still unknown even for general memoryless sources, let alone the characterization for general stationary or non-stationary sources and algorithms for designing optimal MDC. A general information-theoretical analysis on the end-to-end distortion for the proposed cross-layer framework of a successive refinable source with Gaussian distribution over Gaussian broadcast channel will be determined in this chapter. Hence, a fundamental problem here is to investigate whether the use of an erasure coding like MDC or any generic (n, k_l) protection code on successive refinable data coupled with SPC broadcast signals can lead to a new optimization framework for wireless data broadcast/multicast that generalizes the previously reported schemes. With such an optimization framework, the next interesting problem is when and under what conditions an

improved overall quality can always be obtained. These form the motivation of this chapter to answer these questions while solving related problems.

4.1 System Model and Notations

It is assumed that each information unit from the original data source is encoded by a scalable codec into a source symbol with multiple successive refinable layers, with each being a codeword corresponding to specific quality of information. Before the BS launches the source symbols for broadcast transmissions, the codeword of each layer is further encoded by a protection code into a set of protection symbols. The set of protection symbols in each layer is then modulated individually, and the modulated symbols of all layers are superimposed altogether as a single layered broadcast channel symbol for wireless transmission. Since the framework involves interactions between both the source and channel coding schemes, a cross-layer architecture is presented below to illustrate the advantages in dealing with multi-user channel diversity and transmission losses under the fading effect.

4.1.1 Protected Successive Refinement and Layered Broadcast

As shown in Figure 4-1, a memoryless source is assumed to generate each source symbol independently and identically according to a zero-mean unit variance real-valued Gaussian distribution. Each source symbol, S , has L successive refinable layers, and layer l refines the information of a lower layer $l-1$. A source symbol is then encoded into n protected symbols (i.e., V_1, \dots, V_n) for higher robustness, in which layer l in a source symbol is protected by a (n, k_l) code as shown in Figure 1. A smaller k_l provides a better protection for the information of layer l in the

source symbol against any loss/error out of n protection symbols. Hence, each protected symbol, V_i , also has L layers, and is transmitted over a layered broadcast channel.

Letting π_l denote the transmitted power allocated to layer l , the channel symbol x can be expressed as:

$$x = \sqrt{\pi_1}x_1 + \dots + \sqrt{\pi_L}x_L, \quad (4.1)$$

where x_1, \dots, x_L are independent and identical Gaussian random variables referring to the individual channel symbol of layer 1, \dots, L , and π_l is the power allocation to layer l under a total power constraint π , where $\pi = \pi_1 + \dots + \pi_L$. The transmitted channel symbol, x , contains symbols of L resolutions, which is broadcasted to a group of receivers.

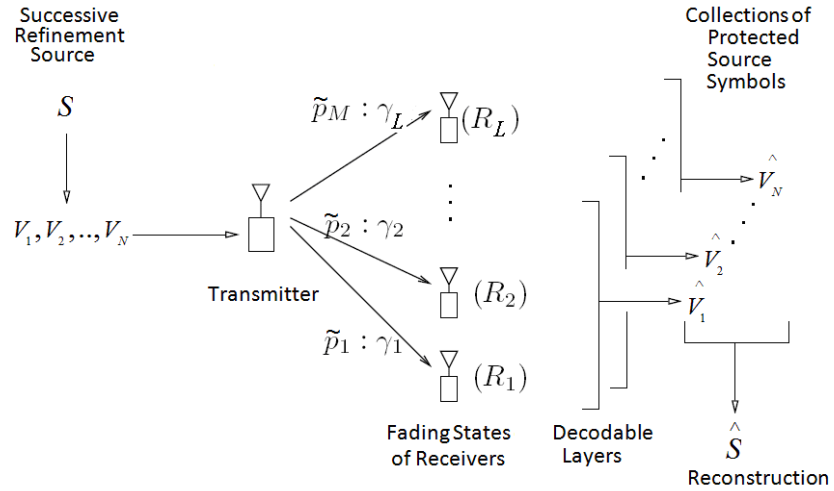


Figure 4-1. A generic cross-layer architecture of protected successive refinement over layered broadcast channels.

4.1.2 Channel Demodulation and Source Reconstruction

With a single antenna at the transmitter and each receiver, the wireless channel is described by:

$$y = Hx + z, \quad (4.2)$$

where y is the received signal, H is the channel gain under fading, x is the transmitted signal, and z is a unit variance noise. A probability mass function (PMF) of a fading distribution in a broadcast network with L discrete states [34] is assumed, such that a receiver has L possible channel power gains in an increasing order $\gamma_L > \dots > \gamma_l > \dots > \gamma_1 \geq 0$, where $\gamma_l = |h_l|^2$. h_l is a realization of H with probability \tilde{p}_l for $l = 1, \dots, L$. The values of \tilde{p}_l are obtained by splitting the probability density function (PDF) of a channel gain distribution into a number of even discrete portions that are equal to the possible number of fading states to decode the layered broadcast signal with the corresponding h_l . The possible values of channel gain h_j in a distribution are collected over two possible scenarios: 1) from a group of receivers within the same wireless video multicast/broadcast network; 2) from a wireless receiver over a long-term period. In other words, a channel symbol y is demodulated by a receiver to reconstruct a protected symbol, \hat{V}_i , either completely with L layers or partially up to layer l . Note that the number of fading states is assumed to be the same as the number of successive layers in a source/protected symbol for simplicity, even though the results in this work are indeed not limited to this assumption.

Depending on the channel conditions in collecting n channel symbols, a receiver in Figure 1 obtains n protected symbols, \hat{V}_i , where $i=1, \dots, n$, and each may have a different number of layers. The original information of layer l in the source symbol, S , can be recovered/reconstructed from any loss/error when at least k_l symbols of that layer are obtained from the n protected symbols. A

complete successive layer l can refine the lower successive layer $l-1$, which is similarly recovered/reconstructed from k_{l-1} symbols of that layer from the same N protected symbols.

According to the number of recovered/reconstructed successively layers, a final information, \hat{S}_i , can be reconstructed up to successive layer l , where $l=1, \dots, L$.

4.2 Distortion Analysis

The end-to-end distortion of the proposed system is derived, and is used to determine the scenario for such a system to yield better end-to-end distortion performance over other possibilities. This section outlines the approach in analyzing the end-to-end distortion over a general Gaussian broadcast channel under the described system model. The analysis starts with a nice closed-form formula for the average end-to-end distortion, denoted by \bar{D}_0 , in a non-layered source-channel coding system derived in [38]:

$$\begin{aligned} \bar{D}_0 &= \left(1 - \frac{Mp_{err}}{M-1}\right) D_Q + \frac{Mp_{err}}{M-1} \sigma^2 + \frac{Mp_{err}}{M-1} S_Q \\ &\approx (1 - p_{err}) D_Q + p_{err} \sigma^2 + p_{err} S_Q \end{aligned} \quad (4.3)$$

where D_Q is the conventional quantization distortion of the source code used, M is the number of codewords in the source code, σ^2 is the source variance, p_{err} is the average channel symbol error rate, and S_Q is the scatter factor of the source code. The approximation in Eq. (4.3) is accurate when M is relatively large, which is the case in high rates of source coding. The above formula was established under the assumption that quantized source symbols (or vectors) are randomly mapped into channel symbols in a one-to-one manner, and was shown in [39] to provide a good end-to-end

distortion approximation for any deterministic mapping from quantized source symbols to channel symbols when the underlying channel is very noisy. In this work, each source symbol is a super-symbol resulting n protected source symbols, which will be mapped to n channel symbols.

Studies on quantization design using the channel information based on Eq. (4.3) show that for optimal quantizers that minimize the end-to-end distortion in Eq. (4.3), the scatter factor, S_Q is significantly smaller than the source variance [39]. A small S_Q can be achieved by simply assigning a large proportion of the source codewords to the source mean. An interesting fact is found that if the receiver can somehow be aware of the transmission error whenever the channel output symbol is erroneous, it can actually improve \bar{D}_0 by simply declaring the loss of the channel symbol and estimating the source symbol using the source mean rather than using the wrong channel symbol. In this case, the distortion \bar{D}_0 is reduced to

$$\bar{D}_0 \approx D_Q(1 - p_{err}) + \sigma^2 p_{err} \quad (4.4)$$

In this work, each source symbol is a super-symbol consisting of n protected source symbols, which are mapped to n channel symbols for layered broadcast transmissions. The right side of Eq. (4.4) may be regarded as the distortion for a system where the receiver detects a source symbol loss due to any loss of n channel symbols. A simple yet intelligent detection scheme, such as the cyclic redundancy check, can be adopted in the system to allow the receiver to declare a source symbol loss whenever an error/loss of channel symbol occurs. This chapter analyzes the impacts to the distortion after applying protection on the successive refinable source symbols over layered broadcast channels.

Given a Gaussian source described at a rate of nR bits per source symbol with a normalized variance, the quantization distortion D_Q in Eq. (4.4) is described as follows [40]:

$$D_Q = c 2^{-nR}, \quad (4.5)$$

where c is some constant, but generally becomes 1 for a source with the normalized variance; and n is the bandwidth ratio defined as $n = \alpha / S$ to describe the number of channel uses per source symbol such that when each fading block spans α channel uses; the transmitter describes S source symbols (i.e., the number of channel symbols required to send one source symbol); and R is the rate in bits per channel symbol. Since the source variance is an upper bound of the quantization distortion, D_Q , an inequality is obtained for any source as follows:

$$c 2^{-nR} \leq \sigma^2. \quad (4.6)$$

By considering both Eqs. (4.4) and (4.5), the distortion becomes:

$$\bar{D} \approx c 2^{-nR} (1 - p_{err}) + \sigma^2 p_{err}, \quad (4.7)$$

where p_{err} is now defined as the average compound channel symbol error probability due to the transmission of n channel symbols to describe a single source symbol at the receiver.

In application of the above distortion model to a system where protected successive refinable data are transmitted over layered broadcast channels, the method for a receiver to decode the information up to the successive layer l is first considered. This happens when the channel of a receiver achieves a rate of $\sum_{j=1}^l R_j$, where R_j is the achievable rate for transmitting data of layer j

in the channel when a channel gain h_j is realized with probability \tilde{p}_j . The achievable rate, R_j , for transmitting data of layer j can be derived as:

$$R_j = \log \left(1 + \frac{h_j \pi_j}{1 + h_j \sum_{g=j+1}^L \pi_g} \right), \quad (4.8)$$

where π_j is the power allocated to layer j , and L is the total number of layers in a layered broadcast signal. When a receiver realizes a channel rate at $\sum_{j=1}^l R_j$ to decode the source symbol in the layered broadcast signal up to layer l with an average compound symbol error rate, $p_{err,l}$, Eq. (4.4) nicely approximates the perceived end-to-end distortion with an upper bound below:

$$\bar{D}_l \approx c \cdot 2^{-n \sum_{j=1}^l R_j} (1 - p_{err,l}) + \sigma^2 p_{err,l}, \quad (4.9)$$

since a (n, k_l) protection code is applied on a successive layer l of each source symbol before being transmitted in a layered broadcast signal. The source information bits in layer l originally transmitted by k_l channel symbols are now encoded into protected information bits that require n channel symbols for layer l . Hence, only $(k_l/n) R_l$ bits in each channel symbol describes successive layer l in the source symbol. With such discount factor of (k_l/n) on each channel symbol, layer l of the source symbol is eventually described by an effective rate of $k_l R_l$ bits over n channel symbol transmissions, which refines Eq. (4.9) as follows:

$$\bar{D}_l \approx c \cdot 2^{-\sum_{j=1}^l k_j R_j} (1 - p_{err,l}) + \sigma^2 p_{err,l}. \quad (4.10)$$

Similar to Eq. (4.6), the quantization distortion up to layer l is upper-bounded by a source variance σ^2 up to layer l , which obtains an inequality:

$$c2^{-\sum_{j=1}^l k_j R_j} \leq \sigma^2, \quad \text{for } k_l = 1, 2, \dots, n. \quad (4.11)$$

Using the effective rate, $k_l R_l$, to describe a source symbol, the average compound symbol error rate, $p_{err,l}$, associated to a channel that decodes the layered broadcast signal up to layer l is:

$$p_{err,l} = 1 - \prod_{i=1}^l \left(1 - \sum_{j=0}^{k_i-1} \binom{n}{j} (1 - p_{M,i})^j (p_{M,i})^{n-j} \right), \quad (4.12)$$

where $p_{M,i}$ is the average symbol error rate affected by the signal-to-noise ratio (SNR) realized at layer l , which is in turn, also affected by the selection of a set of M -ary modulation schemes and the allocated power, ρ_l , in layer l , where:

$$P_{M,l} \leq 1 - \left(1 - 2 \left(1 - \frac{1}{\sqrt{2^{R_l}}} \right) e^{-\frac{1}{2} \left(\frac{3}{2^{R_l} - 1} \right) \left(\frac{h_j \pi_j}{1 + h_j \sum_{g=j+1}^L \pi_g} \right)} \right)^2 \quad (4.13)$$

In view of Eqs. (4.10)-(4.13) and averaging over different channel conditions with probability \tilde{p}_l , an upper bound of the expected distortion, \bar{D} , of the system with successive refinement over layered broadcast channel is defined as:

$$\bar{D} \approx \sum_{l=1}^L \tilde{p}_l \left\{ \begin{array}{l} c \cdot 2^{-\sum_{j=1}^l k_j R_j} \left[\prod_{i=1}^l \left(1 - \sum_{j=0}^{k_i-1} \binom{n}{j} (1-p_{M,i})^j (p_{M,i})^{n-j} \right) \right] \\ \sigma^2 \left[1 - \prod_{i=1}^l \left(1 - \sum_{j=0}^{k_i-1} \binom{n}{j} (1-p_{M,i})^j (p_{M,i})^{n-j} \right) \right] \end{array} \right\} \quad (4.14)$$

Note that a system without using the protection code (n, k_l) on layer l is indeed a special case of the system with $k_l = n$ for $l=1, \dots, L$. The average compound symbol error rate, denoted as, $p_{err,l}$, of layer l in this special case is:

$$p_{err,l} = 1 - \prod_{i=1}^l (1 - p_{M,i})^n \quad (4.15)$$

Using Eqs. (4.9) and (4.15), the expected distortion, \bar{D} , of a system without protection is yielded as follows:

$$\bar{D} \approx \sum_{l=1}^L \tilde{p}_l \left[\begin{array}{l} c \cdot 2^{-n \sum_{j=1}^l R_j} \left(\prod_{i=1}^l (1 - p_{M,i})^n \right) \\ + \sigma^2 \left(1 - \prod_{i=1}^l (1 - p_{M,i})^n \right) \end{array} \right] \quad (4.16)$$

Based on the derived closed-form formula in Eq. (4.14), the distortion can be jointly optimized over operational parameters across the source and channel, namely the values of k_l in the (n, k) protection codes, power allocation, and modulation selection for different layers. However, such joint optimization across the source and channel parameters is always a huge challenge in many cross-layer frameworks when actual operation and deployment are considered, since after such joint optimization, it is indeed impractical to redo the encoding and protection of the source in real-time right before the transmission at a BS. In addition, a source in the proposed cross-layer framework could connect with multiple transmission systems (i.e., BSs) for a broadcast service. It is more suitable to optimize power and modulation selection separately according to the channel conditions of a particular BS. Therefore, a 2-stage optimization methodology with a feedback mechanism in Figure 4-2 is considered here to realize the actual optimization operation and deployment for the cross-layer architecture in this thesis. During the 1st-stage optimization, the optimal k_l values are determined in an encoding and protection system to generate protected successive layers based on the n value of an adopted protection code, an aggregated prior knowledge of power allocations, modulation rates, and the channel gain distribution in the previous broadcast transmissions. Once the protected successive layers arrives in single or multiple transmission systems (i.e., BSs), an individual 2nd-stage optimization can determine the most appropriate power allocation and modulation rate based on the optimized k_l values from the 1st-stage optimization, as well as the local information about the channel conditions. After this 2nd-stage optimization, optimized k_l values, power allocation and modulations for different layers are therefore determined for the layered broadcast transmissions. The newly determined power allocations, modulation rates, and updated channel gain distributions acts as a feedback to update the aggregated prior knowledge in the encoding and protection system for the next 1st-stage optimization.

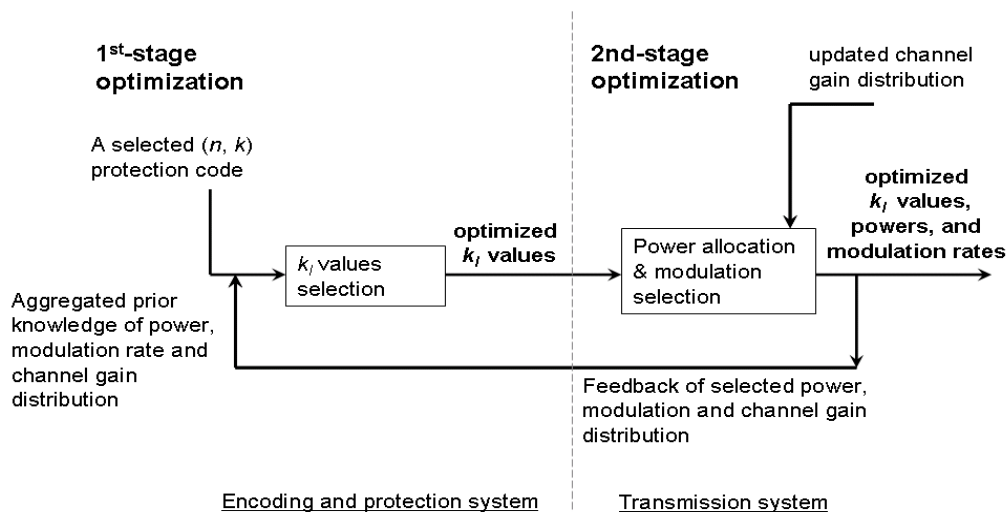


Figure 4-2. Two-stage optimization for the cross-layer framework

The optimization techniques over power allocation or/and modulation selection for the typical approaches of successive refinable source over layered broadcast are reported in previous literatures [33],[34],[45], which could be also adopted to handle the 2nd stage optimization separately in the proposed cross-layer framework. Therefore, it is the focus of this chapter to determine the optimal k_l values in the 1st-stage optimization that minimizes the end-to-end distortion, especially in comparison to a system without protection. For a fair comparison, a system with and without protection on each successive layer will both use the same bandwidth ratio, n . Comparing Eqs. (4.14) and (4.16), the system using protection under some optimal k_l values in each layer l can be proven to yield a smaller expected distortion at the receiver than that without using protection. Given the power allocation, modulation rate, and channel conditions (i.e., $p_{M,l}$ and the channel gain distribution), optimal k_l values in each layer l can be determined by solving the optimization problem of the following objective function:

$$\min_{k_1, \dots, k_L} \sum_{i=1}^L \tilde{p}_i \left\{ \begin{aligned} & c \cdot 2^{-\sum_{j=1}^l k_j R_j} \left[\prod_{i=1}^l \left(1 - \sum_{j=0}^{k_i-1} \binom{n}{j} (1-p_{M,i})^j (p_{M,i})^{n-j} \right) \right] \\ & + \sigma^2 \left[1 - \prod_{i=1}^l \left(1 - \sum_{j=0}^{k_i-1} \binom{n}{j} (1-p_{M,i})^j (p_{M,i})^{n-j} \right) \right] \end{aligned} \right\} \quad (4.17)$$

subject to the constraints:

$$0 < p_{M,i} \leq 1,$$

$$l = 1, \dots, L,$$

$$\tilde{p}_i \geq \tilde{p}_j \text{ for } i < j,$$

$$k_l \leq n.$$

4.3 A Novel Search Algorithm

Taking derivatives on a cost function is a standard optimization technique to verify the convexity of an optimization problem. Some approximation approaches could be used to make Eq. (4.17) continuous for the convexity test. To cope with the huge computation complexity, the proposed search algorithm can significantly reduce the search space from $O(n^2)$ to $O(n \log n)$ by taking advantage of the results of convexity test. The rest of the section will focus on the scenario with $L = 2$, for the sake of manageability and relevance in practical situations. However, the presented approach can be easily expanded to multiple layers with $L > 2$.

4.3.1 The Global Minimum

As the first step towards solving the optimization problem, the binomial CDF in Eq. (4.17) is approximated using the normal distribution as shown in Eq. (4.18).

$$F = \sum_{i=1}^L \tilde{p}_i \left[c \cdot 2^{-\sum_{j=1}^L k_j R_j} (1 - \phi(z_i)) + \sigma^2 \left(1 - \prod_{i=1}^L (1 - \phi(z_i)) \right) \right], \quad (4.18)$$

where $z_i = \frac{k_i - 0.5 - \mu_i}{\sigma_{c,i}}$, $\mu_i = n(1 - p_{M,i})$, and the channel variance of the i -th layer is

$\sigma_{c,i}^2 = n(1 - p_{M,i})p_{M,i}$. With $L = 2$, Eq. (4.18) can be expanded as follows:

$$\begin{aligned} F &= \tilde{p}_1 c \cdot 2^{-k_1 R_1} (1 - \phi(z_1)) \\ &\quad + \tilde{p}_1 \sigma^2 [1 - (1 - \phi(z_1))] \\ &\quad + \tilde{p}_2 c \cdot 2^{-(k_1 R_1 + k_2 R_2)} (1 - \phi(z_1))(1 - \phi(z_2)) \\ &\quad + \tilde{p}_2 \sigma^2 [1 - (1 - \phi(z_1))(1 - \phi(z_2))] \\ &= f_1 + f_2 + f_3 + f_4, \end{aligned} \quad (4.19)$$

where

$$\begin{aligned} f_1 &= \tilde{p}_1 c \cdot 2^{-k_1 R_1} (1 - \phi(z_1)), \\ f_2 &= \tilde{p}_1 \sigma^2 (1 - (1 - \phi(z_1))), \\ f_3 &= \tilde{p}_2 c \cdot 2^{-(k_1 R_1 + k_2 R_2)} (1 - \phi(z_1))(1 - \phi(z_2)), \\ f_4 &= \tilde{p}_2 \sigma^2 [1 - (1 - \phi(z_1))(1 - \phi(z_2))]. \end{aligned}$$

Let $F = f_1 + f_2 + f_3 + f_4$, and let $F_1 = f_1 + f_3$ and $F_2 = f_2 + f_4$. In the study, the convexity test simply takes the derivative on F with respect to one of the variables (in this case, k_1 is taken without loss of generality), i.e.,

$$F' = \frac{\partial F}{\partial k_1} = \frac{\partial(f_1 + f_2 + f_3 + f_4)}{\partial k_1} = (f_1 + f_3)' + (f_2 + f_4)' \quad (4.20)$$

Incorporating the necessary condition of $F' = 0$ for the existence of the optimality into Eq. (4.20) results in:

$$(f_2 + f_4)' = -(f_1 + f_3)' \quad (4.21)$$

Since both f_1 and f_3 are exponential functions with respect to k_1 under a given value of k_2 , $(f_1 + f_3)$ is a monotonously decreasing function with respect to k_1 as shown in Figure 4-3. Thus, $-(f_1 + f_3)'$ leads to a monotonously decreasing curve that can be illustrated in Figure 4-4 for any k_2 . On the other hand, $(f_2 + f_4)$ is an increasing convex and concave function with respect to k_1 in Figure 4-5 with an arbitrary k_2 value, which can be confirmed by a lemma here.

Lemma 4.1: $(f_2 + f_4)$ is an increasing convex and concave function with respect to k_1 in Figure 5 with an arbitrary k_2 value.

Proof: $(f_2 + f_4)$ is a function that could be expressed as:

$$(f_2 + f_4) = a - b(1 - \phi(z_1)) = a - b + b\phi(z_1), \text{ where } a \text{ and } b \text{ are both positive constant.}$$

Because $\phi(z_1)$ is a well-known increasing convex and concave function with respect to k_1 , so $(f_2 + f_4)$ will have the same property. ■

Hence, the derivative of $(f_2 + f_4)$ yields a bell-shape curve as shown in Figure 4-6. It is observed that a higher k_2 yields a higher starting point of the curve, or vice versa. Therefore, F' is the subtraction the two curves in Figure 4-4 and Figure 4-6, respectively, where the k_1 values corresponding to the intersection of the two curves result in $F' = 0$.

With the knowledge of $-(f_1 + f_3)'$ and $(f_2 + f_4)'$, four relations between the two functions seen in Figure 4-7 can be concluded: (relation-1) $-(f_1 + f_3)'$ intersects $(f_2 + f_4)'$ at a single point; (relation-2) two intersections are formed by the two function, and they are separated by the mean of the bell curve $(f_2 + f_4)'$; (relation-3) two intersections are after the mean of the bell curve $(f_2 + f_4)'$; (relation-4) there is no intersection found between the two functions. Note that an intersection of the two curves results in a critical point (i.e., minimum/maximum) for Eq. (4.20) such that $F' = 0$.

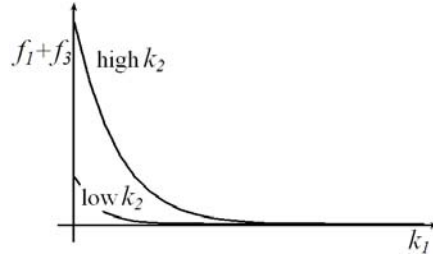


Figure 4-3. A function of f_1+f_3

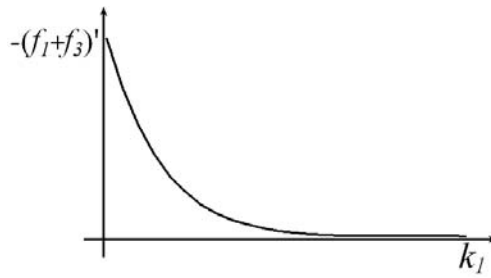


Figure 4-4. $-(f_1+f_3)'$

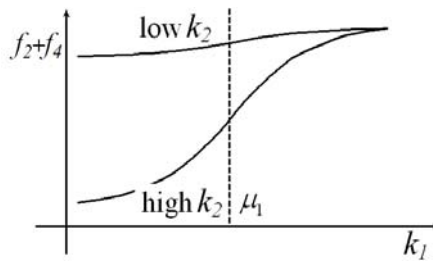


Figure 4-5. A function of f_2+f_4

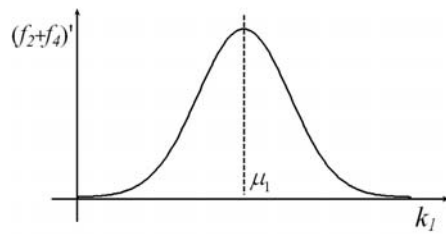


Figure 4-6. $(f_2+f_4)'$

Based on the four possible relations between $-(f_1 + f_3)'$ and $(f_2 + f_4)'$, there are 7 possible cases of trends in the original distortion function with respect to k_1 for any given k_2 , which are summarized as follows.

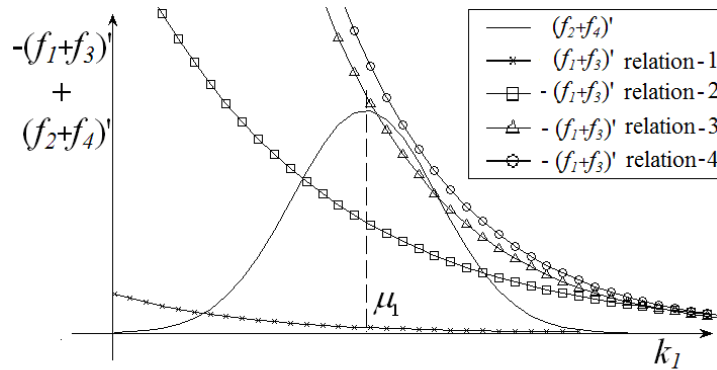


Figure 4-7. Four possible cases

- **Cases 1(a), 1(b), 2(a) and 2(b) :**

There are two types of trends in both cases 1 and 2: (a) $F|_{k_1=0} \leq F|_{k_1=n}$; and (b) $F|_{k_1=0} > F|_{k_1=n}$.

Regardless of either type in any case here, a common observation is found in the trend of the distortion function when $k_1 \leq \mu_1$. Since a negative sum of the derivatives appears before the first intersection in Figure 4-7 and is followed by a positive derivatives sum, the first intersection acts as a minimum in either type of any case for $k_1 \leq \mu_1$ as shown in Table 4-1. However, a second intersection only appears in case 2(a) and 2(b) for $k_1 > \mu_1$. A positive derivative sum appears before the intersection and is followed by a negative one, indicating the second intersection acts as a

maximum. Hence, the one and only one minimum in either cases 1(a), 1(b), 2(a), and 2(b) must be the global minimum, which must exist within the range $k_1 \leq \mu_1$.

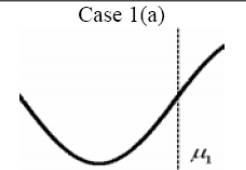
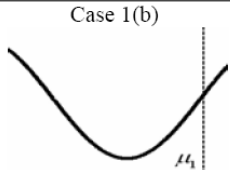
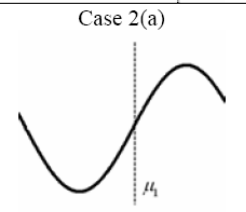
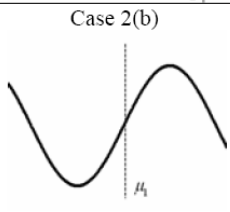
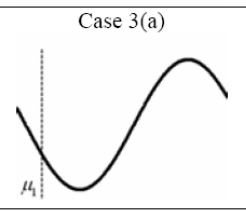
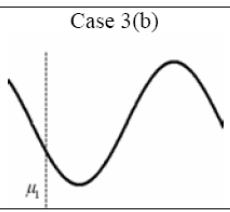
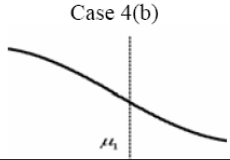
- **Case 3(a) and 3(b):**

Similarly, two types are in case 3: (a) $F|_{k_1=0} \leq F|_{k_1=n}$; (b) $F|_{k_1=0} > F|_{k_1=n}$. However, in contrast to cases 1 and 2 above, both the minimum and maximum must exist for $k_1 > \mu_1$. As shown in Figure 4-7, the first intersection only appears after $k_1 = \mu_1$ with a negative sum of derivatives before the intersection and is followed by a positive sum. This indicates that intersection acts as a minimum. A second intersection also appears at a larger k_1 value, initially with a positive derivative sum but followed by a negative one afterwards. The second intersection is therefore a maximum. Hence, the only minimum in both cases 3(a) and 3(b) must be the global minimum that exists within the range $k_1 > \mu_1$.

- **Case 4:**

Since no intersections exist in Figure 4-7 with negative sum of derivatives for any k_1 , the global minimum can only be possible at the boundary condition of $k_1 = n$.

Table 4-1. Only 7 possible trends of the distortion function with respect to k_1 .

Sign of $\left. \frac{\partial F}{\partial k_1} \right _{k_1=\mu_1}$	$F _{k_1=0} \leq F _{k_1=n}$	$F _{k_1=0} > F _{k_1=n}$
> 0	Case 1(a) 	Case 1(b) 
	Case 2(a) 	Case 2(b) 
< 0	Case 3(a) 	Case 3(b) 
	Case 4(a) Not Applicable	Case 4(b) 

Although these cases are developed based on the normal approximation, they can accurately indicate if the global minimum exists at the range of $k_1 \leq \mu_1$ and $k_1 > \mu_1$. By knowing that the range of search space is convex for the global minimum and some additional information, the exact optimal pairs of k_1 and k_2 for the global minimum can be efficiently searched. A lemma is derived here to identify the range for global minimum and the required information for a very efficient searching algorithm.

Lemma 2: Given k_2 on a successive refinable source following the Gaussian distribution, the global minimum of the expected distortion only exists in type (a) of cases 1, 2, and 3.

Proof: The proof can be derived by using the fact from Eq. (4.11) showing $c2^{-\sum_{j=1}^l k_j R_j} \leq \sigma^2$.

For any $k_1=0$ and any k_2 ,

$$\begin{aligned}
 & \tilde{p}_1 \sigma^2 \geq \tilde{p}_1 c \\
 \Rightarrow & \tilde{p}_1 \sigma^2 + \tilde{p}_2 \sigma^2 \geq \tilde{p}_1 c + \tilde{p}_2 c 2^{-k_2 R_2} \\
 \Rightarrow & \tilde{p}_1 \sigma^2 + \tilde{p}_2 \sigma^2 (1 - \phi(z_2)) \\
 & \geq \tilde{p}_1 c + \tilde{p}_2 c 2^{-k_2 R_2} (1 - \phi(z_2)) \\
 \Rightarrow & F|_{k_1=n} \geq F|_{k_1=0} \\
 \Rightarrow & \text{type (a) in case 1, 2 and 3.}
 \end{aligned}$$

Hence, the global minimum exists before μ_1 in cases 1(a), 2(a), and 3(a) for any successive refinable source following the Gaussian distribution. \square

4.3.2 Proposed Search Algorithm

The proposed search algorithm is developed based on *Lemma 2*, by which the range of where the optimal k_1 is located can be determined. Thus, the search complexity can be reduced from $O(n^2)$ to $O(n \log n)$. The following three decision principles are first provided before a further detailed description of the proposed search algorithm.

- (1) Compute the derivative of the distortion at $k_1 = \mu_1$ to see if it is positive or zero for types 1(a) and 2(a). Otherwise, it is for type 3(a);
- (2) If type 1(a) or 2(a) is identified, the global minimum occurs within the convex portion left of the point $k_1 = \mu_1$, and can be efficiently determined within the range of $0 < k_1 \leq \mu_1$ using a simple midpoint search with $O(\log n)$ complexity;

- (3) If type 3(a) is identified, an additional step is necessary to determine if the derivative at each sample mid-point is negative. With a negative derivative, the distortion at the midpoint is compared with the distortion at $k = 0$ to determine whether the left or right search boundary is to be updated. Once a positive midpoint derivative is found, the global minimum can be found using the mid-point search previously outlined in the range of the resultant boundaries for $k > \mu_1$ while maintaining $O(\log n)$ complexity.

A detailed description on the proposed algorithm is presented as follows in a form of pseudo code, where the algorithm searches in the dimension of k_1 while taking a given k_2 value. Note that the algorithm can entirely operate in the same manner with the k_2 dimension. However, due to the dependency of the two dimensions, the optimality can be guaranteed only when the algorithm is applied to one of the two dimensions while leaving the other to be sequentially searched. Therefore, the global minimum is the minimum of all minimums along k_1 under n different k_2 values, which yields the worst-time complexity of this algorithm as $O(n \log n)$. In spite of this, the algorithm is reasonably efficient for implementation into practical systems.

Algorithm 1 Finding k_1^* and k_2^* for minimum distortion

```

1: for all  $k_2 \in (0, n]$  do
2:   if  $D(\mu_1 - 1) < D(\mu_1)$  then
3:      $k_{1,\text{left}} = 0, k_{1,\text{right}} = \mu_1$ 
4:   else do
5:      $k_{1,\text{left}} = \mu_1, k_{1,\text{right}} = N, k_{1,\text{mid}} = (k_{1,\text{left}} + k_{1,\text{right}}) / 2$ 
6:     while  $D(k_{1,\text{mid}}) < D(k_{1,\text{mid}} - 1)$  do
7:       if  $D(k_{1,\text{mid}}) < D(k_1 = 0)$  do
8:          $k_{1,\text{left}} = k_{1,\text{mid}}$ 
9:       else do
10:         $k_{1,\text{right}} = k_{1,\text{mid}}$ 
11:      end if
12:       $k_{1,\text{mid}} = (k_{1,\text{left}} + k_{1,\text{right}}) / 2$ 
13:    end while
14:     $k_{1,\text{right}} = k_{1,\text{mid}}$ 
15:  end if
16:   $k_{1,\text{mid}} = (k_{1,\text{left}} + k_{1,\text{right}}) / 2$ 
17:  while  $D(k_{1,\text{mid}}) > D(k_{1,\text{mid}} - 1)$  or  $D(k_{1,\text{mid}}) > D(k_{1,\text{mid}} + 1)$  do
18:    if  $D(k_{1,\text{mid}}) < D(k_1 = 0)$  do
19:       $k_{1,\text{left}} = k_{1,\text{mid}}$ 
20:    else do
21:       $k_{1,\text{right}} = k_{1,\text{mid}}$ 
22:    end if
23:     $k_{1,\text{mid}} = (k_{1,\text{left}} + k_{1,\text{right}}) / 2$ 
24:  end while
25:   $k_1^*(k_2) = k_{1,\text{mid}}$ 
26: end for
27: return  $k_1, k_2^*$  such that  $k_1^*(k_2 = k_2^*)$  yields  $D_{\min}$ 

```

Algorithm 1. The proposed search algorithm for determining optimal k values.

4.4 Numerical Analysis

Numerical analysis is conducted in this section for two purposes: 1) to verify the conclusions and the curves that are mathematically proved in the previous section; 2) to gain deeper understanding on the developed closed-form equations. The expected distortion by the proposed closed-form solution is presented with respect to different values of k_1 and k_2 , followed by different average compound symbol errors, i.e., $p_{M,1}$ and $p_{M,2}$. A smaller k_1 indicates that less information bits from layer 1 are launched in each channel symbol (i.e., $k_1 R_1$) while more bits are used for protection (i.e., $(n - k_1) R_1$), where n is total number of transmissions (i.e., channel symbols) required for each source symbol. In the numerical study, $n = 30$ is used. A special case is when $k_1 = n$ and $k_2 = n$, where the system behaves as one without using protection as described in Eq. (16). A system without protection is used as a benchmark in comparison with the general case using various k_1 and k_2 values.

It can be observed from the distortion curves in Figure 4-8 to Figure 4-11 that the existence of the convexity in the distortion function is confirmed. In addition, it is in line with *Lemma 4.1* that the system always yields a lower distortion than that without any protection (i.e., the distortion at $k_1 = k_2 = n$). It is also observed that a minimized distortion exists with some optimized protection values in the graphs.

Figure 4-8 and Figure 4-9 show the expected distortion over various combinations of k_1 and k_2 , where the system in Figure 4-8 experiences a higher average compound symbol error, $p_{M,1}$, in layer 1 while with the same average compound symbol error, $p_{M,2}$, in layer 2 as the system in Figure 4-9. It can be observed that more protection for layer 1 (i.e., a smaller value of k_1) is required in the system of Figure 4-8 to minimize the distortion; thus, the minimized distortion exists in the area closer to lower values of k when compared with the system in Figure 4-9. From

the numerical results, optimized protection configurations are $(k_1^* = 5$ and $k_2^* = 2)$ and $(k_1^* = 14$ and $k_2^* = 2)$ for minimized distortions in Figure 4-8 and Figure 4-9, respectively.

Similarly, Figure 4-10 and Figure 4-11 show the expected distortion over various combinations of k_1 and k_2 protection values, where the system in Figure 4-10 experiences a higher compound symbol error rate, $p_{M,2}$, in layer 2. It is demonstrated that more protection is required in layer 2 (i.e., a smaller k_2) for the system in Figure 4-10 to approach the region with a lower or minimized distortion when compared to that in Figure 4-11. From the numerical results, $k_2^* = 3$ and $k_2^* = 1$ are the optimized protection values in layer 2 for their minimized distortion in Figure 4-10 and Figure 4-11, respectively.

It is interesting to observe that the region resulting in lower distortion is much wider along the dimension of k_1 when $p_{M,1}$ is smaller. This also happens along the k_2 dimension when $p_{M,2}$ is reduced. There are many possible choices of k_1 and k_2 values observable from this low distortion region, which actually gives relatively lower distortion comparable to the optimal configuration for the global minimum. This observation reveals a tradeoff for practical situations where the use of sub-optimal protection configurations may be sufficient in exchange for feasible implementation from lower computation complexities.

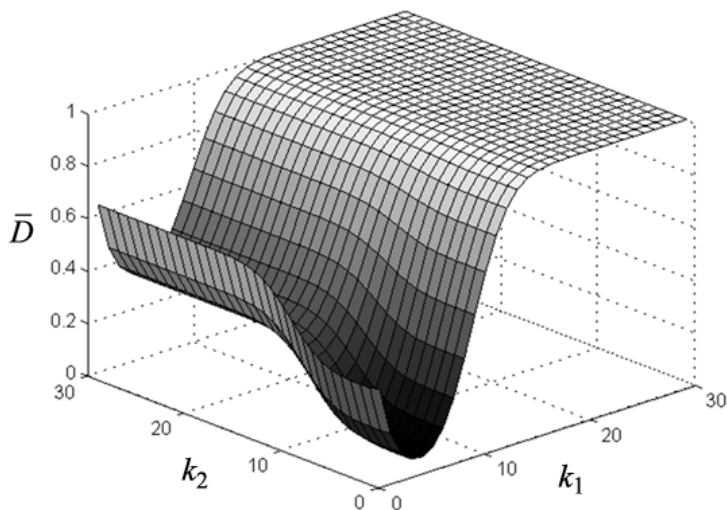


Figure 4-8. The system with a higher average compound symbol error, $p_{M,1}$. (optimized protections are $k_1^* = 5$ and $k_2^* = 2$)

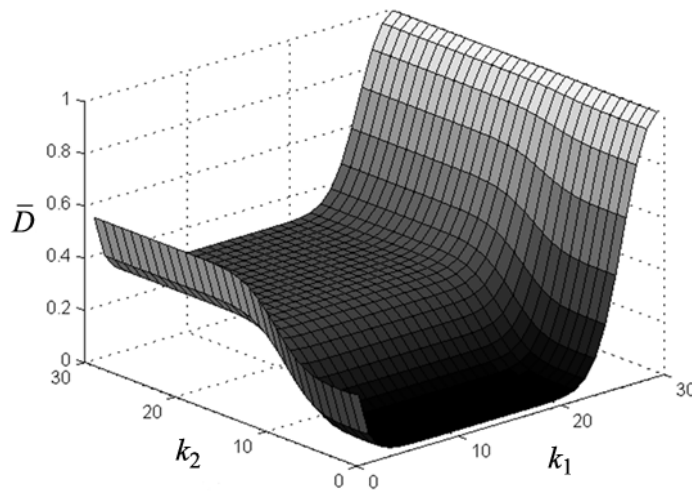


Figure 4-9. The system with a lower average compound symbol error, $p_{M,1}$. (optimized protections are $k_1^* = 14$ and $k_2^* = 2$)

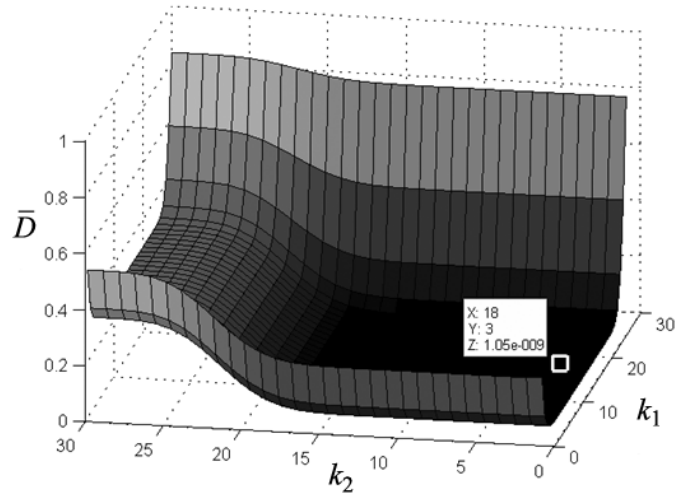


Figure 4-10. The system with a higher average compound symbol error, $p_{M,2}$. (optimized protection in layer 2 – $k_1^* = 18$ and $k_2^* = 1$)

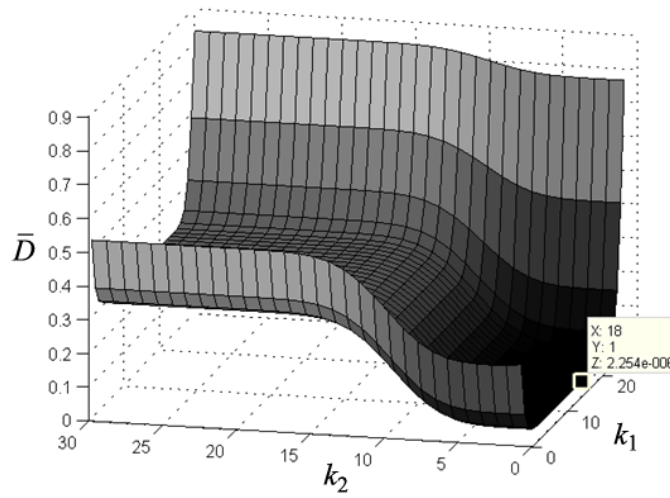


Figure 4-11. The system with a lower average compound symbol error, $p_{M,2}$. (optimized protection in layer 2 – $k_1^* = 18$ and $k_2^* = 3$)

Figure 4-12 compares the optimized distortions of two systems with respect to various average compound symbol errors, $p_{M,1}$ and $p_{M,2}$, where a system has optimized protection configurations and the other without any protection. The numerical results show that a system always gives a better or equivalent distortion with protection when compared to a system without protection under constant channel distributions and power allocations to the video quality layers.

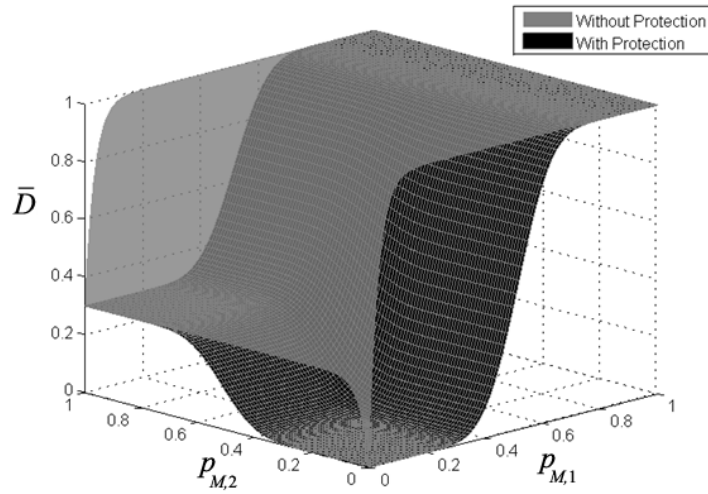


Figure 4-12. The expected distortions of two systems with respect to various $p_{M,1}$ and $p_{M,2}$.

4.5 Summary

The chapter investigated a wireless system with protected successive refined sources over layered broadcast channel, wherein a closed-form formula on the upper bound of the expected distortion was developed. It is claimed that such a wireless system generalizes all previously reported schemes. The obtained formula nicely reveals a special case that refers to a system without using

protection, which can be used for analytical comparison and numerical evaluation. Based on the closed-form formula, conditions were identified for the system with two successive layers such that a global minimum for the end-to-end distortion can be found and proven to be always better than a system without protection. An efficient iterative search algorithm is developed, which always determines the exact optimal k values for the two layers with the worst-time complexity of $O(n \log n)$, where n is number of channel uses per source symbol. Numerical analysis was developed to give a visual intuition on the distortion performance and to verify the obtained optimum by using the proposed search algorithm under various scenarios of system parameters. It is concluded that the end-to-end distortion in the system with protected successive refined sources over layered broadcast channels can be optimized with respect to the k values to be always be lower than a system without protection.

Chapter 5

Logical Superposition Modulation

Superposition coding is a key modulation technique adopted in the proposed cross-layer framework of coded wireless video broadcast/multicast in this thesis. In spite of the aforementioned advantages from previous chapters, very few commercially available wireless systems and industry standards on wireless video broadcast/multicast have defined the SPC modulation. The absence of SPC modulation in wireless video multicast applications is likely due to the requirement of additional system support. Dedicated hardware components and circuitry are required to superimpose two or multiple modulated signals together to form a SPC signal in the physical (PHY) layer. Also, software modifications are required to enable the cross-layer mapping between the successively refinable video sources and the layered SPC multicast signals. Such additions of dedicated hardware and software supports could hardly be justified in current 3G/4G technologies and previous wireless systems mainly due to the lack of broadband digital media applications on video broadcast/multicast and their subscriptions back then. Nonetheless, by envisioning the prevalence of bandwidth-intensive video multicast services provisioned via the emerging BWA networks, it is becoming crucial to develop a practical implementation of SPC modulation for wireless video multicast that offers minimal barrier to industry acceptance.

In this chapter, a proposed logical SPC modulation/demodulation scheme is presented. It can serve as an alternative means to realize multi-resolution modulated broadcast/multicast for scalable video if the hardware-based SPC is not available in a wireless system. The proposed modulation scheme at transmitters in generating such a logical SPC broadcast/multicast signal is described first, followed by the corresponding design at the receiver-end which demodulates and finally retrieves video information from the received SPC broadcast/multicast signal. Analytical formulations of the proposed logical SPC modulation will be presented. Numerical and testbed results will be demonstrated to justify the feasibility of using the proposed scheme to realize the coded wireless video multicast, when a hardware-based SPC modulation is not available in a system.

5.1 Proposed Logical Superposition Coded Modulation

In this section, the proposed logical SPC modulation/demodulation scheme is presented, which incorporates with a cross-layer design framework for wireless video multicast. The proposed modulation scheme at transmitters in generating such a logical SPC multicast signal is described first, followed by the corresponding design at the receiver-end which demodulates and finally retrieves video information from the received SPC multicast signal.

5.1.1 One-shot Modulation at Transmitter

For conceptual demonstration, it is assumed that an SPC modulated signal contains information bits of two quality layers from a scalable video bitstreams. Recall the example of superposition coding/decoding in Section 2.2 of Chapter 2, a superimposed signal x can be taken as the summation of the two vectors expressed in terms of the corresponding amplitudes and phases in a

constellation diagram formed by the conventional approach using the modulation schemes of BPSK and QPSK. The resultant constellation diagram of signal x has 8 symbols, each with an associated amplitude and phase. This translates into an observation that such superimposed signal can be directly generated at the transmitter through dynamic phase shift keying (i.e., the angle of x in the constellation diagram) and energy (power) allocation (i.e., the amplitude of x) during the signal transmission, which have become feasible by commercially available chipsets [41]. The amplitude and angle of each point in the constellation designates its own actual location, which also depends on the allocation ratio of energies in each transmission for modulating signals using BPSK and QPSK in the conventional approach, denoted by E_1 and E_2 , respectively. There is a total energy constraint $E = E_1 + E_2$ in each transmission instant described with a relationship by a single parameter β :

$$E_1 = \beta E \quad (5.1a)$$

$$E_2 = (1 - \beta)E \quad (5.1b)$$

By identifying the required number of constellation points and manipulating the value of β , the proposed logical SPC modulation can generate an 8-point constellation diagram that is similar to that by the conventional hardware-based SPC. The proposed approach can be generically used to generate SPC multicast signals equivalent to any combination of common modulation schemes. As illustrated in Table 5-1, with knowledge of the modulation schemes for the base layer and enhancement layer, the total number of points in the constellation diagram can be identified. It is observed that a conventional modulation scheme (i.e., 8-QAM in our example here) can lead to a similar or equivalent constellation diagram in *one-shot* without going through a superposition process of two modulated signals (i.e., BPSK and QPSK in our case). The generated *one-shot* constellation symbols in the constellation diagram can be configured to have amplitudes and phases

equal to those generated by a conventional hardware-based SPC approach. To make those constellation points logically equivalent to those generated from the conventional approach, the two approaches must have identical information bits from each constellation point.

Table 5-1. Equivalency in the number of constellation symbols between logical and conventional SPC modulations.

modulation for base layer m_1 points per symbol			
modulation for enhancement layer (m_2 points per symbol)	BPSK ($m_1 = 2$)	QPSK ($m_1 = 4$)	16-QAM ($m_1 = 16$)
QPSK ($m_2 = 4$)	8 pts	-	-
16-QAM ($m_2 = 16$)	32 pts	64 pts	-
64-QAM ($m_2 = 64$)	128 pts	256 pts	1024 pts

5.1.2 A Cross-layer Mapping at Transmitter

To realize the proposed logical SPC modulation for video multicast, strategically mapping a symbol of m bits from the base layer data and n bits from the enhancement layer into a $(m + n)$ -bit symbol block is required. Referring back to the example of using BPSK and QPSK, each symbol block contains 1 bit from the base layer and 2 bits from the enhancement layer, and the 3-bit symbol block is mapped by a constellation diagram with 8 points as shown in the lower portion of

Figure 5-1. The symbol block can be alternatively expressed as a combination of two conventional modulation schemes as shown in the upper portion of Figure 5-1. The mapping of the 3-bit symbol block to the 8-point constellation is based on the knowledge regarding the information bits of the scalable video bitstreams in the application layer. For a symbol referring to ‘0’ in the base layer with BPSK and a symbol referring to ‘01’ in the enhanced layer with QPSK, a corresponding 3-bit symbol block containing “001” (i.e. “0”+”01”) can be formed and mapped to the symbol ‘0, 01’ in the *one-shot* constellation diagram of the existing modulation scheme for generating a logical SPC modulated signal equivalent to the conventional approach.

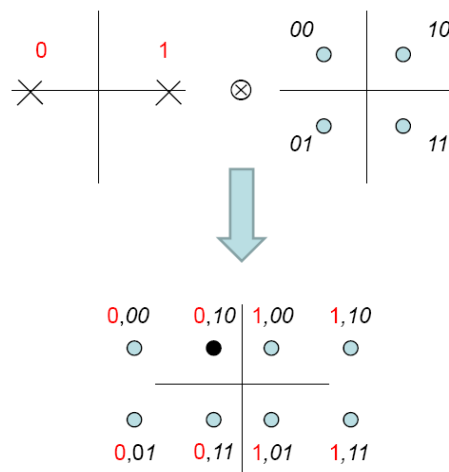


Figure 5-1. Mapping a 3-bit symbol block to one of the 8 constellation symbols. “⊗” stands for superposition operation.

- **Implementation Issues**

To implement the illustrated logical SPC modulation at the transmitter, a new software module is required in the existing MAC layer to obtain the dependency knowledge of information bits

between bitstreams of two quality layers from the scalable video source, which are buffered in the corresponding queues at the transmitter. The modified MAC software then interacts with the modulation chipset in the PHY layer through a set of primitives to execute *one-shot* modulation for generating logical SPC multicast signal as shown in Figure 5-2. The primitives act as the passage for the MAC software to define the *one-shot* modulation scheme in PHY, by which a constellation point will be selected to map the 3-bit symbol block formed by the set of bits at the head-of-line of the corresponding queues. In the modulation chipset, on the other hand, more functions should be added such that some service access points (SAPs) are defined in order to receive and recognize the parameters passed from the upper MAC software. Furthermore, the chipset should be able to generate the logical SPC modulated signals accordingly along with allocation of energy for each modulation level.

Note that the locations of the symbols in the constellation diagram can be dynamically determined by the given amplitude and phase for each symbol through the control of β , which can determine the transmission performances required for the application, in terms of the symbol error rate (SER) or overall symbol throughput.

Since the energy allocation and phase keying assignment are becoming common functionalities in modern wireless chipsets, the aforementioned software modifications should not introduce much overhead at a powerful base station system. Therefore, the proposed logical SPC modulation scheme is expected to be feasible and implementable in currently available commercial BS systems.

5.1.3 Leveraging Existing Receiver Demodulators

In contrast to the hardware-based SPC demodulation using SIC, the proposed logical SPC demodulation allows the decoding of the base layer information directly using a standard 8-QAM modulation scheme regardless of the channel condition. For example, when the channel condition

is poor, the first bit in the example of Figure 5-1 (that carries the base layer information) can always be obtained as “0” if the received logical SPC signal is interpreted as any point on the left-hand-side of the constellation diagram. This is due to the way every 3-bit symbol block is assigned to a constellation point as shown in Figure 5-1. In forthcoming sections, using 8-QAM instead of BPSK for the first bit in a symbol block is proved to yield the same error probability as that by using a standard BPSK demodulator. When the channel condition is good, instead of subtracting the base layer symbol for decoding the enhancement layer symbol using SIC as the conventional SPC demodulation, the receiver simply decodes the three bits from the 8-QAM demodulator.

Since no hardware subtraction is required, the received logical SPC modulated signals can be decoded using an existing demodulator already implemented in commercially available hardware chipsets. Additional software support is needed to retrieve the original video bitstream for playback, which is discussed in the next subsection.

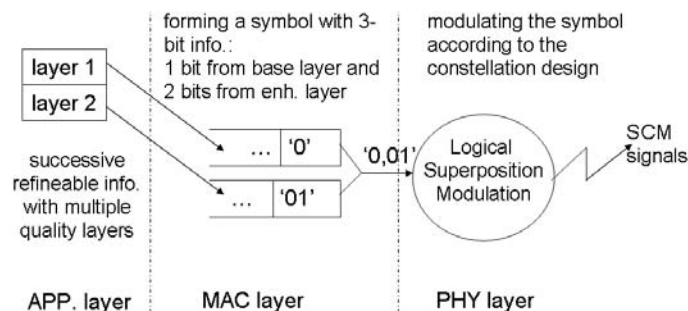


Figure 5-2. Operation and interactions between layers of the required software support.

5.1.4 Software Support at Receiver

The proposed software support for logical SPC demodulation at the receiving end is designed for simple implementation with minimal overhead. Such design requirements are critical for customer premise equipments (CPE) that are considered low-cost devices under mass-production.

To demodulate the logical SPC multicast signal with the proposed logical SPC demodulation, the receiver only requires knowledge of the two modulation schemes employed for the signal at the transmitter. The performance by using a single standard 8-QAM demodulator will be close to that by using the hardware-based SIC approach, which will be further examined in the next section. Letting the result from the BPSK demodulation be a_1 and the result from the 8-QAM demodulation be $b_1b_2b_3$, the application layer takes the 3-bit symbol block as $a_1b_2b_3$. Since a_1 is the most important bit, it is obtained by using the most reliable demodulation scheme (i.e., BPSK) such that the base video quality is highly secured. Furthermore, a better perceived video quality can be achieved if the two additional bits from the higher layer, b_2b_3 , are successfully decoded.

The aforementioned design incurs very limited additional signaling and software modifications. Firstly, the signaling between the transmitter and receivers just need to define two modulation schemes for each SPC symbol block. Secondly, the MAC software needs to split each obtained symbol into two portions, where the bits of the first part are assigned to the buffer for the base layer and the bits of the remaining are assigned to the buffer for the enhancement layer. Thirdly, the video decoder in the application at the receiver has to extract the bits from both queues and reconstruct the original video bitstream.

Compared with the conventional SIC based demodulation process, both schemes need separate buffers and interfaces to handle the individual streams of information bits from the multi-stage decoding process. On the contrary, the modified software in the proposed scheme could take all the information bits from a single demodulation process in one-shot, and then assigns the first

$(\log m_1)$ bits and subsequent $(\log m_2)$ bits into the buffers of base and enhancement quality layers, which is a relatively light-weighted process.

5.2 Analysis of Symbol Errors – A Case study

Conventionally, the points in a constellation diagram are equidistantly located to achieve optimal overall symbol error rate. The requirement of equidistance is based on the assumption of equal importance of each bit encoded in a symbol block. However, this is not necessarily a desirable feature when transmitting successively refinable information using SPC modulation due to the dependency of information bits between successive layers in a transmission as well as the scalability issues in the presence of multi-user channel diversity under wireless multicasting.

In the section, the bounds on the power allocation (in terms of the value of β) is first derived such that a standard demodulator can be feasibly applied for demodulating the proposed logical SPC signal. Without loss of generality, the following analysis will be based on the superposition of BPSK and QPSK signals, where a constellation with 8 points is yielded. An analysis of SER for the proposed scheme will be conducted.

5.2.1 Feasibility of using a Standard 8-QAM Demodulator

Simply using a standard 8-QAM demodulator at the receiving end instead of a specialized demodulator for SPC demodulation bears many advantages for implementation and industry acceptance, which is one of unique features of the proposed cross-layer design. The necessary condition for feasibly using a standard 8-QAM demodulator is that any one of the 8 constellation points by logical SPC modulation should be positioned within a proper decision region for the

corresponding constellation point that is identifiable by a standard 8-QAM detector. This places constraints on the energy allocation factor β , which is the major factor that determines the resultant locations of the constellation points.

Let a logical SPC modulated signal be generated according to a given set of energy (denoted as E_1 and E_2) and phase shift keys, which is equivalent to the superposition of two BPSK and QPSK signals with E_1 and E_2 as the corresponding energy. The resultant constellation diagram has 8 constellation points as shown in Figure 5-3(a).

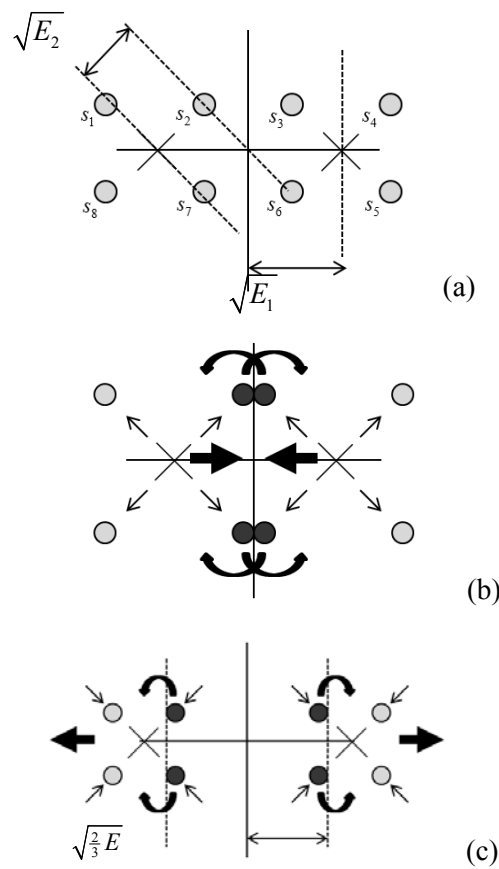


Figure 5-3 (a-c). The bounds and impacts of β towards the location of constellation points limited by the decision boundary of a standard 8-QAM detector.

It is now important to identify the situations where any of the 8 points in the constellation formed by a 3-bit symbol block could not be identified by a standard 8-QAM demodulator. As β is decreased (or equivalently, more energy is weighted on the enhancement layer information), the locations of the four points $s_1, s_2, s_7,$ and s_8 (or, $s_3, s_4, s_5,$ and s_6) move further away from each other, while their centre (marked as X) moves closer to the origin, as shown in Figure 5-3 (b). When β is decreased such that s_3 overlaps with s_2 (and s_7 overlaps with s_6), a persistent error occurs in case a standard 8-QAM demodulator is used for decoding. Therefore, β should be lower-bounded as follows: $\sqrt{E_1} > \sqrt{E_2/2}$, or $\sqrt{\beta E} > \sqrt{(1-\beta)E/2}$. Thus, the lower bound on β is $\beta > 0.333$.

On the other hand, when β is increased, the four symbols $s_1, s_2, s_7,$ and s_8 (or, $s_3, s_4, s_5,$ and s_6) move closer with each other while their centre moves further away from the origin, as shown in Figure 5-3 (c). When β is increased such that s_5 and s_6 (or, s_2 and s_7) cross the dashed line on the right (or left) side of the constellation, a persistent error in distinguishing s_3 from s_4 (or s_6 from s_5, s_2 from $s_1,$ and s_8 from s_7) will occur in case a standard 8-QAM demodulator is used for decoding the signal. Therefore, β should be upper-bounded as: $\sqrt{E_1} - \sqrt{E_2/2} < \sqrt{2E/3}$, or $\sqrt{\beta E} - \sqrt{(1-\beta)E/2} < \sqrt{2E/3}$. Thus, $\beta < 0.949$ is obtained. From the above discussion, it is concluded that $0.333 < \beta < 0.949$ is a necessary condition for the feasibility of using a standard 8-QAM demodulator in the proposed logical SPC modulation scheme.

Although with the same number of points in the constellation diagram, the performance of the proposed logical SPC modulation/demodulation could be different from that by the conventional hardware-based SPC, which will be further analyzed in the following subsection.

5.2.2 Analysis of Symbol Error Rate (SER)

Analysis is conducted in this section to evaluate the SERs in decoding the logical SPC modulated signals at a receiver. Without loss of generality, the following analysis is conducted based on logical SPC modulation with 8 points in the constellation diagram along with an Additive White Gaussian Noise (AWGN) channel, where the receivers perform SPC demodulation based on the BPSK+QPSK combination. Due to the AWGN channel, the coordinates of symbol s_c can be disturbed by the normally distributed Gaussian noise, N_0 , on top of the allocated energies E_1 and E_2 . Thus, the coordinates of the 8 points in the constellation diagram, $s_c: (x_1, x_2)$, have with the following means and variances:

$$\begin{aligned} x_1 &\sim N\left[\pm\sqrt{E_1} \pm \sqrt{\frac{E_2}{2}}, \frac{N_0}{2}\right] \\ x_2 &\sim N\left[\pm\sqrt{\frac{E_2}{2}}, \frac{N_0}{2}\right] \end{aligned} \quad (5.2)$$

The demodulation mechanism in the analysis is briefed as follows. A standard 8-QAM demodulator is employed to decode the SPC modulated signal. Although a one-shot demodulator is used on the SPC symbol, it is necessary to determine both the symbol error of the base layer and of the entire SPC symbol to accurately reflect the dependency between the base and enhancement layers for successively refinable video bitstreams.

Due to symmetry, the crossover probability of the base layer, $P_{e,1}$, of all 8 points can be categorized into two sets of equations, expressed as:

$$P_{e,1|s_c} = \begin{cases} Q \left[\sqrt{\frac{2}{N_0}} \left(\sqrt{E_1} + \sqrt{\frac{E_2}{2}} \right) \right], & \text{for } c = 1, 4, 5, \text{ and } 8. \\ Q \left[\sqrt{\frac{2}{N_0}} \left(\sqrt{E_1} - \sqrt{\frac{E_2}{2}} \right) \right], & \text{for } c = 2, 3, 6, \text{ and } 7. \end{cases}, \quad (5.3)$$

where the location of each s_c can be referred to in Figure 5-3 (a).

With the assumption that each of the 8 points is equally likely to occur at the transmitter, the overall SER under poor channel conditions using BPSK for demodulation is denoted by $P_{2,4}^{s,1}$, and can be expressed as:

$$P_{2,4}^{s,1} = \frac{1}{2} Q \left[\sqrt{\frac{2E}{N_0}} \left(\sqrt{\beta} + \sqrt{\frac{1}{2}(1-\beta)} \right) \right] + \frac{1}{2} Q \left[\sqrt{\frac{2E}{N_0}} \left(\sqrt{\beta} - \sqrt{\frac{1}{2}(1-\beta)} \right) \right], \quad (5.4)$$

where $E_1 = \beta E$ and $E_2 = (1 - \beta)E$ as described before.

Similarly, the overall SER, P_e , can be expressed using the following two sets of equations:

$$P_e | s_c = \begin{cases} 1 - Q \left[\sqrt{\frac{2E}{N_0}} \left(\sqrt{\frac{2}{3}} - \sqrt{\beta} - \sqrt{\frac{1}{2}(1-\beta)} \right) \right] Q \left[-\sqrt{\frac{E}{N_0}} \left(\sqrt{1-\beta} \right) \right] \\ \text{for } c = 1, 4, 5 \text{ and } 8. \\ 1 - \left\{ \begin{array}{l} Q \left[\sqrt{\frac{2E}{N_0}} \left(-\sqrt{\frac{2}{3}} + \sqrt{\beta} - \sqrt{\frac{1}{2}(1-\beta)} \right) \right] - \\ Q \left[\sqrt{\frac{2E}{N_0}} \left(\sqrt{\beta} - \sqrt{\frac{1}{2}(1-\beta)} \right) \right] \end{array} \right\} Q \left[-\sqrt{\frac{E}{N_0}} \left(\sqrt{1-\beta} \right) \right] \\ \text{for } c = 2, 3, 6 \text{ and } 7. \end{cases}. \quad (5.5)$$

By assuming that each of the 8 points is equally likely to occur, the overall SPC SER $P_{2,4}^{s,2}$ can be expressed as:

$$\begin{aligned}
P_{2,4}^{s,2} &= \frac{1}{2} \left\{ 1 - Q \left[\sqrt{\frac{2E}{N_0}} \left(\sqrt{\frac{2}{3}} - \sqrt{\beta} - \sqrt{\frac{1-\beta}{2}} \right) \right] Q \left[-\sqrt{\frac{2E(1-\beta)}{N_0}} \right] \right\} \\
&\quad + \frac{1}{2} - \frac{1}{2} \left\{ Q \left[\sqrt{\frac{2E}{N_0}} \left(-\sqrt{\frac{2}{3}} + \sqrt{\beta} - \sqrt{\frac{1-\beta}{2}} \right) \right] - \right. \\
&\quad \left. Q \left[\sqrt{\frac{2E}{N_0}} \left(\sqrt{\beta} - \sqrt{\frac{1-\beta}{2}} \right) \right] \right\} Q \left[-\sqrt{\frac{E(1-\beta)}{N_0}} \right] \\
&= \frac{1}{2} Q \left[\sqrt{\frac{2E}{N_0}} \left(\sqrt{\beta} + \sqrt{\frac{1-\beta}{2}} \right) \right] + \frac{1}{2} Q \left[\sqrt{\frac{2E}{N_0}} \left(\sqrt{\beta} - \sqrt{\frac{1-\beta}{2}} \right) \right]
\end{aligned} \tag{5.6}$$

The symbol throughput is measured in terms of the average number of correct bits per transmission at a receiver. By taking each transmission as a symbol block, the symbol throughput of the receiver j , T_j , can be expressed in Eq. (5.7), where the dependency between the successively refinable data in the enhancement and base quality layers embedded in a SPC signal is considered. Note that receiver j has an SNR denoted as $\gamma = E/N_0$.

$$T_j(\gamma) = (1 - P_{2,4}^{s,1}) + 2(1 - P_{2,4}^{s,1})(1 - P_{2,4}^{s,2}) \tag{5.7}$$

The overall system performance, S , is defined as the number of bits obtained from the total symbol throughput that is realized by all receivers from decoding the same received SPC signal. To address the issue of multi-user channel diversity, receivers are divided into two groups based on their respective instantaneous channel conditions. Each group is characterized by the number of users (N_{low} , N_{high}) in the group and their collective average SNR (γ_{low} , γ_{high}). The average SNR for each group is used to evaluate the performance of the specific group. For this purpose, an SNR threshold, denoted as γ_{th} is defined, such that user j belongs to bad-channel group if $\gamma_j < \gamma_{\text{th}}$, and it

belongs to a good-channel group otherwise. Thus, the overall system throughput, $S_{2,4}$, can be expressed as follows:

$$S_{2,4} = T_j(\gamma_{\text{low}}) \times N_{\text{low}} + T_j(\gamma_{\text{high}}) \times N_{\text{high}}. \quad (5.8)$$

5.3 Generalized Formulations for Logical SPC

The design mechanisms and consideration of logical superposition modulation for mimicking a conventional BPSK/QPSK SPC modulation can be easily extended to any combination consisting of modulation schemes (e.g., QPSK, 16QAM, a64QAM) adopted in current and emerging wireless standards such as LTE and WiMAX. As shown in Table 5-1, any combination of modulation schemes in conventional SPC with m_1 points and m_2 points per symbol, respectively, can be theoretically decoded by a standard m_1m_2 demodulator.

5.3.1 Bounds on β

Similar to the use of an 8-QAM detector for decoding a logical SPC signal of the modulation pairs (BPSK/QPSK), there exists a lower and upper bound for the energy allocation factor, β , to restrict the resultant locations of the constellation points of any modulation pair with m_1 points and m_2 points per symbol, such that a standard m_1m_2 demodulator can be employed for decoding with a reasonable SER. The upper and lower bounds of β for L-SPC is determined by numerically solving equations determined from the constellation diagram using geometry. The bounds of β for the modulation combination of interest are presented in Table 5-2.

Table 5-2. Upper and lower bounds for β under various L-SPC combinations of modulation schemes.

Combination	β_{\min}	β_{\max}
BPSK/QPSK	0.333	0.9499
QPSK/16QAM	0.645	0.864
16QAM/64QAM	0.9234	0.9521

5.3.2 General Formulation of SER

A single closed-form formulation is developed as follows for obtaining SERs of logical SPC modulation/demodulation for any combination containing QPSK, 16QAM and 64QAM or any M -ary QAM modulation.

Due to the dependency of the enhancement layer on the base layer, it is important to determine not only the overall crossover probability of the SPC symbol to be decoded using a generalized m_1m_2 -QAM, but also the probability of crossover error of the base layer portion of the logical SPC symbol. For each of the two types of symbol error probability, the goal is to first determine the probability that each received symbol occurs within its corresponding correct decision boundaries when being subject to AWGN noise. Since the abscissa (x-axis) and ordinate (y-axis) components of the noise are uncorrelated, the correctness probability for each axis of any symbol can be determined independently. Due to symmetry, only one quadrant of the constellation needs to be considered, as seen in Figure 5-4.

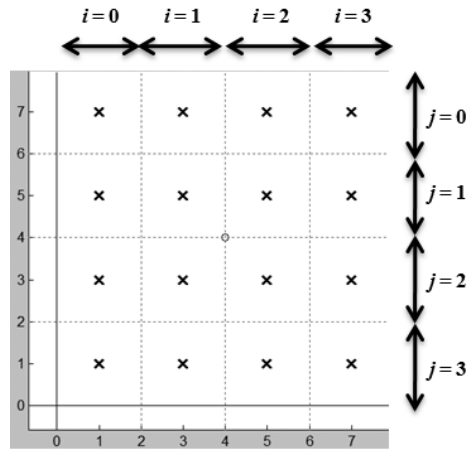


Figure 5-4. Sample first quadrant of QPSK/16QAM constellation denoting reference to each decision region using i and j .

When considering strictly 4^p -QAM modulation schemes for positive integer p , the abscissa and ordinate of the first quadrant in the constellation diagram can each be divided into $\sqrt{M/4}$ regions and be referenced respectively by i and j , as shown in Figure 5-4. However, since there is the same number of regions for both the abscissa and ordinate, it suffices to consider only the abscissa. Defining P_i as the probability of correctly receiving the abscissa of SPC symbols in the i^{th} region, and assuming each point to be equally likely to occur, the probability of SPC SER, denoted as $P_{m_1, m_2}^{s,2}$, with m_1 and m_2 symbols in the base and enhancement layers, respectively, can be expressed as:

$$P_{m_1, m_2}^{s,2} = 1 - P_{m_1, m_2}^{c,2} = 1 - \frac{4}{M} \left(\sum_{i=0}^{\sqrt{M/4}-1} P_i \right)^2. \quad (5.9)$$

Similarly, defining $P_{i,l}$ as the probability of correctly receiving the abscissa of the base layer portion of SPC symbols in the i -th region, the probability of base layer symbol error, $P_{m_1, m_2}^{s,1}$, with m_1 and m_2 symbols in the base and enhancement layers, respectively, can be expressed as:

$$P_{m_1, m_2}^{s,1} = 1 - \frac{4}{M} \left(\sum_{i=0}^{\sqrt{\frac{M}{4}}-1} P_{i,1} \right)^2. \quad (5.10)$$

Thus, the symbol throughput of the receiver j , T_j , can be expressed in Eq. (5.11) in both cases of using conventional SPC (denoted as C-SPC) and proposed logical SPC (denoted as L-SPC) scheme, respectively, where the dependency between the successively refinable data in the enhancement and base quality layers embedded in a SPC signal is considered. Eq. (5.11) summarizes the scenarios where the user SNR is above or below the threshold SNR γ_{th} :

$$T_j(\gamma) = \left. \begin{cases} \log_2(m_1)(1 - P_{m_1, m_2}^{s,1}) + \log_2(m_2)(1 - P_{m_1, m_2}^{s,1})(1 - P_{m_2-QAM}) & \text{for C-SPC} \\ \log_2(m_1)(1 - P_{m_1, m_2}^{s,1}) + \log_2(m_2)(1 - P_{m_1, m_2}^{s,2}) & \text{for L-SPC} \end{cases} \right\}. \quad (5.11)$$

The overall system performance, S_{m_1, m_2} , is defined as the number of bits obtained from the total symbol transmission that is realized by all receivers from decoding the same received SPC signal:

$$S_{m_1, m_2} = T_j(\gamma_{low}) \times N_{low} + T_j(\gamma_{high}) \times N_{high}. \quad (5.12)$$

5.4 Numerical Results

In this section, the goal is to investigate and compare the performance of logical SPC (L-SPC) with the conventional hardware-based SPC (C-SPC) within the operational ranges of β values for each modulation combination under various channel environments. Extensive numerical experiments are conducted for evaluating the per-symbol performance as well as the overall system throughput in a wireless video multicast network. The configuration of the experiments involve video bitstreams with 2 quality layers, where three possible combinations of modulation pairs (i.e., BPSK/QPSK, QPSK/16QAM, 16QAM/64QAM) are evaluated. Both L-SPC and C-SPC are also compared with the one using mono-modulation (denoted as MONO), which serves as a fundamental benchmark to justify the benefits of SPC modulation in general. MONO is a simple implementation only maintaining the use of a single modulation/demodulation scheme (either BPSK, QPSK, 16QAM, 64QAM in this experiment) supportable by the majority of receivers. With both L-SPC and C-SPC, the same cross-layer information mapping mechanism between the application and physical layers is employed, which leads to identical modulated signals provided with the same video source using the same power allocation ratio. In the demodulation process, on the other hand, C-SPC uses a specialized SPC demodulator based on SIC.

5.4.1 Overall System Performance with Multi-User Channel Diversity

Three scenarios are examined, where the SNR thresholds, γ_{th} , that divides the recipients into the two groups, are selected as 14 dB, 23 dB, and 31 dB, respectively. To quantify multi-user channel diversity, a number of cases are defined to describe the histograms of multi-user channel conditions, which are approximated as Normal distributions with various means. In addition to the histogram of the receiver channels, the behavior of the overall system performance, S , is observed over the operational range of β values under different histograms of receiver channels.

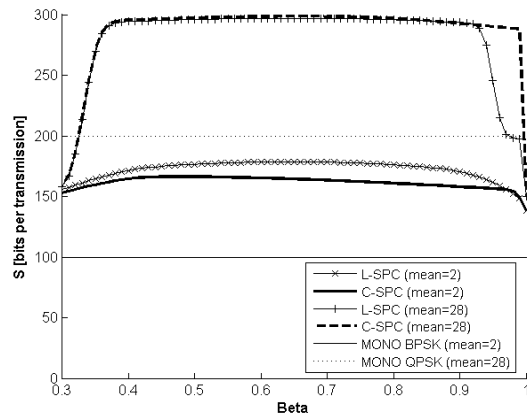
From the results in Figure 5-6 (a)-(c), three observations can be concluded: 1) When the majority of the users are only able to decode the base layer, both L-SPC and C-SPC perform equivalently, since the receivers are basically decoding the information bits of the base layer using the lower-order modulation, i.e., BPSK as shown in Figure 5-6(a), QPSK as shown in Figure 5-6(b) and 16QAM as shown in Figure 5-6(c); 2) When the mean of user channel SNR is relatively sufficient to support the higher order modulation in each combination, L-SPC can achieve the possible maximum per symbol throughput with some β values within the corresponding operational range; 3) the performance of simply using BPSK, QPSK, 16QAM alone, as indicated by the flat lines in Figure 5-6(a)-(c), respectively, are generally outperformed by C-SPC and L-SPC within the operational range of β values; 4) In addition to the advantages of easier implementation in the proposed L-SPC, the receivers equipped with the conventional SPC based on the SIC technique can still be supported to demodulate the logical SPC signal with reasonable per-symbol performance for compatibility purposes.

Since SPC modulation is employed to solve the issue of multi-user channel diversity in wireless video multicast networks, it is important to evaluate its performance under different standard deviations of receiver channel distribution in order to characterize the diversity of multi-user channel in the entire system. Figure 5-8 (a)-(c) illustrates the performance of L-SPC and C-SPC for the three combinations of 2-level SPC signal of interest at low and high SNR standard deviations, yielding two sets of data for each implementation of SPC. From the results, two observations can be drawn. 1) it is observed that for a fixed SNR mean, increased standard deviation reduces the overall system throughput due to the increase in channel diversity between the two groups of receivers (i.e., the receivers can only decode the base layer, and the receivers can decode both layers); 2) for both low and high SNR standard deviation conditions, L-SPC is able to achieve comparable performance to C-SPC within the operational range of β .

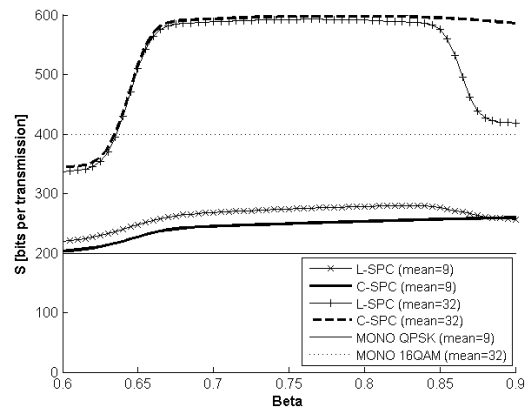
With 2-level SPC signals, SNR standard deviations should be large enough to fully demonstrate the benefits of multi-rate video transmission by the SPC signals in accommodating for the two user groups experiencing lower and higher channel SNRs. However, such SNR standard deviation should not be too large to prevent the distribution from becoming uniform. Otherwise, the number of levels in a SPC signal should include more quality layers instead of two, so that the SPC signal can offer more multi-rates to better cater for more receivers with diverse channel conditions due to the high variance of receiver SNR.

5.4.2 Achieving Comparable Optimal System Performance

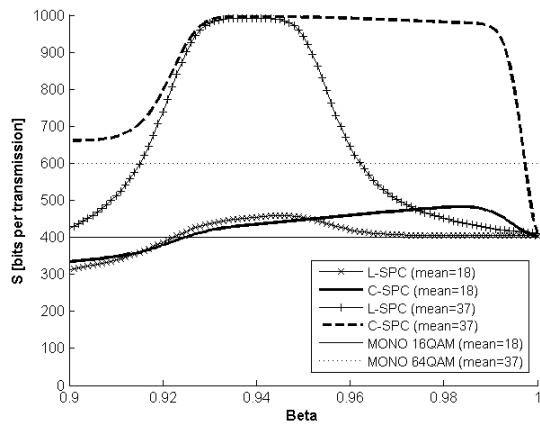
From the results in Figure 5-6, it is observed that both C-SPC and L-SPC achieve their optimal system symbol throughputs at different β values, which is verified repeatedly over 2 different sets of means of user channel conditions as well as different combinations of modulation schemes, respectively. For attaining the achievable optimal system performance of the proposed approach in each multicast transmission, β should be chosen based on a given receiver channel distribution characterized by the mean. From the results in Figure 5-8 (a)-(c), two conclusions can be solidly drawn: 1) L-SPC is shown to achieve comparable optimal system throughput in the wireless video multicast network for two different group size of receivers (i.e., 100 and 10000 receivers) under different average SNR values of a Normal SNR distribution with all combinations, respectively. Both approaches of L-SPC and C-SPC are evaluated and compared their optimal system performance by using the β values that maximizes their individual performances, which can be derived by solving the first order derivative of Eq. (5.8) (i.e., $\partial S / \partial \beta = 0$); 2) L-SPC in fact achieves a comparable optimal system performance like C-SPC independent from the number of receivers (i.e., 10000 receivers) within a wireless video multicast, while also offering a much easier implementation and deployment in realizing the SPC modulation/ demodulation.



(a)



(b)



(c)

Figure 5-5. Overall system throughput of L-SPC and C-SPC for combinations: (a) BPSK/QPSK, (b) QPSK/16QAM, (c) 16QAM/64QAM, over varying β values under the Normal distributions with various means for the multi-user channel histogram.

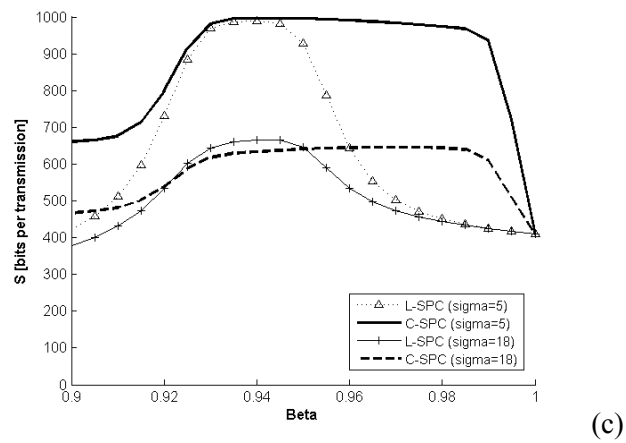
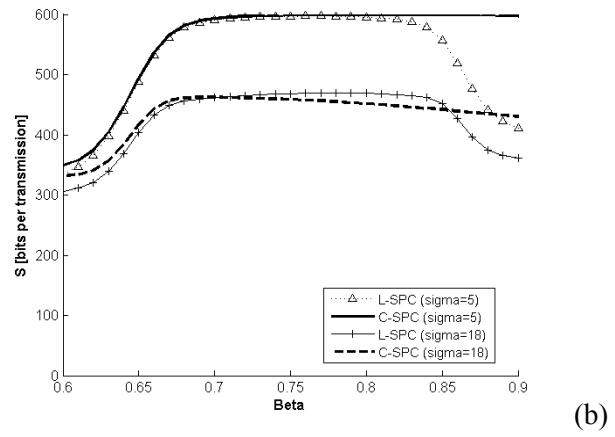
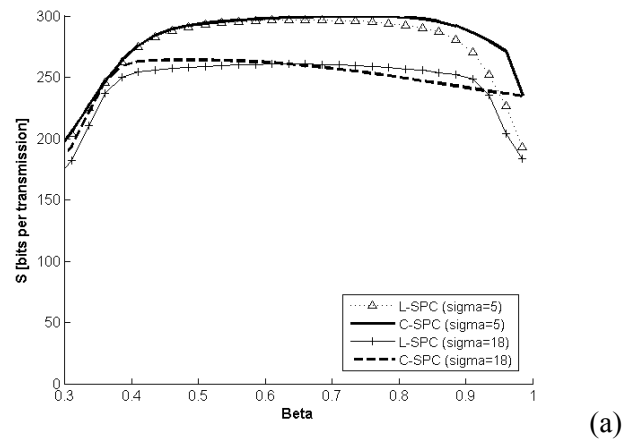


Figure 5-6. Overall system throughputs of the proposed and standard approaches over different values under the normal distribution with various standard deviations for the SPC combination (a)

QPSK/BPSK, (b) QPSK/16QAM and (c) 16QAM/64QAM

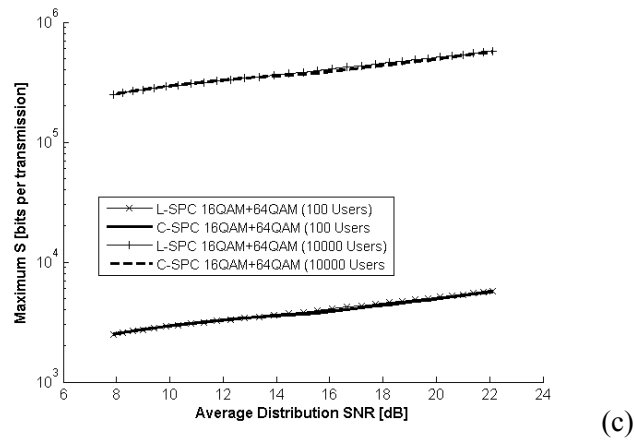
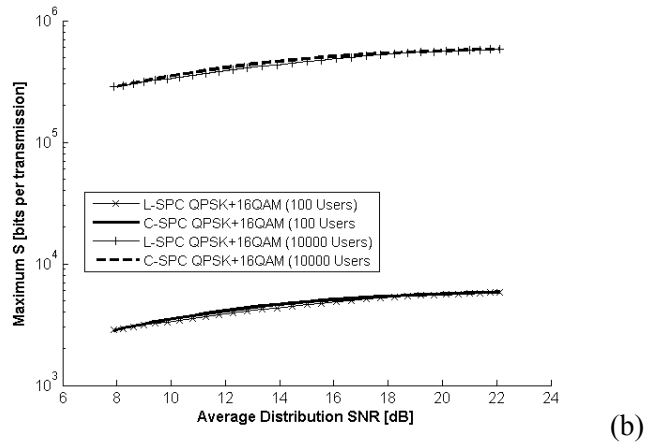
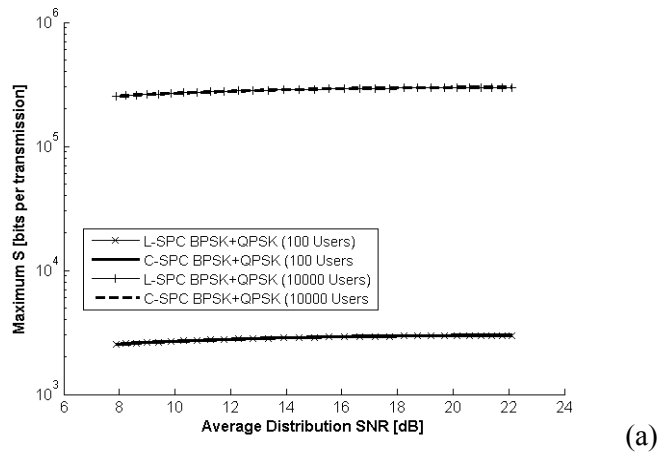


Figure 5-7. Comparable optimal system performance between the proposed and conventional approaches under various multi-user channel histograms modeled using Normal distributions of different means and variances.

5.5 Testbed Results

In addition to the comprehensive simulations, GNU Radio [42] was used to demonstrate the implementation feasibility of logical SPC on a practical small-scale testbed of wireless video multicast. The software for the basic signal processing blocks is from the open source GNU Radio project. A commodity PC as the transmitter is connected to a Universal Software Radio Peripheral (USRP) motherboard, in which 2 modulation schemes (i.e., BPSK and QPSK) and the information bit mapping of L-SPC modulation scheme along the use of 8-QAM modulation are developed for multicast transmissions in the testbed. The RFX2400 daughterboard, which operate in the 2.4 GHz range, were used. The transmitter generates packets according to the trace file of a real video with the HDTV quality from [11] in the PC, which is encoded with two quality layers (i.e., base and enhancement) by H.264/AVC. The trace file provides the amount of base and enhancement bitstreams of each video frames to be transmitted. On the other side, PCs act as the multicast receivers connected to USRP boards has implemented the decoding mechanisms of L-SPC in addition to the standard demodulations. Two different receiver channel conditions are created by adding noise through the signal processing at one of the receiver group, in which receivers with a lower mean of SNR channel condition around 10dB and the others with a mean SNR around 20dB are selected. Successfully received packets will be tracked at the receivers for the computation of video quality of each video frame in the trace. The results reveal the following findings.

- Due to the dependency of enhancement bitstreams on the base layer one, the transmitter without any SPC capability can only exercise BPSK (the mono-rate) to reliably transmit the video bitstreams to all multicast receivers by sending the base layer bitstreams first followed by the enhancement layer one. Much longer transmission timeslots must be required for transmitting both the base and enhancement layer bitstreams for the full high-definition video quality. Otherwise, the

tradeoff is to multicast a lower video quality wirelessly (such as only the base quality or not the original full quality) to all receivers to occupy less transmission timeslots.

- With the logical SPC implemented at the transmitter, it successfully realizes the benefits of the SPC modulation to the transmitter by using less transmission timeslots, and/or offering multi-rate transmissions to all wireless receivers to secure the base quality but with the opportunity to obtain higher video quality or almost the original full quality.

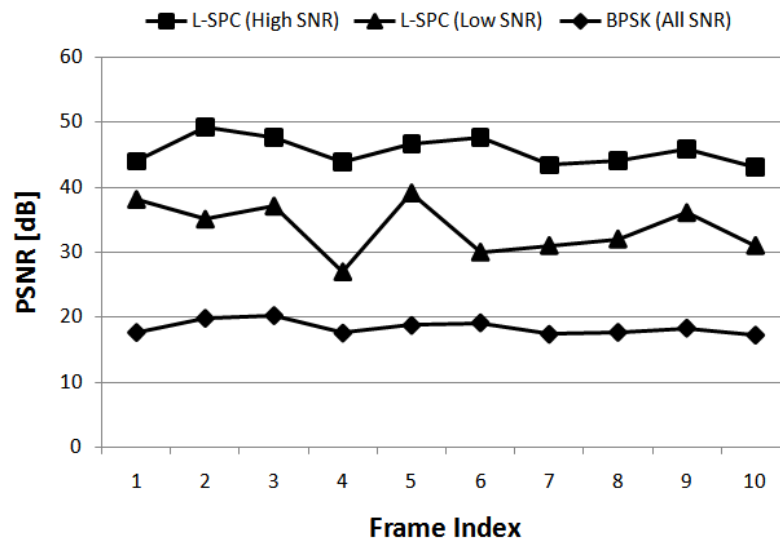


Figure 5-8. Received PSNR from the transmission of a scalable HDTV video trace using 2 layered L-SPC and mono-rate BPSK.

In Figure 5-8, it shows the video quality of the first 10 video frames in terms of peak-signal-to-noise ratio (PSNR) achievable by receivers with a lower and higher SNR means of channel condition at 10dB and 20dB, respectively. Higher PSNR values can always be obtained by receivers with the use of SPC realized by L-SPC, whereas a much lower PSNR value is resulted due to the mono-rate of BPSK with the transmitter without implementing L-SPC.

5.6 Summary

Superposition coded (SPC) modulation/demodulation has been well proven as an effective approach to mitigating the vicious effect caused by multi-user channel diversity in wireless video multicast. However, due to the requirement of additional hardware, SPC modulation/demodulation has not been commonly employed in most industry standards and practical implementations for wireless video multicast in spite of the obvious advantages.

The chapter introduced a novel cross-layer design framework of logical SPC modulation for wireless video multicast, which takes advantage of the successively refinable feature of scalable video bitstreams and a logical mapping onto the constellation of SPC modulated signals. The logical SPC signals are characterized by their comparable performances under various receiver channel distributions. Rather than installing additional hardware circuitry, the proposed framework simply performs software-based dynamic energy allocation and phase keying to generate the logical SPC signals in a single shot. Each receiver, on the other hand, selects a demodulation scheme on the received logical SPC signals according to its channel condition, where users with good channels can obtain both base and enhancement layer bits, while users with poor channels can at least obtain the base layer bits. Generalized closed-form formulations were derived to evaluate and analyze the proposed approach in terms of symbol error rate (SER). Numerical experiments were conducted, and the results showed that the proposed logical SPC modulation/demodulation can achieve much better performance than that by using only mono-rate modulation in the multicast of scalable video bitstreams. In contrast with the scheme of conventional hardware-based SPC with SIC, the proposed logical SPC modulation can completely avoid additional hardware at the sender and receivers without any compromise in the overall performance by manipulating the value of β . A test bed is developed based on GNU Radio to demonstrate the implementability and its advantages of the proposed framework. It is concluded that the proposed logical SPC

modulation not only provides an alternative means of realizing SPC modulation for mitigating the vicious effect of multi-user channel diversity in wireless video multicast applications, but also serves as a powerful transition tool to bridge the gap in adopting SPC modulation for any future wireless technologies.

Chapter 6

Contributions and Conclusions

In this chapter, the contributions of this thesis are concluded, followed by the future work.

6.1 Major Research Contributions

The major research contributions from this doctoral thesis work are summarized as follows:

- (1) A cross-layer framework, called Superposition Coded Multicast (SCM), is proposed by exploring the intrinsic layered natures of advanced scalable video coding (e.g., H.264/MPEG-4 AVC) and the use of superposition coding at the channel. The results concluded that multi-resolution modulations and scalable video source are two unavoidable design components.
- (2) Extensive simulations and experiments with real trace files of high-definition television (HDTV) are conducted to compare a system using the proposed framework and a legacy multicast scheme that always transmits with the best supported modulation rate. The results revealed the benefits of jointly considering a successive refinement coding at the source and layered broadcast coding at the channel for wireless video broadcast/multicast. Such coded wireless video broadcast/multicast signal practically utilized the diverse channel conditions of

all individual receivers at each reception moment. Each receiver can therefore acquire a better video quality regardless of its average channel condition.

- (3) A novel cross-layer framework of the interplay between applying protections on successively refinable video source and layered modulation at the channel is proposed, which effectively tackles the multi-user channel diversity and error control problems.
- (4) An analytical model using the total receivable/recoverable video bitstreams from each coded wireless broadcast/multicast signal is developed, which serves as a video quality measurement for system analysis and optimization.
- (5) An efficient optimization technique is developed to practically determine the optimal power allocations and modulation selections to improve the broadcast/multicast video quality at the receivers. Most importantly, this framework can be realistically implemented by using scalable video source, a modified multiple description coding (MDC) as the protection, and SPC at the channel for layered broadcast/multicast.
- (6) Comprehensive simulations are conducted on various standard video sequences, which confirm the effectiveness of this framework of coded wireless video broadcast/multicast for effectively tackling with the problems of multi-user channel diversity and error control.
- (7) From the information-theoretical point of view, a closed-form formula is derived for the distortion analysis of the proposed framework using any (n, k) protection code in a successive refinable source with Gaussian distribution over a layered Gaussian broadcast channel. The closed-form formula can determine the situations in which coded wireless video broadcast/multicast can yield a lower distortion than a system with any protection.
- (8) An efficient iterative search algorithm is developed that can always identify the global optimal for distortion at the worst-time complexity of $O(n \log n)$, where n is the number of channel symbols required to send a source symbol after protection.

- (9) Numerical analyses for performance evaluation are conducted to show the effectiveness of the proposed search algorithm. The results confirmed that the optimized k values searched by the $O(n \log n)$ algorithm can yield the lowest distortion.
- (10) The chapter introduced a novel cross-layer design framework of logical SPC modulation for wireless video multicast, which takes advantage of the successively refinable feature of scalable video bitstreams and a logical mapping onto the constellation of SPC modulated signals.
- (11) Generalized closed-form formulations were derived to evaluate and analyze the proposed logical SPC approach in terms of symbol error rate (SER).
- (12) Numerical experiments were conducted, and the results showed that the proposed logical SPC modulation/demodulation can achieve much better performance than that by using only mono-rate modulation in the multicast of scalable video bitstreams.
- (13) In contrast with the scheme of conventional hardware-based SPC with SIC, the proposed logical SPC modulation can completely avoid additional hardware at the sender and receivers without any compromise in the overall performance by manipulating the value of β . A test bed is developed based on GNU Radio to demonstrate the implementability and its advantages of the proposed framework.

More importantly, this thesis contributes to the advancement in the related fields in communication engineering and information theory by introducing a new design dimension in terms of protection. This is unique when compared to previously-reported layered approaches that are often manipulating conventional parameters alone such as power and modulation scheme. The impact of this dimension was unapparent in the past, but is now proven as an effective means to enable high-quality, efficient, and robust wireless video broadcast/multicast for media applications even with high-definition content in the future.

6.2 Future Works

Due to the vibrant broadband access technologies based on WiMAX and Ethernet passive optical networks (EPONs) [43], next-generation video broadcast/multicast services are envisioned to be offered in such cost-effective hybrid wired/wireless access network like Figure 6-1. Due to a higher economy of scale in the operations, operators can secure the bigger successes in video businesses (e.g., IPTV) along with their existing broadband and mobile services. By investigating and tackling the interferences and other related issues in the future works, the proposed framework in this thesis could be extended to operate over multiple cooperative BSs in such emerging hybrid access network. A very large-scale, high-capacity and HD-quality wireless video broadcast/multicast network is foreseeable to happen to benefit end-users with many innovative all-IP wireless media applications. Preliminary studies are conducted in this direction with some promising results below, which confirm the potentials of required future research works.

6.2.1 EPON-WiMAX Network - A hybrid wired/wireless access network

Figure 6-2 shows an emerging integrated access network architecture based on EPON and WiMAX technologies. An EPON consists of a central optical line terminal (OLT) and multiple optical network units (ONUs) that are connected to the OLT through fibers of a tree topology. Given a certain optical split ratio, only a limited number of ONUs can be connected to an optical splitter and then to a common OLT. For example, a 1:16 splitter can maximally connect 16 ONUs. As a root node, the OLT is often located in a central office (CO) which provides an access to the core IPTV network that is beyond an EPON-WiMAX access network.

Within the EPON-WiMAX access network, an EPON ONU and a WiMAX base station (BS) are integrated into a single device box, called an ONU-BS [43]. In addition to hardware cost saving,

such integration achieves a flat control plane and seamless integration between the EPON and WiMAX systems, where signaling and control messages are exchanged directly between the OLT and end users (i.e., subscriber stations [SSs], which could be fixed stations or mobile stations [MSs]). Besides directly extending the comprehensive class of services for various traffic types (i.e., UGS, rtPS, nrPS, and BE) defined in WiMAX standards, broadcast/multicast services (MBS) [44] should also be adopted from the standards to support both unicast and multicast applications in the EPON-WiMAX networks. Due to the tree topology of EPON and the broadcast nature of WiMAX, the EPON-WiMAX access networks are ideal to provision bandwidth-intensive IPTV content to multiple receivers simultaneously using wireless multicasting without duplicated deliveries, especially for ongoing scheduled TV channels. However, there are new challenges to be addressed for preserving the use of broadcasting/multicasting in such integrated networks for IPTV services.

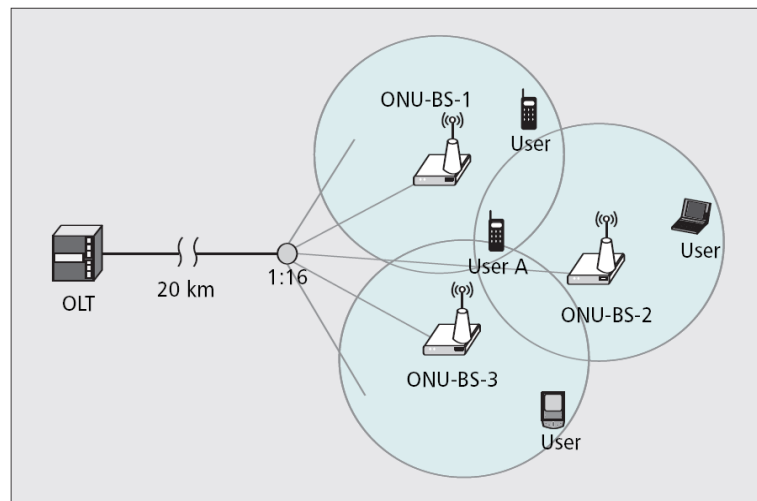


Figure 6-2. Integrated access network architecture based on EPON and WiMAX.

6.2.2 Cooperative Coded Video Multicast

A cooperative coded framework can be developed by jointly exercising a space-time coding (STC) with the proposed wireless coded video broadcast/multicast framework in this thesis above. With orthogonal codes equipped in each distributed ONU-BS that enables STC-based cooperative transmission initiated by the OLT, a receiver could be provisioned by multiple ONU-BSs cooperatively to obtain aggregated power assigned for each layer of MDC protected bitstreams. As shown in Figure 3-4 in Chapter 3, the video bitstream of a quality layer will first be encoded by the modified layered MDC at the source. The ONU-BSs, upon receiving the MDC bitstreams, will perform superposition coding on the bitstreams of different quality layers. The superimposed signal, which corresponds to a GoF of an IPTV channel, is further encoded with an assigned space-time code, which is orthogonal to that used by the other ONU-BSs. Therefore, according to STC, a receiver in area A will perceive aggregated power from the three ONU-BSs, which yields a much higher signal-to-interference-plus-noise ratio (SINR) than the situation where the conventional transmission with simply a single ONU-BS is adopted. Due to the higher perceived SINR, the three ONU-BSs can adopt a pair of more aggressive modulation schemes in the two quality layers of video bitstreams under the cooperative provisioning scenario while ensuring that a receiver in area A can still decode the received signal. In summary, the proposed CCVM framework is designed to effectively solve the impacts of long-term user diversity and short-term channel fluctuation by jointly exercising SPC and the modified MDC, respectively, as well as to overcome the inter-cell interferences by STC-based cooperative communications under coordination of the OLT. The use of MDC contributes not only to the robustness of the video quality, but also to mitigate the channel condition fluctuations due to user mobility. It is notable that the timescale of channel fluctuation that can be defended by using the modified MDC is in milliseconds, which is much larger than that by other redundancy code added in the MAC layer (which are as short as several microseconds).

Such larger timescales of protection are considered more effective in dealing with non-spontaneous channel fluctuations.

A simple case study is conducted to examine the possible future work framework in terms of cooperation among ONU-BSs. In particular, the performance improvement by initiating cooperative transmission among distributed ONU-BSs is investigated. The scenario where a broadcasted/multicast IPTV channel over an EPON-WiMAX access network with 3 ONU-BSs as shown in Figure 6-3. Without loss of generality, two quality layers of video bitstream are assumed for every GoF. Each ONU-BS is considered at the origin of a cell, and a SS (receiver) will associate with and be served by at least one ONU-BS (i.e. the home ONU-BS) that is closest to the SS with the strongest SINR. An exponential path loss model with Rayleigh fading is assumed in determining the individual SINR of a signal from an ONU-BS to a receiver with the distance and allocated power. Polar coordinates $P(r, \theta)$ are used with the home ONU-BS at the origin. The distance of a SS at (r, θ) from the i -th ONU-BS at (r_i, θ_i) can be expressed as $d_i(r, \theta) = \sqrt{r^2 + r_i^2 - 2rr_i \cos(\theta - \theta_i)}$. Simulations were conducted using MATLAB to obtain the highest achievable SINRs of each quality layer in the multicast signals for the scenarios with and without cooperative coded multicasting. The same system parameters and fading channel environments in **Error! Reference source not found.** are used, and the best pairs of modulation schemes with the optimized power of each quality layer in superposition coding are selected universally across all ONU-BSs in the EPON-WiMAX network. As demonstrated by Eq. (3.8) of Chapter 3 in this thesis, the video quality of a GoF perceived by a receiver depends on the total amount of receivable/recoverable bitstream of the GoF, which is further affected by the factors of bit error rates (or layer error rates) and the throughput of each received cross-layer coded multicast signal in both quality layers. These factors are essentially determined by the aggregated SINR of each quality layer perceivable by a receiver. Therefore, averaged SINRs of SS₁, SS₂, SS₃, and SS₄

are measured in three interested areas A1, A2 and A3, for each quality layer with and without employing the cooperative communications of over 5,000 simulated timeslots.

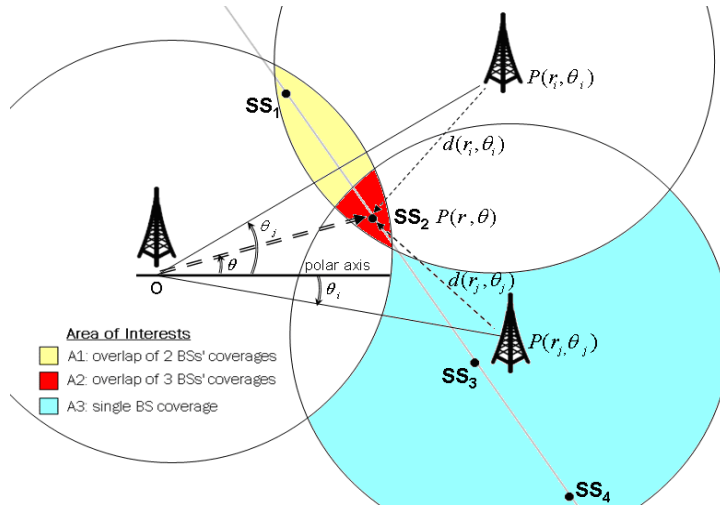


Figure 6-3. Multiple ONU-BSs and 4 SSs in the polar coordinates.

Figure 6-4 illustrates the SINR for each quality layer at the SSs in the three interested areas under the best achievable modulation schemes for the two quality layers. For SS₁ and SS₂, the proposed CCVM framework can solidly help to perceive required SINRs to support modulations in both quality layers of the multicast signals in the presence of the inter-cell interferences (i.e. 11.8dB and 11.4dB in average for base quality, and 7.0dB and 9.8dB in average for enhancement quality at SS₁ and SS₂, respectively). However, the one without CCVM fails to provide the minimal SINRs for even the lowest order of modulation in any quality layer for SS₁ and SS₂ in both areas A1 and A2 under interferences. On the other hand, the integration of CCVM does not affect the SINR of the multicast signals perceived by SS₃ and SS₄ if there are no inter-cell interferences from the other ONU-BSs in area A3. However, SS₄ in area A3 only has the required SINR to support the lowest order of modulation, BPSK, for the base quality layer, but not enough SINR to support any

modulation type for the enhancement quality layer. On the contrary and interestingly, as shown in Figure 6-4, although those SSs located at areas A1 and A2 are subject to severe interferences from neighboring ONU-BSs, they can actually have sufficient SINR to support an even higher-order modulation scheme to maintain better transmission capacity for provisioning IPTV services when compared to those SSs at the cell boundary of their home ONU-BS without much of interference (i.e. SS₃ and SS₄ in A3). This indicates that the proposed CCVM framework not only effectively mitigates the inter-cell interference, but also promotes the ultimate gain of video multicasting in a large-scale deployment of multiple ONU-BSs in EPON-WiMAX access networks with wireless access and mobility.

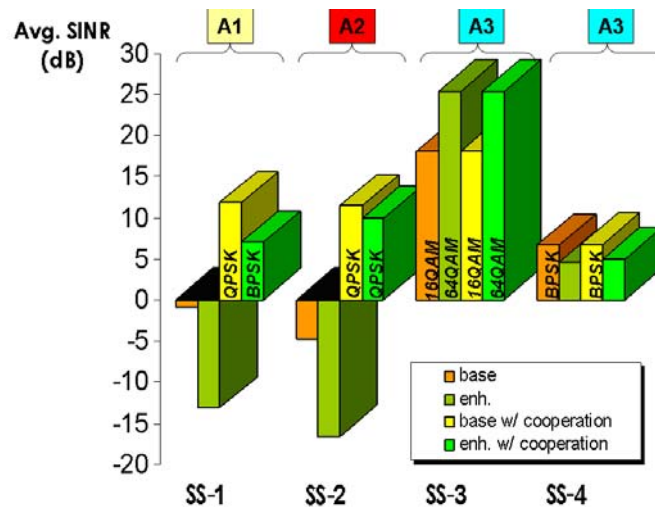


Figure 6-4. Achievable SINRs and best supportable modulation pair for both quality layers by SSs in different interference areas.

6.3 Final Remarks

Promising results are obtained from the preliminary investigation in the previous section for EPON-WiMAX access networks, in which the proposed framework is extended to deal with the wireless video broadcast/multicast under the scenario of multiple BSs. This thesis has been investigating the use of protections on a successive refinable source over layered broadcast channel in a single-hop wireless access network. The contributions and conclusions from this thesis also established solid research groundwork in terms of a closed-form cross-layer distortion model, which facilitate researchers/engineers to understand if and how protections in future cross-layer designs under cooperative wired/wireless access networks can lead to a better video broadcast/multicast performance.

References

- [1] IEEE Standard 802.16-2004, "IEEE Standard for Local and Metropolitan Area Networks-Par 16:Air Interface for Fixed Broadband Wireless Access Systems," 2004.
- [2] F. Khan, "LTE for 4G Mobile Broadband - Air Interface Technologies and Performance", *Cambridge University Press*, 2009.
- [3] D. Coates, "Low Power Large-Area Cholesteric Displays," *Info. Display*, nol. 25, no. 3, pp.18, 2009.
- [4] D. Marpe, T. Wiegand, and G. J. Sullivan, "The H.264/MPEG4 Advanced Video Coding Standard and Its Applications," *IEEE Commun. Mag.*, vol. 44, no. 8, Aug. 2006, pp. 134–43.
- [5] J. She, F. Hou, and P.-H. Ho, "An Application-Driven MAC-layer Buffer Management with Active Dropping for Real-time Video Streaming in 802.16 Networks", *Proc. of IEEE 21st International Conference on Advanced Networking and Applications*, pp.451-458, Niagara Falls, Canada, 2007.
- [6] J. Gross, J. Klaue, H. Karl and A. Wolisz, "Cross-layer Optimization of OFDM Transmission Systems for MPEG-4 Video Streaming," *Comp. Commun.*, vol. 27, no. 11, pp. 1044–55, Jul. 1, 2004.

- [7] Y. Shan and A. Zakhori, "Cross Layer Techniques for Adaptive Video Streaming over Wireless Networks," *IEEE Int'l. Conf. Multimedia and Expo*, Lausanne, Switzerland, Aug. 26–29, 2002.
- [8] P. Buccioli, G. Davini, E. Masala, E. Filippi and J.C. De Martin, "Cross-layer Perceptual ARQ for H.264 Video Streaming over 802.11 Wireless Networks," *Proc. of IEEE GLOBECOM*, vol. 5, pp. 3027-3031, Nov.-Dec. 2004.
- [9] M. van der Schaar, S. Krishnamachari, S. Choi and X. Xu, "Adaptive Cross-Layer Protection Strategies for Robust Scalable Video Transmission over 802.11 WLANs," *IEEE JSAC*, vol. 21, no. 10, pp. 1752–63, Dec. 2003.
- [10] J. Song and K. J. Ray Liu, "An Integrated Source and Channel Rate Allocation Scheme for Robust Video Coding and Transmission over Wireless Channels," *EURASIP Journal on Applied Signal Processing*, vol. 2004, no. 2, pp. 304-316, 2004.
- [11] Video Traces, <http://trace.eas.asu.edu/>
- [12] I. Djama and T. Ahmed, "A Cross-Layer Interworking of DVB-T and WLAN for Mobile IPTV Service Delivery", *IEEE Trans. on Broadcasting*, vol. 53, no. 1, Part 2, pp.382–390, Mar. 2007.
- [13] J. Byers, M. Luby, M. and M. Mitzenmacher, "A digital fountain approach to asynchronous reliable multicast," *IEEE JSAC*, vol. 20, no. 8, pp. 1528-1540, Oct. 2002.
- [14] V. K. Goyal, "Multiple description coding: Compression meets the network", *IEEE Signal Processing Magazine*, pp. 74–93, Sep 2001.

- [15] W. Ge, J. Zhang and S. Shen, "A Cross-Layer Design Approach to Multicast in Wireless Networks", *IEEE Trans. on Wireless Communications*, vol. 6, no. 3, pp. 1063-1071, 2007.
- [16] A. El Gamal and T. M. Cover, "Achievable rates for multiple descriptions", *IEEE Trans. Info. Theory*, vol.28, pp.851-857, November 1982.
- [17] L. Ozarow, "On a source-coding problem with two channels and three receivers", *Bell Syst. Tech. J.*, vol. 59, pp. 1909-1921, 1980.
- [18] R. Venkataramani, G. Kramer, and V. K. Goyal, "Multiple description coding with many channels", *IEEE Trans. Info. Theory*, vol.49, pp.2106-2114, September 2002.
- [19] P. A. Chou, H. J. Wang, and V. N. Padmanabhan, "Layered multiple description coding," *Proc. PV 13th Int'l. Packet Video Workshop*, Nantes, France, Apr. 2003.
- [20] A. Albanese, J. Blomer, J. Edmonds, M. Luby, M. Sudan, "Priority encoding transmission", *IEEE Trans. Info. Theory*, vol. 42, pp.1737-1744, Nov. 1996.
- [21] John G. Proakis, "Digital Communication", Fourth Edition, McGraw-Hill, New York, 2000.
- [22] R. Theodore, "Wireless Communication", Prentice Hall, 1996.
- [23] L. Li, R. Alimi, R. Ramjee, J. Shi, Y. Sun, H. Viswanathan, Y. R. Yang, "Superposition coding for wireless mesh networks", *Proc. of the 13th annual ACM Int'l. Conf. on Mobile Computing and Networking*, pp. 330 – 333, Montreal, Canada, 2007.

- [24] S. Bopping and J. M. Shea, “Superposition Coding in the Downlink of CDMA Cellular Systems,” *IEEE Wireless Commun. and Networking Conf.*, vol. 4, Apr. 3–6, 2006, pp. 1978–83.
- [25] A. El Gamal and T. M. Cover, “Achievable rates for multiple descriptions,” *IEEE Trans. Info.Theory*, vol.28, pp.851-857, November 1982.
- [26] L. Ozarow, “On a source-coding problem with two channels and three receivers,” *Bell Syst. Tech. J.*, vol. 59, pp. 1909-1921, 1980.
- [27] R. Venkataramani, G. Kramer, and V. K. Goyal, “Multiple description coding with many channels,” *IEEE Trans. Info. Theory*, vol.49, pp.2106-2114, September 2002.
- [28] T. M. Cover, “Broadcast Channels,” *IEEE Trans. Info. Theory*, vol. IT-18, Jan. 1972, pp. 2-4.
- [29] S. Bopping and J. M. Shea, “Superposition Coding in the Downlink of CDMA Cellular Systems,” *IEEE Wireless Commun. and Networking Conf.*, vol. 4, Apr. 3-6, 2006, pp. 1978-83.
- [30] S. Shamai (Shitz), “A broadcast strategy for the Gaussian slowly fading channel,” in *Proc. IEEE Int’l. Symp. Info. Theory*, June 1997, p. 150.
- [31] S. Shamai (Shitz) and A. Steiner, “A broadcast approach for a single-user slowly fading MIMO channel,” *IEEE Trans. Info. Theory*, vol. 49, no. 10, pp. 2617–2635, Oct. 2003.
- [32] C. Tian, A. Steiner, S. Shamai (Shitz) and S. N. Diggavi, “Successive Refinement Via Broadcast: Optimizing Expected Distortion of a Gaussian Source Over a Gaussian Fading Channel,” *IEEE Trans. on Info. Theory*, vol. 54, no 7, pp.2903-2918, Jul. 2008.

- [33] Y. S. Chan, J. W. Modestino, Q. Qu and X. Fan, "An End-to-End Embedded Approach for Broadcast/multicast of Scalable Video over Multiuser CDMA Wireless Networks", *IEEE Trans. on Multimedia*, vol. 9, no. 3, pp. 655-667, Apr. 2007.
- [34] Chris T. K. Ng, Deniz Gündüz, Andrea J. Goldsmith and Elza Erkip, "Recursive Power Allocation in Gaussian Layered Broadcast Coding with Successive Refinement," *IEEE Int'l. Conf. on Commun. (ICC)*, June 24–27, 2007, Glasgow, Scotland, pp. 889–896.
- [35] Qualcomm, "MediaFLO FLO Technology Overview", http://www.mediaflo.com/news/pdf/tech_overview.pdf
- [36] Qualcomm Incorporated, "Hierarchical Coding With Multiple Antennas In A Wireless Communication System", *WO/2005/032035, Patent Application, Patent Cooperation Treaty*, Sep. 2004.
- [37] J. She, F. Hou, P.-H. Ho and L.-L. Xie, "IPTV over WiMAX: Key Success Factors, Challenges, and Solutions", *IEEE Commun. Mag.*, vol. 45, no 8, pp.87-93, Aug. 2007.
- [38] X. Yu, H. Wang, and E.-H. Yang, "Optimal quantization for noisy channels with random index assignment", *Proc. of the 2008 IEEE Int'l. Symp. Inform. Theory*, Toronto, Canada, July 6-11, 2008.
- [39] X. Yu and E.-H. Yang, "Design and analysis of optimal noisy channel quantization with random index assignment," *to appear in IEEE Trans. on Info. Theory*, 2009
- [40] T. M. Cover et al., "Element of Information Theory", New York, NY, Wiley, 1991
- [41] picoChip, <http://www.picochip.com/>
- [42] "GNU Radio: The GNU Software Radio," <http://www.gnu.org/software/gnuradio/>

- [43] G. Shen, R. S. Tucker, and C.-J. Chae, "Fixed Mobile Convergence (FMC) Architectures for Broadband Access: Integration of EPON and WiMAX," *IEEE Commun.Mag.*, Aug. 2007, pp. 44–50.
- [44] T. Jiang, W. Xiang, H.-H. Chen, and Q. Ni, "Multicast Broadcast Services Support in OFDMA-Based WiMAX Systems," *IEEE Commun. Mag.*, vol. 45, no. 8, Aug. 2007, pp. 78–86.
- [45] J. She, X. Yu, P.-H. Ho, and E.-H. Yang, "A Cross-Layer Design Framework for Robust IPTV Services over IEEE 802.16 Networks", *IEEE JSAC*, vol. 27, no. 2, Feb. 2009, pp. 235-245.